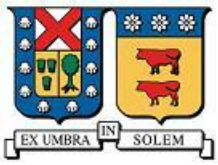

Universidad Técnica Federico Santa María.
Departamento de Física.

Phenomenology in Rare Meson Decays

Jilberto Antonio Zamora Saá
Advisor: Gorazd Cvetic, Ph.D.

A thesis submitted in partial fulfillment for the degree of Doctor in Science, Universidad Técnica Federico Santa María.

May 2015

THESIS TITLE:

Phenomenology in Rare Meson Decays

AUTHOR:

Jilberto Antonio Zamora Saá

A thesis submitted in partial fulfillment for the degree of Doctor in Science, Universidad Técnica Federico Santa María.

THESIS EXAM COMMITTEE:

Gorazd Cvetic, Ph.D. .....

Dr. Sergey Kovalenko .....

Dr. Alfonso R. Zerwekh .....

Marco A. Díaz, Ph.D. .....

Valparaiso, June 2015

to my family.

Abstract

In this thesis we studied the leptonic pion decays with intermediate on-shell (and off-shell) neutrinos N into two electrons and a muon, $\pi^{\pm} \to e^{\pm} N \to e^{\pm} e^{\pm} \mu^{\mp} \nu$. We investigated the branching ratios $\mathrm{Br}_{\pm} = [\Gamma(\pi^- \to e^- e^- \mu^+ \nu) \pm \Gamma(\pi^+ \to e^+ e^+ \mu^- \nu)]/\Gamma(\pi^- \to \text{all})$ and the CP asymmetry ratio $\mathcal{A}_{\mathrm{CP}} = \mathrm{Br}_-/\mathrm{Br}_+$ for such decays, in the scenario with two different on-shell neutrinos N_j ($j = 1, 2$). If N is Dirac, only the lepton number conserving (LC) decays contribute (LC: $\nu = \nu_e$ or $\bar{\nu}_e$); if N is Majorana, both LC and lepton number violating (LV) decays contribute (LV: $\nu = \nu_\mu$). Furthermore, we studied the CP violation in lepton number violating semihadronic decays $M^{\pm} \to \ell_1^{\pm} \ell_2^{\pm} M^{'\mp}$, where M and $M^{'}$ are pseudoscalar mesons, $M = K, D, D_s, B, B_c$ and $M^{'} = \pi, K, D, D_s$, and the charged leptons are $\ell_1, \ell_2 = e, \mu$. Our calculations show that the asymmetry becomes largest when the masses of N_1 and N_2 are almost degenerate, i.e., when the mass difference ΔM_N becomes comparable with the (small) decay widths Γ_N of these neutrinos: $\Delta M_N \not\gg \Gamma_N$. We showed that in such a case, the CP asymmetry ratio $\mathcal{A}_{CP}$ becomes a quantity ~ 1. The observation of CP violation in these decays would be consistent with the existence of the well-motivated νMSM model with two almost degenerate heavy neutrinos in the mass range between $M_N \sim 0.1\text{-}10^1$ GeV.

Moreover, in the context of the semihadronic decays in particular (LV: $B^{\pm} \to \mu^{\pm} e^{\mp} \pi^{\mp}$) and (LC: $B^{\pm} \to \mu^{\pm} e^{\mp} \pi^{\pm}$) we studied the possibilities to detect the effects of heavy neutrino oscillation of the intermediated on-shell neutrinos. We pointed out that such decays may present detectable effects of heavy neutrino oscillation, allowing us to extract the oscillation length and thus the heavy neutrino mass difference ΔM_N, as well as a CP-violating Majorana phase.

Aknowledgements

Firstly I would like to thanks the support and kindness of my advisor Gorazd Cvetic who gave me more than "academic guidance" during this time.

I would like to thanks the support and confidence of my family Jilberto Zamora, Juana Saá, Margarita Zamora and Juan Molinari who have believed in my project of become a physicist.

I would like to thanks to my professors at Universidad Técnica Federico Santa María Dr. Sergey Kovalenko, Dr. Alfonso Zerwekh, Claudio Dib Ph.D., Ivan Schmidt Ph.D. for their fruitful discussions and advice and Dr. Carlos Contreras for his advice and friendship.

I would like to thanks to my friends and colleagues from UTFSM, Felipe Rojas, Bastián Díaz, Marcela Gonzalez, Nicolás Neill, Pedro Allendes, Dr. Gastón Moreno, Dr. Cristobal Corral, Dr. Oscar Castillo and to my friends "De la vida" Jorge Reyes, Carlos Silva and Felipe Cubillos.

Finally I would like to thanks "the National Commission for Scientific and Technological Research", CONICYT, Chile. By support the development of this thesis, under the grant No. 21100023.

Contents

Chapter 1

Introduction

Neutrinos are one of the most enigmatic particles in the Standard Model (SM) and their history goes back to 1930 when Wolfang Pauli proposed the existence of one undetectable particle [1] to explain the non-conservation of the energy in beta decay ($n \rightarrow p + e^- + \nu_e$). This hypothetical particle did not have electric charge and had a very small mass, could even be massless. This fact leads to the name *neutrino*, which mean *small neutron* in Italian. Twenty-six years after the Pauli prediction, Cowan and Reines [2] discovered the first neutrinos (actually they discovered electron antineutrino $\overline{\nu_e}$) , produced in Savannah River nuclear power plant in South Carolina, USA. These neutrinos were created in association with an electron and were detected in the inverse beta decay in which an antineutrino interacts with an atomic nucleus and induces the transformation of a proton into a neutron ($\overline{\nu_e} + p \rightarrow n + e^+$).

Six years later in 1962, Leon Max Lederman, Melvin Schwartz and Jack Steinberger discovered a new type of neutrino [3], this time associated with the muon (the muon neutrino ν_μ). Finally, in 2000 the DONUT collaboration in FERMILAB, found a neutrino associated with the tau lepton (the tau neutrino ν_τ).

Up to date we know that neutrinos are extremely abundant in the Universe and continually pass through the Earth. They come from different sources such as fusion reactions in the Sun, the interaction of cosmic rays with the atmosphere, radioactivity of the Earth and also in nuclear power plant. It is believed that very low energy neutrinos from the Big Bang exist in the Universe, although it has still not been possible to experimentally detect them in a direct way. Since neutrinos hardly interact with matter, they are very difficult to detect. Billions of neutrinos pass through our body every second without leaving a trace, but every now and then one of them will end up interacting with an atom of our body. Current particle detectors are not suited for directly detecting neutrinos because the latter are not sensitive to the electromagnetic field. However, neutrinos can interact (be absorbed) with a nucleon producing a charged lepton, or scatter from an electron. In both cases, the products can be detected.

Toward the end of the 20th century, a deficit was observed with respect to the predictions in the flux of electron neutrinos coming from the Sun and in the muon neutrinos produced in the atmosphere, this was a mystery that lasted 30 years. The disappearance of neutrinos was verified much later in neutrinos produced in nuclear reactors and particle accelerators. The result could be explained by the phenomenon that today we call *oscillations* [4–7].
Oscillation means that a neutrino created with a specific lepton flavor (e, μ or τ) can later be measured having a different flavor, this was experimentally demonstrated for the first time by the Super-Kamiokande (SK) experiment. This detector, a 50,000 ton water tank located 1000 m underground in a mine in Japan, was able to demonstrate that atmospheric neutrinos on their way through the Earth, are transformed from muon neutrinos into tau neutrinos. SK measured a deficit of muon neutrinos with respect to those expected based on the distance traveled and the neutrino energy, unambiguously proving that neutrinos oscillate. This ca-

pacity of transmutation between families of neutrinos is only possible, according to quantum mechanics, if neutrinos are massive particles, but it is in contradiction with the Standard Model (SM), which assumes that neutrinos are massless. Neutrino masses are smaller than 1 eV. If these light masses are produced via a seesaw [8–11] or related mechanism, then the existence of significantly heavier neutrinos is expected.

Neutrinos are detected via weak interactions and in these participate the neutrinos ν_e, ν_μ and ν_τ, called flavor eigenstates and they are not mass eigenstates. Any measurement that involves neutrinos is quite complicated, but the measurement of their masses is perhaps the hardest, because they have extremely small masses.

In oscillation experiments it is not possible to get information about the absolute value of neutrino mass since the probability of one type of neutrino oscillating to another is a function of the difference between their squared masses. The effects of the neutrino mass itself can be observed in phenomena such as weak nuclear and particle decays, in which the energy and momentum of the decay products depend on the neutrino mass. These methods are called direct, because the only physical requirement is that the neutrino has finite mass; up to now they have only managed to set upper limits on the neutrino mass. On the other hand, there are various other experiments that can indirectly get information of neutrinos since the amplitude of their process depends on the value of the neutrino mass and also on the other properties that are not predicted by the SM. The most promising are the neutrinoless double beta decay ($0\nu\beta\beta$) [12–19], and rare meson decays [20–27], in most cases these processes are possible if the neutrino is a Majorana particle (i.e., if neutrino and antineutrino are the same particle), it is still unknown whether neutrinos are Majorana ($\overline{\nu} = \nu$) or Dirac particles ($\overline{\nu} \neq \nu$).

Among the principal tasks in neutrino physics are the ascertainment of the nature of the neutrino mass (Dirac or Majorana) and the CP violation in the neutrino sector. If neutrinos are Dirac particles, they must have right-handed electroweak singlet components in addition to the known left-handed ν_e, ν_μ and ν_τ; in such case lepton number remains as a conserved quantity. Alternatively, if they are Majorana particles (as required for $0\nu\beta\beta$ and semihadronic rare meson decay), the lepton number in the reactions involving them may be violated. There is a possibility of CP violation in the neutrino sector, both if neutrinos are Dirac or Majorana particles CP violations in the neutrino sector is important for baryon number asymmetry of the universe.

In this thesis, we investigate the possibility of measuring the CP asymmetry in decays of pseudo-scalar mesons (π, K, D, D_s, B, B_c). The CP violation in the neutrino sector can be measured by neutrino oscillations [28]. However, here we consider a scenario in which CP violation of the neutrino sector can be measured by investigating rare meson decays, i.e; decays mediated by (on-shell) neutrino exchange.
We consider scenarios that include two additional, sterile, almost degenerate neutrinos N_j ($j = 1, 2$) with masses in the range $M_N \sim 0.1 - 6$ GeV. Such neutrinos are predicted in low scale seesaw scenarios [29–31].

We note that the model νMSM [29–31] proposes two almost degenerate Majorana neutrinos with mass between 100 MeV and a few GeV, in addition to a light Majorana neutrino of mass $\sim 10^2$ keV. The existence of such neutrinos with CP violation is strongly significant, because it can explain simultaneously the baryon asymmetry of the Universe, the pattern of light neutrino masses and oscillations, and can provide a dark matter candidate, cf. Ref [32–34] for a review.

The requirement that the lightest sterile neutrino be the dark matter candidate reduces the parameters of the model in such a way as to make the two heavier neutrinos nearly degenerate in mass. Recently CERN-SPS has proposed a search of such heavy neutrinos, Ref. [35], in the decays of D_s mesons. We are interested in the question if in such models the CP violation can be detected in rare mesons decays and if it cover the parameter space favored by theoretical models.

We investigated the possibility of measuring the CP asymmetry in the rare leptonic decays of charged pions $\pi^\pm \to e^\pm e^\pm \mu^\mp \nu$ and in rare semihadronic decays of charged pseudoscalar mesons $M^\pm \to \ell_1^\pm \ell_2^\pm M'^\mp$, where $M = K, D, D_s, B, B_c$ and $M' = \pi, K, D, D_s$, and the charged leptons are $\ell_1, \ell_2 = e, \mu$. We focus on signals of CP violation in such processes, working in scenarios with two on-shell sterile neutrinos N_1 and N_2.

In the leptonic decay the relevant processes are the lepton number conserving (LC) processes $\pi^\pm \to e^\pm N_j \to e^\pm e^\pm \mu^\mp \nu$ where $\nu = \nu_e$ for π^+ and $\nu = \bar{\nu}_e$ for π^-; and the lepton number violating (LV) processes, where $\nu = \nu_\mu$ if the N_j neutrinos are Dirac, only LC decays contribute; if they are Majorana, both LC and LV decays contribute. In the rare semihadronic decays only the lepton number violating (LNV) processes take part, thererefore, the neutrinos mediating them must be of Majorana type.

In Chapter 2 we present the relevant formulas and concepts which are used in this thesis. In Chapter 3 we outline the formalism and results of the calculation of the various leptonic decay widths, branching ratios and CP asymmetries. The details of the calculation are given in Appendices A and D. In Chapter 4 we present the same analysis as in Chapter 3, but this time for rare semihadronic decays adding estimation of the possibilities to detect the CP asymmetries in future experiments as SHiP [36], and the details of the calculation are given in Appendix E. In Chapter 5 we discuss neutrino oscillations in semihadronics decays of heavy pseudoscalar mesons (such as B, B_C, D_S) mediated by two on-shell Majorana neutrinos, and in Appendix F we show the consistency of the oscillation amplitude method applied. In Chapter 6 we summarize the conclusions of this thesis.

Chapter 2

Some Useful Remarks About Majorana and Dirac Neutrinos.

In this chapter we shall present some relevant and useful definitions which we shall use in this thesis. Some points that we shall present here have not a fundamental role in neutrino physics, but are very helpful to improve our understanding about it and the processes involved in it.

2.1 Dirac and Majorana Fields

To understand the differences between the Dirac and Majorana particles it is instructive to look at the expansion of their quantum field in terms of the plane-wave modes. For a Dirac field the expansion has the form [37]:

$$\psi(x)^D = \int \frac{d^3p}{(2\pi)^3\sqrt{2E_p}} \sum_{s=\pm\frac{1}{2}} \left[b_s(\mathbf{p})u_s(\mathbf{p})e^{-ipx} + d_s^\dagger(\mathbf{p})v_s(\mathbf{p})e^{ipx}\right] \tag{2.1}$$

where $u_s(\mathbf{p})$ and $v_s(\mathbf{p})$ are the positive and negative energy solutions of the Dirac equation in the momentum space, respectively. The operators $b_s(\mathbf{p})$ and $d_s^\dagger(\mathbf{p})$ are the annihilation operator for the particle and the creation operator for the antiparticle, respectively.
Majorana fields have to satisfy an extra contidion, given by:

$$(\psi(x)^M)^c = \psi(x)^M \tag{2.2}$$

If we impose the condition (2.2) in Eq. (2.1), we get a Majorana field:

$$\psi(x)^M = \int \frac{d^3p}{(2\pi)^3\sqrt{2E_p}} \sum_{s=\pm\frac{1}{2}} \left[b_s(\mathbf{p})u_s(\mathbf{p})e^{-ipx} + b_s^\dagger(\mathbf{p})v_s(\mathbf{p})e^{ipx}\right] \tag{2.3}$$

Comparing Eqs. (2.1) and (2.3), we see that, while in the Dirac field the difference between particle and anti-particle is present, this difference dissapears in the Majorana case.

Eqs. (2.1) and (2.3) are presented sometimes with a phase factor λ in front of the creation operators [38]. Here we choose $\lambda = 1$, as in [39].

2.2 Neutrino Mixing Matrix

Neutrino oscillation leads to the conclusion that neutrinos are massive particles. Furthermore, in the electroweak interaction (SM interaction lagrangian) participate flavor states (ν_e, ν_μ, ν_τ) which are mixtures of left-handed components of the neutrino fields with definite masses (ν_i). Some extensions [29–34] of the SM include sterile neutrinos (N_ℓ) which have no interaction with charged leptons of SM.
As a result, we have additional neutrinos (N_k) which have a definite (higher) mass and are mostly made of sterile neutrinos (N_ℓ). Then the usual neutrino flavor fields ν_ℓ ($\ell = e, \mu, \tau$) are:

$$\nu_\ell = \sum_{i=1}^{3} B_{\ell\nu_i}\nu_i + (B_{\ell N_1}N_1 + B_{\ell N_2}N_2 + ... + B_{\ell N_k}N_k + ... + B_{\ell N_n}N_n) \ , \tag{2.4}$$

where ν_i ($i = 1, 2, 3$) are the light mass eigenstates, N_k are the heavier mass eigenstates, and the (unitary) PMNS matrix B is in this scenario a $(3 + n) \times (3 + n)$ matrix.

The B matrix is unitary and the number of its independent parameters depends on the neutrino nature (Dirac or Majorana) [39]. We can divide the parameters in two categories, "real parameters" or angles, and "complex parameters" or phases. While the angles do not depend on the neutrino nature, the phases do.

The number n_θ of angles in a $(\omega \times \omega)$ B matrix is:

$$n_\theta = \frac{\omega(\omega - 1)}{2} \tag{2.5}$$

The number of physical phases n_ϕ in a $(\omega \times \omega)$ B matrix are; for the case of Dirac and Majorana neutrinos, respectively

$$n_\phi^D = \frac{(\omega - 1)(\omega - 2)}{2} \quad ; \quad n_\phi^M = \frac{\omega(\omega - 1)}{2} \tag{2.6}$$

In this thesis we are interested in the case when at least two sterile neutrinos are added. Then, our relevant electroweak flavor states are

$$\nu_\ell = \sum_{k=1}^{3} B_{\ell\nu_k}\nu_k + (B_{\ell N_1}N_1 + B_{\ell N_2}N_2) \ , \tag{2.7}$$

where $B_{\ell\nu_k}$ is the PMNS mixing matrix [40]. We shall refer here even to the extended B matrix (with B_{eN1}, B_{eN2}) as the PMNS mixing matrix.

As a final comment, we mention that B matrix is an object of central interest for theoreticians and experimentalist, because it is a source of CP violation in the neutrino sector and it is the responsable for the strong suppression in the interaction between active and sterile neutrinos.

2.3 Neutrinos and Neutral Current Interaction

In the standard model (SM), neutrinos interact by means of weak interaction. While the charged current (CCI) can distinguish the nature of neutrinos, the neutral current interaction (NCI) can not distinguish between Majorana and Dirac neutrinos (in the relativistic limit). In this section we shall explain why, and we shall present a example to clarify this fact.

As we know, neutrinos are fermions and any fermion fields anticommute:

$$\overline{\nu}\gamma_\mu\nu = -\overline{\nu^c}\gamma_\mu\nu^c \tag{2.8}$$

The Equation (2.8) is valid for Dirac and Majorana fermions (e.g. the vector current of positron is opposite to the vector current of electron). As we wrote in Eq. (2.2), Majorana particle must satisfy the condition $(\nu^M)^c = \nu^M$, therefore Eq. (2.8) has an inconsistency unless $\overline{\nu^M}\gamma_\mu\nu^M = 0$. This fact means: The vector current of a Majorana fermion is zero.
The only contribution of a Majorana neutrino to the NCI is the axial-vector current $\overline{\nu^M}\gamma_\mu\gamma_5\nu^M$.

In order to get the matrix elements, we have to perform the Wick contraction between NCI $\overline{\nu^M}\gamma_\mu\gamma_5\nu^M$ and the final and initial states $|\nu_f^M\rangle$, $|\nu_i^M\rangle$, respectively.

$$\langle\nu_f^M|\overline{\nu^M}\gamma_\mu\gamma_5\nu^M|\nu_i^M\rangle = -2\ \overline{u_f}\gamma_\mu\gamma_5 u_i \tag{2.9}$$

Majorana neutrinos can be contracted with both initial and final states; for this reason we have a factor two in front of Eq. (2.9).

Besides, the matrix elements for Dirac neutrinos is:

$$\langle\nu_f^D|\overline{\nu^D}\gamma_\mu(1-\gamma_5)\nu^D|\nu_i^D\rangle = \overline{u_f}\gamma_\mu(1-\gamma_5)u_i \tag{2.10}$$

From quantum field theory we know that massive neutrinos (fermions) [37] obey :

$$\gamma_5\ \nu = h\ \nu + \mathcal{O}\left(\frac{M_\nu}{E_\nu}\right)\nu, \tag{2.11}$$

where h is the helicity operator. In a neutrino experiment, the neutrino beam is left-handed ($h\ \nu = -\nu$) [38] and relativistic ($\frac{M_\nu}{E_\nu} \to 0$) , therefore, the second term at the right side in Eq. (2.11) disappears and this leads to:

$$-\ 2\ \overline{u}_f\gamma_\mu\gamma_5 u_i = \overline{u}_f\gamma_\mu(1-\gamma_5)u_i \tag{2.12}$$

Equation (2.12) shows that there is no difference between the neutral current matrix elements for Majorana and Dirac neutrino in the relativistic limit.

2.3.1 A Short Exanple: The Neutrino Decay

Here we shall present a short example where Eqs. (2.9) and (2.10) manifest themselves in the relativistic limit.
We are interested in the neutrino (Dirac or Majorana) decay mediated by Z boson, as shown in figure 2.1.

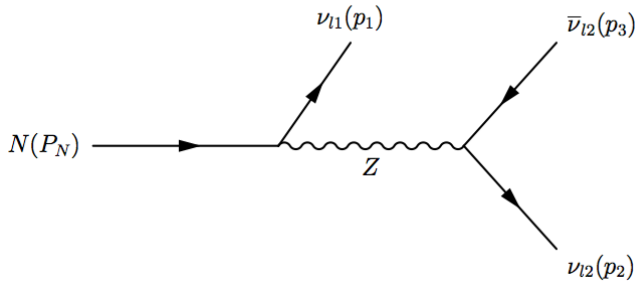

Figure 2.1: *Feynman Diagram for Netrino (N) Decay into three light neutrinos (ν_l), mediated by Z Boson.*

The differential of the decay width in the neutrino (N) rest frame, is given by:

$$d\Gamma = \frac{1}{2M_N}\left(\prod_f \frac{d^3p_f}{(2\pi)^3 2E_f}(2\pi)^4|\mathcal{M}_{fi}|^2\ \delta^4(P_N - \sum p_f)\right), \tag{2.13}$$

where M_N is the neutrino mass, $|\mathcal{M}_{fi}|^2$ is the square of the reduce matrix element, and E_f are the energies of the final state particles.

Majorana Neutrino Decay

In order to obtain the decay width, we have to divide the problem in two scenarios:

- Scenario 1, when $l1 = l2$: this provide a symmetry factor 1/3! in front of the decay width, because we cannot distinguish between the frees neutrinos and anti-neutrinos in the final state.

- Scenario 2, when $l1 \neq l2$: this provide a symmetry factor 1/2! in front of the decay width, here we can distinguish the flavors, but we can't distinguish neutrino and anti-neutrino.

Taking into account both scenarios, we get a general expresion for the decay width:

$$\Gamma^M(N \to \nu_{l1}\nu_{l2}\overline{\nu}_{l2}) = \frac{1}{3!}\,\Gamma^M(N \to \nu_e\nu_e\overline{\nu}_e) + \frac{1}{2!}\,\Gamma^M(N \to \nu_e\nu_\mu\overline{\nu}_\mu) + \frac{1}{2!}\,\Gamma^M(N \to \nu_e\nu_\tau\overline{\nu}_\tau)$$
$$+ \frac{1}{2!}\,\Gamma^M(N \to \nu_\mu\nu_e\overline{\nu}_e) + \frac{1}{3!}\,\Gamma^M(N \to \nu_\mu\nu_\mu\overline{\nu}_\mu) + \frac{1}{2!}\,\Gamma^M(N \to \nu_\mu\nu_\tau\overline{\nu}_\tau)$$
$$+ \frac{1}{2!}\,\Gamma^M(N \to \nu_\tau\nu_e\overline{\nu}_e) + \frac{1}{2!}\,\Gamma^M(N \to \nu_\tau\nu_\mu\overline{\nu}_\mu) + \frac{1}{3!}\,\Gamma^M(N \to \nu_\tau\nu_\tau\overline{\nu}_\tau) \tag{2.14}$$

Taking into account the relativistic limit ($m_{\nu e} = m_{\nu\mu} = m_{\nu\tau} = 0$), we get for the partial decay width:

$$\Gamma^M_{(l1\neq l2)} = |B_{lN}|^2\,\frac{G_F^2 M_N^5}{192\pi^3} \qquad ; \qquad \Gamma^M_{(l1=l2)} = |B_{lN}|^2\,\frac{G_F^2 M_N^5}{32\pi^3}, \tag{2.15}$$

where G_F is the Fermi constant and B_{lN} is the mixing between active and sterile neutrino presented in Eq. (2.7). Finally the total decay width for a Majorana neutrino, is given by:

$$\Gamma^M(N \to \nu_{l1}\nu_{l2}\overline{\nu}_{l2}) = \sum_{l=e,\mu,\tau} |B_{lN}|^2\,\frac{G_F^2 M_N^5}{96\pi^3} \tag{2.16}$$

Dirac Neutrino Decay

In the Dirac neutrino decay we shall divide the problem in two scenarios, again, but this time we shall have some differences with the Majorana neutrino case:

- Scenario 1, when $l1 = l2$: this provide a symmetry factor $1/2!$ in front of the decay width, for Dirac particle we can distinguish between neutrino and anti-neutrino, so we have a symmetry factor only due to $l1 = l2$.
- Scenario 2, when $l1 \neq l2$: we don't have a symmetry factor.

Taking into account both scenarios, we get a general expresion for the decay width:

$$\Gamma^D(N \to \nu_{l1}\nu_{l2}\overline{\nu}_{l2}) = \frac{1}{2!}\,\Gamma^D(N \to \nu_e\nu_e\overline{\nu}_e) + \Gamma^D(N \to \nu_e\nu_\mu\overline{\nu}_\mu) + \Gamma^D(N \to \nu_e\nu_\tau\overline{\nu}_\tau)$$
$$+ \Gamma^D(N \to \nu_\mu\nu_e\overline{\nu}_e) + \frac{1}{2!}\,\Gamma^D(N \to \nu_\mu\nu_\mu\overline{\nu}_\mu) + \Gamma^D(N \to \nu_\mu\nu_\tau\overline{\nu}_\tau)$$
$$+ \Gamma^D(N \to \nu_\tau\nu_e\overline{\nu}_e) + \Gamma^D(N \to \nu_\tau\nu_\mu\overline{\nu}_\mu) + \frac{1}{2!}\,\Gamma^D(N \to \nu_\tau\nu_\tau\overline{\nu}_\tau) \tag{2.17}$$

In the relativistic limit ($m_{\nu e} = m_{\nu \mu} = m_{\nu \tau} = 0$), we get, this time for Dirac neutrinos:

$$\Gamma^{D}_{(l1 \neq l2)} = |B_{lN}|^2 \, \frac{G_F^2 M_N^5}{384 \pi^3} \qquad ; \qquad \Gamma^{D}_{(l1 = l2)} = |B_{lN}|^2 \, \frac{G_F^2 M_N^5}{96 \pi^3} \tag{2.18}$$

therefore, the total decay width for a Dirac neutrino, is given by:

$$\Gamma^{D}(N \to \nu_{l1} \nu_{l2} \overline{\nu}_{l2}) = \sum_{l=e,\mu,\tau} |B_{lN}|^2 \, \frac{G_F^2 M_N^5}{96 \pi^3} \tag{2.19}$$

We see that there are no differences between Eqs (2.16) and (2.19), this is a clear manifestation of the aspects discussed in Sec.2.3 in Eq. (2.12).

Chapter 3

The Rare $\pi^{\pm} \to e^{\pm}e^{\pm}\mu^{\mp}\nu$ Leptonic Decay

We shall consider first the rare pion decay $\pi^+ \to e^+e^+\mu^-\nu_e$ mediated by exchange of neutrinos, with a view to construct a CP-violating asymmetry involving this decay and its charge-conjugate partner decay $\pi^- \to e^-e^-\mu^+\nu_e$.

The rare leptonic pion decay $\pi^+ \to e^+e^+\mu^-\nu_e$ happens by means of two different diagrams (t-channel and s-channel). The literature [41] show that the t-channel is in general suppressed by an order of magnitude, due to this fact we shall concentrate only on the s-channel. This Section is based mainly on our work [42] (see also [43])

Further, if the exchange neutrino in the s-channel is on-shell, this channel dominates over the t-channel by many orders of magnitude. The process can occur via a Majorana neutrino, violating the lepton number (LV) by two units ($\Delta l = 2$) or via a Dirac neutrino conserving the lepton number (LC), but violating the lepton flavor. The s-channel has two contributions, these contributions are: direct-channel and crossed-channel.

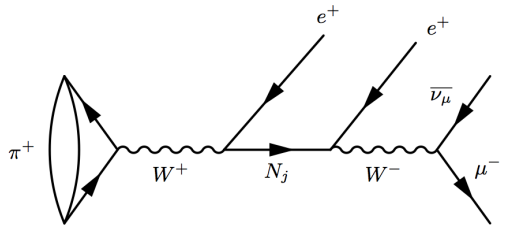

FIGURE 3.1: *Direct Channel of (LV) Decay*

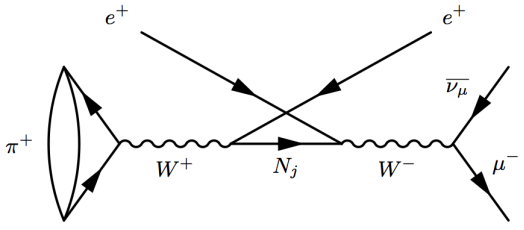

FIGURE 3.2: *Crossed Channel of (LV) Decay*

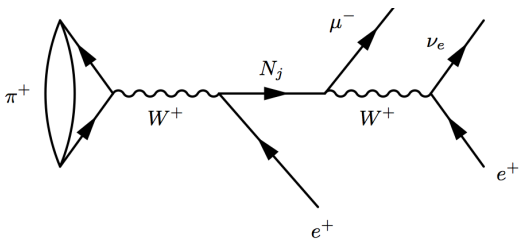

FIGURE 3.3: *Direct Channel of (LC) Decay*

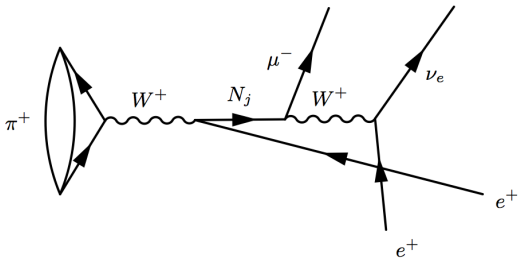

FIGURE 3.4: *Crossed Channel of (LC) Decay*

In this chapter we shall study an extensive range [0.01-6.3] GeV of neutrino mass, passing through off-shell and on-shell regions.

3.1 The Formalism for the rare leptonic pion decay

First we present the formalism for the decays $\pi^+ \to e^+e^+\mu^-\nu$ where the intermediate neutrinos can be on-shell or off-shell.

In order to keep an easy notation from now on, unless otherwise stated, we shall use the simplified notations of some relevant parameters, involved in this rare decay:

$$\Gamma^{(X)}(\pi^{\pm}) \equiv \Gamma^{(X)}(\pi^{\pm} \to e^{\pm}e^{\pm}\mu^{\mp}\nu) \ , \quad (\mathrm{X} = \mathrm{LNV} = \mathrm{LV};\ \mathrm{X} = \mathrm{LNC} = \mathrm{LC}) \ . \tag{3.1}$$

The decay widths $\Gamma^{(X)}(\pi^{\pm})$ can be written in the form

$$\Gamma^{(X)}(\pi^{\pm}) = \frac{1}{2!}\frac{1}{2M_{\pi}}\frac{1}{(2\pi)^8}\int d_4\ |\mathcal{T}^{(X)}(\pi^{\pm})|^2 \ , \tag{3.2}$$

where $1/2!$ is the symmetry factor due to two final state electrons, and d_4 denotes the integration over the 4-particle final phase space.

$$d_4 = \left(\prod_{j=1}^{2}\frac{d^3\vec{p}_j}{2E_e(\vec{p}_j)}\right)\frac{d^3\vec{p}_{\mu}}{2E_{\mu}(\vec{p}_{\mu})}\frac{d^3\vec{p}_{\nu}}{2|\vec{p}_{\nu}|}\delta^{(4)}\left(p_{\pi} - p_1 - p_2 - p_{\mu} - p_{\nu}\right) \ , \tag{3.3}$$

and we denoted by p_1 and p_2 the momenta of $e^{\pm}$ from the left and the right vertex of the direct channels, respectively (and for the crossed channels just the opposite). The squared matrix element $|\mathcal{T}^{(X)}(\pi^{\pm})|^2$ in Eq. (3.2) is a combination of contributions from $N_1, N_2, ..., N_n$ (n: number of sterile neutrinos) and from the two channels D (direct) and C (crossed).

$$\begin{aligned}
|\mathcal{T}^{(X)}(\pi^+)|^2 &= K_{\pi}^2\sum_{i=1}^{n}\sum_{j=1}^{n}k_i^{(X)*}k_j^{(X)} \\
&\times\Big[P_i^{(X)}(D)P_j^{(X)}(D)^*T^{(X)}(DD^*) + P_i^{(X)}(C)P_j^{(X)}(C)^*T^{(X)}(CC^*) \\
&+\Big(P_i^{(X)}(D)P_j^{(X)}(C)^*T_+^{(X)}(DC^*) + P_i^{(X)}(C)P_j^{(X)}(D)^*T_+^{(X)}(CD^*)\Big)\Big], \qquad (3.4a) \\
|\mathcal{T}^{(X)}(\pi^-)|^2 &= K_{\pi}^2\sum_{i=1}^{n}\sum_{j=1}^{n}k_i^{(X)}k_j^{(X)*} \\
&\times\Big[P_i^{(X)}(D)P_j^{(X)}(D)^*T^{(X)}(DD^*) + P_i^{(X)}(C)P_j^{(X)}(C)^*T^{(X)}(CC^*) \\
&+\Big(P_i^{(X)}(D)P_j^{(X)}(C)^*T_-^{(X)}(DC^*) + P_i^{(X)}(C)P_j^{(X)}(D)^*T_-^{(X)}(CD^*)\Big)\Big], \qquad (3.4b)
\end{aligned}$$

where

$$K_{\pi}^2 = G_F^4 f_{\pi}^2 |V_{ud}|^2 \approx 2.983 \times 10^{-22}\ \mathrm{GeV}^{-6} \ , \tag{3.5}$$

and we have used the following notation for the N_j propagators of the direct and crossed

channels:

$$P_j^{(LC)}(D) = \frac{1}{\left[(p_\pi - p_1)^2 - M_{N_j}^2 + i\Gamma_{N_j} M_{N_j}\right]},\ P_j^{(LV)}(D) = M_{N_j} P_j^{(LC)}(D), \tag{3.6a}$$

$$P_j^{(LC)}(C) = \frac{1}{\left[(p_\pi - p_2)^2 - M_{N_j}^2 + i\Gamma_{N_j} M_{N_j}\right]},\ P_j^{(LV)}(C) = M_{N_j} P_j^{(LC)}(C), \tag{3.6b}$$

and $k_j^{(X)}$ represent the combinations of the corresponding heavy-light mixing elements presented in (2.7):

$$k_j^{(LV)} = B_{eN_j}^2\ , \qquad k_j^{(LC)} = B_{eN_j} B_{\mu N_j}^*\ . \tag{3.7}$$

The expressions for the direct (DD^*), crossed (CC^*) and direct-crossed interference (DC^*, CD^*) elements [$T^{(X)}(DD^*)$, $T^{(X)}(CC^*)$, $T^{(X)}(DC^*)$, $T^{(X)}(CD^*)$] appearing in Eqs. (3.4) are given in Appendix A.

Combining Eqs. (3.2) and (3.4), we obtain

$$\begin{aligned}\Gamma^{(X)}(\pi^+) &= \sum_{i=1}^{n}\sum_{j=1}^{n} k_i^{(X)*} k_j^{(X)} \big[\widetilde{\Gamma}^{(X)}(DD^*)_{ij} + \widetilde{\Gamma}^{(X)}(CC^*)_{ij} \\ &\quad + \widetilde{\Gamma}_+^{(X)}(DC^*)_{ij} + \left(\widetilde{\Gamma}_+^{(X)}(DC^*)_{ji}\right)^* \big]\ , \end{aligned} \tag{3.8a}$$

$$\begin{aligned}\Gamma^{(X)}(\pi^-) &= \sum_{i=1}^{n}\sum_{j=1}^{n} k_i^{(X)} k_j^{(X)*} \big[\widetilde{\Gamma}^{(X)}(DD^*)_{ij} + \widetilde{\Gamma}^{(X)}(CC^*)_{ij} \\ &\quad + \widetilde{\Gamma}_-^{(X)}(DC^*)_{ij} + \left(\widetilde{\Gamma}_-^{(X)}(DC^*)_{ji}\right)^* \big]\ , \end{aligned} \tag{3.8b}$$

Here we denoted the elements $\Gamma^{(X)}(YZ^*)_{ij}$ $(i,j = 1,2,...,n)$ of the decay width matrices $\Gamma^{(X)}(YZ^*)$ $(X = LV, LC;\ Y, Z = D, C)$ as

$$\widetilde{\Gamma}^{(X)}(DD^*)_{ij} = K_\pi^2 \frac{1}{2!}\frac{1}{2M_\pi}\frac{1}{(2\pi)^8}\int d_4\ P_i^{(X)}(D) P_j^{(X)}(D)^*\ T^{(X)}(DD^*)\ , \tag{3.9a}$$

$$\widetilde{\Gamma}^{(X)}(CC^*)_{ij} = K_\pi^2 \frac{1}{2!}\frac{1}{2M_\pi}\frac{1}{(2\pi)^8}\int d_4\ P_i^{(X)}(C) P_j^{(X)}(C)^*\ T^{(X)}(CC^*)\ , \tag{3.9b}$$

$$\widetilde{\Gamma_+}^{(X)}(DC^*)_{ij} = K_\pi^2 \frac{1}{2!}\frac{1}{2M_\pi}\frac{1}{(2\pi)^8}\int d_4\ P_i^{(X)}(D) P_j^{(X)}(C)^*\ T_+^{(X)}(DC^*)\ , \tag{3.9c}$$

$$\widetilde{\Gamma_-}^{(X)}(DC^*)_{ij} = K_\pi^2 \frac{1}{2!}\frac{1}{2M_\pi}\frac{1}{(2\pi)^8}\int d_4\ P_i^{(X)}(D) P_j^{(X)}(C)^*\ T_-^{(X)}(DC^*)\ , \tag{3.9d}$$

On the basis of these expressions, and the expressions in Appendix A, we can see that the following symmetry relations hold between the elements of the decay width matrices:

$$\widetilde{\Gamma}^{(X)}(DD^*)_{ij} = \widetilde{\Gamma}^{(X)}(CC^*)_{ij}\ , \quad \widetilde{\Gamma}^{(X)}(DD^*)_{ji} = \left(\widetilde{\Gamma}^{(X)}(DD^*)_{ij}\right)^*\ , \tag{3.10a}$$

$$\widetilde{\Gamma}^{(X)}(CD^*)_{ij} = \widetilde{\Gamma}^{(X)}(DC^*)_{ji} = \left(\widetilde{\Gamma}^{(X)}(CD^*)_{ji}\right)^*\ . \tag{3.10b}$$

The branching ratios are obtained by dividing the decay widths $\Gamma^{(X)}(YZ^*) = k_i^{(X)*}k_j^{(X)}\widetilde{\Gamma}^X(YZ^*)$ $(X = LV, LC;\, Y, Z = D, C)$ by the total decay width of the charged pion $\Gamma(\pi^+ \to \text{all})$

$$\text{Br}^{(X)}(YZ^*) = \frac{\Gamma^{(X)}(YZ^*)}{\Gamma(\pi^+ \to \text{all})} = \frac{k_i^{(X)*}k_j^{(X)}\widetilde{\Gamma}^X(YZ^*)}{\Gamma(\pi^+ \to \text{all})} \tag{3.11}$$

where

$$\Gamma(\pi^+ \to \text{all}) = 2.529 \times 10^{-17}\ \text{GeV} \approx \frac{1}{8\pi}G_F^2 f_\pi^2 M_\mu^2 M_\pi |V_{ud}|^2 \left(1 - \frac{M_\mu^2}{M_\pi^2}\right)^2 . \tag{3.12}$$

Another important quantity in the evaluations of $\Gamma^{(X)}(YZ^*)$ and $\text{Br}^{(X)}(YZ^*)$ is the total decay width Γ_{N_j} of the intermediate on-shell neutrinos, which for the mass range of interest can be approximated in the following way:

$$\Gamma_{N_j}^{Ma} \approx \widetilde{\mathcal{K}}_j^{Ma}\ \overline{\Gamma}(M_{N_j})\ , \quad \Gamma_{N_j}^{Di} \approx \widetilde{\mathcal{K}}_j^{Di}\ \overline{\Gamma}(M_{N_j}) \tag{3.13}$$

where

$$\overline{\Gamma}(M_{N_j}) \equiv \frac{G_F^2 M_{N_j}^5}{96\pi^3}\ , \tag{3.14}$$

$\Gamma_{N_j}^{(Ma)}$ was defined for Majorana neutrinos, and $\Gamma_{N_j}^{(Di)}$ for Dirac neutrinos.

From now on, all parameter with over-bar represent a quantity without any mixing, dependence, as in Eqs. (3.14).

The factor $\widetilde{\mathcal{K}}_j^T$ $(T = Di, Ma)$, includes the heavy-light mixing factors dependence, from all charged channels and all neutral channels mediated by $W^{\pm}$ and Z bosons, respectively.

We define the factor $\widetilde{\mathcal{K}}_j^T$, as:

$$\widetilde{\mathcal{K}}_j^T(M_{N_j}) \equiv \widetilde{\mathcal{K}}_j^T = \mathcal{N}_{eN_j}^T\ |B_{eN_j}|^2 + \mathcal{N}_{\mu N_j}^T\ |B_{\mu N_j}|^2 + \mathcal{N}_{\tau N_j}^T\ |B_{\tau N_j}|^2)\ , \quad (j = 1, ..., n)\ . \tag{3.15}$$

Here, $\mathcal{N}_{\ell N}(M_N) \equiv \mathcal{N}_{\ell N}$ $(\ell = e, \mu, \tau)$ are the effective mixing coefficients; they are numbers $\sim 10^0$-10^1 which depend on the mass M_N $(N = N_1, N_2, ..., N_n)$ and the nature of the mass term (Dirac or Majorana).

In Appendix B we write down the relevant formulas for the calculation of these coefficients. The results of these calculations are given in Figs. 3.5 and 3.6 , for the relevant neutrino mass interval 0.01 GeV $< M_N <$ 0.5 GeV.

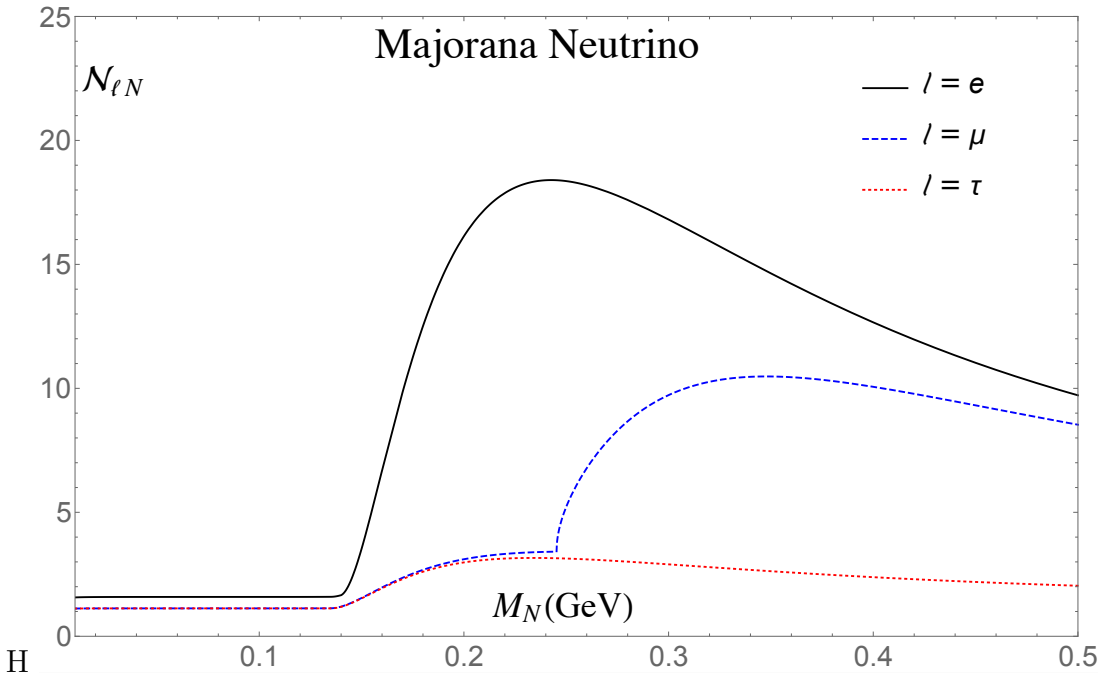

H

Figure 3.5: *The effective mixing coefficients* $\mathcal{N}_{\ell N}^{(LV)}$ $(\ell = e, \mu, \tau)$, *as a function of the mass* M_N *of the Majorana neutrino* N.

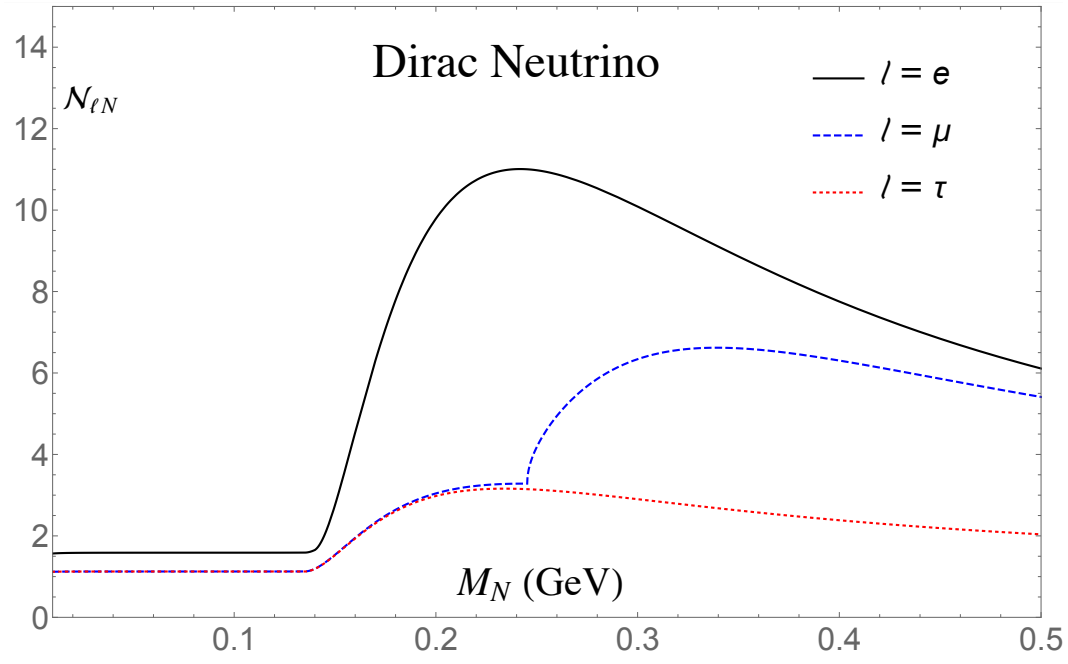

Figure 3.6: *The effective mixing coefficients* $\mathcal{N}_{\ell N}^{(LC)}$ $(\ell = e, \mu, \tau)$, *as a function of the mass* M_N *of the Dirac neutrino* N.

By comparison between Fig. 3.5 and Fig. 3.6, we can infer:

1. There are no differences between $\widetilde{\mathcal{K}}^{Ma}$ and $\widetilde{\mathcal{K}}^{Di}$ in $[0-0.140]$ GeV mass range. This fact is due to the fact that only the neutral current contribution ($N \to \nu_{l1}\overline{\nu}_{l2}\nu_{l2}$) contributes in this mass range, and as we have seen in section 2.3 there are no differences between Dirac and Majorana neutrinos in this decay.

2. The charged current contribution is the clearly dominant contribution to $\widetilde{\mathcal{K}}^{(T)}$ for $M_N > 200$ MeV.

3.2 $\pi^+ \to e^+e^+\mu^-\nu_e$ via one intermediate neutrino

At this point we are interested in determining the branching ratio for $\pi^+ \to e^+e^+\mu^-\nu_e$ via one intermediate neutrino ($n = 1$) in a M_{N1} mass range [0.01-6.3] GeV. In order to get the branching ratio, we can divide the M_{N1} mass range in two regions: on-shell and off-shell mass region.

For a scenario with $n = 1$ (one intermediate neutrino) Eqs. (3.9) adopt the following form:

$$\widetilde{\Gamma}^{(LV)}(DD^*)_{11} = K_\pi^2 \frac{1}{2!}\frac{1}{2M_\pi}\frac{1}{(2\pi)^8}\int d_4\ P_1^{(LV)}(D)P_1^{(LV)}(D)^*\ T^{(LV)}(DD^*)\ , \quad (3.16a)$$

$$\widetilde{\Gamma}^{(LV)}(CC^*)_{11} = K_\pi^2 \frac{1}{2!}\frac{1}{2M_\pi}\frac{1}{(2\pi)^8}\int d_4\ P_1^{(LV)}(C)P_1^{(LV)}(C)^*\ T^{(LV)}(CC^*)\ , \quad (3.16b)$$

$$\widetilde{\Gamma}^{(LV)}(DC^*)_{11} = K_\pi^2 \frac{1}{2!}\frac{1}{2M_\pi}\frac{1}{(2\pi)^8}\int d_4\ P_1^{(LV)}(D)P_1^{(LV)}(C)^*\ T_+^{(LV)}(DC^*)\ , \quad (3.16c)$$

here: $T^{(LV)}(DD^*)$, $T^{(LV)}(CC^*)$ and $T^{(LV)}(DC^*)$ are given in Apendix A.

3.2.1 $\pi^+ \to e^+e^+\mu^-\nu_e$ via one on-shell neutrino

In order to have analitical expresion of $\Gamma^{(LV)}(DD^*)$ and $\Gamma^{(LV)}(CC^*)$, and taking into account the limit $\Gamma_{N1} \to +0$, ($\Gamma_{N1} \ll M_{N1}$), we can approximate the propagator in on-shell (0.106 GeV $< M_{N1} < 0.139$ GeV) M_{N1} mass range through the narrow width approximation:

$$P^{(LV)}(D)P^{(LV)}(D)^* = \left|\frac{M_{N1}}{[(p_\pi - p_1)^2 - M_{N1}^2 + i\Gamma_{N1}M_{N1}]}\right|^2 \approx \frac{\pi}{\Gamma_{N1}}\ \delta\left((p_\pi - p_1)^2 - M_{N1}^2\right) \quad (3.17a)$$

$$P^{(LV)}(C)P^{(LV)}(C)^* = \left|\frac{M_{N1}}{[(p_\pi - p_2)^2 - M_{N1}^2 + i\Gamma_{N1}M_{N1}]}\right|^2 \approx \frac{\pi}{\Gamma_{N1}}\ \delta\left((p_\pi - p_2)^2 - M_{N1}^2\right) \quad (3.17b)$$

$$P^{(LC)}(D)P^{(LC)}(D)^* = \left|\frac{1}{[(p_\pi - p_1)^2 - M_{N1}^2 + i\Gamma_{N1}M_{N1}]}\right|^2 \approx \frac{\pi}{\Gamma_{N1}M_{N1}}\ \delta\left((p_\pi - p_1)^2 - M_{N1}^2\right) \quad (3.18a)$$

$$P^{(LC)}(C)P^{(LC)}(C)^* = \left|\frac{1}{[(p_\pi - p_2)^2 - M_{N1}^2 + i\Gamma_{N1}M_{N1}]}\right|^2 \approx \frac{\pi}{\Gamma_{N1}M_{N1}}\ \delta\left((p_\pi - p_2)^2 - M_{N1}^2\right) \quad (3.18b)$$

Here wee see that the most important on-shell efect is reflected in the on-shell "amplification"

factor $((1/\Gamma_{N1}) \propto (1/\widetilde{\mathcal{K}}_1)$. It turns out that in the on-shell M_{N1} mass region the D-C interference contributions are negligible. Therefore, and taking into account the symmetry relations in Eq. (3.10), the resulting decay widths $\Gamma^{(LV)}(\pi^+)$ and $\Gamma^{(LC)}(\pi^+)$ are:

$$\Gamma^{(LV)}(\pi^+) = 2|B_{eN_1}|^4\ \widetilde{\Gamma}^{(LV)}(DD^*)_{11} \tag{3.19a}$$

$$\Gamma^{(LC)}(\pi^+) = 2|B_{eN_1}|^2|B_{\mu N_1}|^2\ \widetilde{\Gamma}^{(LC)}(DD^*)_{11} \tag{3.19b}$$

Where $\widetilde{\Gamma}^{(LV)}_{11}$ and $\widetilde{\Gamma}^{(LC)}_{11}$ are given by:

$$\widetilde{\Gamma}^{(LV)}(DD^*)_{11} = \frac{\overline{\Gamma}(DD^*)_{11}}{\widetilde{\mathcal{K}}_1^{Ma}}\ ; \quad \widetilde{\Gamma}^{(LC)}(DD^*)_{11} = \frac{\overline{\Gamma}(DD^*)_{11}}{\widetilde{\mathcal{K}}_1^{Di}} \tag{3.20}$$

Here $\overline{\Gamma}(DD^*)_{11}$ is the canonical (without mixing factors) decay width and its general expresion is given by:

$$\begin{aligned}\overline{\Gamma}(DD^*)_{jj} &= = \frac{K_\pi^2}{192(2\pi)^4}\frac{M_{N_j}^{11}}{M_\pi^3\ \overline{\Gamma}_{N_j}}\lambda^{1/2}(x_{\pi j},1,x_{ej}) \\ &\quad \times\left[x_{\pi j}-1+x_{ej}(x_{\pi j}+2-x_{ej})\right]\mathcal{F}(x_j,x_{ej}) \quad ,(j=1,...,n)\ ,\end{aligned} \tag{3.21}$$

where we use the notations:

$$\lambda(y_1,y_2,y_3) = y_1^2+y_2^2+y_3^2-2y_1y_2-2y_2y_3-2y_3y_1\ , \tag{3.22a}$$

$$x_{\pi j} = \frac{M_\pi^2}{M_{N_j}^2}\ , \quad x_{ej} = \frac{M_e^2}{M_{N_j}^2}\ , \quad x_j = \frac{M_\mu^2}{M_{N_j}^2}\ , \quad (j=1,...,n)\ , \tag{3.22b}$$

and the function $\mathcal{F}(x_j,x_{ej})$ is given in Appendix A [Eq. (A.5)] where the derivation of this expression (3.21) is given. When $M_e=0$, the results acquires a simpler form:

$$\lim_{M_e\to 0}\Gamma^{(X)}(DD^*)_{jj} = \frac{K_\pi^2}{192(2\pi)^4}\frac{M_{N_j}^{11}}{\overline{\Gamma}_{N_j}\ M_\pi^3}(x_{\pi j}-1)^2 f(x_j)\ , \tag{3.23}$$

where the function $f(x_j)=\mathcal{F}(x_j,0)$ is:

$$f(x_j) = 1-8x_j+8x_j^3-x_j^4-12x_j^2\ln x_j\ . \tag{3.24}$$

In the range of masses 0.117 GeV $< M_{N_j} <$ 0.136 GeV the expression (3.23) differs from the exact expression (3.21) [with Eq. (A.5)] by less than one per cent. However, for 0.106 GeV $< M_{N_j} <$ 0.117 GeV and for 0.136 GeV $< M_{N_j} <$ 0.139 GeV the deviation is more than one per cent. For values of M_{N_j} close to the lower on-shell bound $M_\mu + M_e$ ($\approx$ 0.1062 GeV) the deviation is very large and the expression (3.21) [with Eq. (A.5)] must be used instead of Eq. (3.23) for $\Gamma^{(X)}(DD^*)_{jj}$. We shall use the general expression (3.21) unless otherwise stated.

On the other hand, taking into account Eq.(3.15), and for the on-shell regime (0.106 GeV $<$ $M_{N_j} <$ 0.139 GeV) Fig. 3.5 and Fig. 3.6, we can write

$$\widetilde{\mathcal{K}}_1^{Di} = \widetilde{\mathcal{K}}_1^{Ma} = \widetilde{\mathcal{K}}_1 \approx 1.6\,|B_{eN_1}|^2 + 1.1\,|B_{\mu N_1}|^2 + 1.1\,|B_{\tau N_1}|^2 \tag{3.25}$$

Finally, the branching ratio defined in (3.11), for (LV) and (LC) processes in the on-shell mass region, are:

$$\mathrm{Br}^{(LV)}(\pi^+) \;=\; \frac{2|B_{eN_1}|^4\;\overline{\Gamma}(DD^*)_{11}}{\widetilde{\mathcal{K}}_1^{Ma}\;\Gamma(\pi^+ \to \mathrm{all})} = \frac{|B_{eN_1}|^4}{\widetilde{\mathcal{K}}_1}\;\overline{\mathrm{Br}}(\pi^+), \tag{3.26a}$$

$$\mathrm{Br}^{(LC)}(\pi^+) \;=\; \frac{2|B_{eN_1}|^2|B_{\mu N_1}|^2\;\overline{\Gamma}(DD^*)_{11}}{\widetilde{\mathcal{K}}_1^{Di}\;\Gamma(\pi^+ \to \mathrm{all})} = \frac{|B_{eN_1}|^2|B_{\mu N_1}|^2}{\widetilde{\mathcal{K}}_1}\;\overline{\mathrm{Br}}(\pi^+), \tag{3.26b}$$

where $\overline{\mathrm{Br}}(\pi^+) = \frac{2\overline{\Gamma}(DD^*)_{11}}{\Gamma(\pi^+ \to \mathrm{all})}$ is the canonical branching ratio. The on-shell "amplification" factor $1/\widetilde{\mathcal{K}}_1$ ($>> 1$) is manifest here, and the mixing effects are $\sim |B_{\ell N1}|^4/\widetilde{\mathcal{K}}_1 \sim |B_{\ell N1}|^2$.

The future pion factories, among them the Project X at Fermilab, will produce charged pions with lab energies E_π of a few GeV (i.e., the Lorentz time dilation factor $\gamma_\pi \sim 10^1$), and luminosities $\sim 10^{22}$ cm^{-2}s^{-1} [44]. If the beam has 1 cm^2 cross section, then $\sim 10^{29}$ charged pions could be expected per year.

The probability [Eq.C.2] of (on-shell) neutrino N to decay inside a detector of length $L \sim 10^1$ m in such pion factories is:

$$P_N \sim 10^{-3}\;\widetilde{\mathcal{K}}. \tag{3.27}$$

where $\widetilde{\mathcal{K}} \sim \widetilde{\mathcal{K}}_j \propto |B_{\ell N_j}|^2$. We should multiply the obtained branching ratios (3.26) by such acceptance factors P_N to obtain the effective branching ratios.

$$\mathrm{Br}^{(LV)}(\pi^+)^{(eff)} \;\approx\; 10^{-3}\;|B_{eN_1}|^4\;\overline{\mathrm{Br}}(\pi^+) = |B_{eN_1}|^4\;\overline{\mathrm{Br}^{\mathrm{eff}}}(\pi^+) \tag{3.28a}$$

$$\mathrm{Br}^{(LC)}(\pi^+)^{(eff)} \;\approx\; 10^{-3}\;|B_{eN_1}|^2|B_{\mu N_1}|^2\;\overline{\mathrm{Br}}(\pi^+) = |B_{eN_1}|^2|B_{\mu N_1}|^2\;\overline{\mathrm{Br}^{\mathrm{eff}}}(\pi^+) \tag{3.28b}$$

Here $\overline{\mathrm{Br}^{\mathrm{eff}}}(\pi^+)$ is the canonical branching ratio and we present it, for the on-shell mass range in Fig. 3.7.

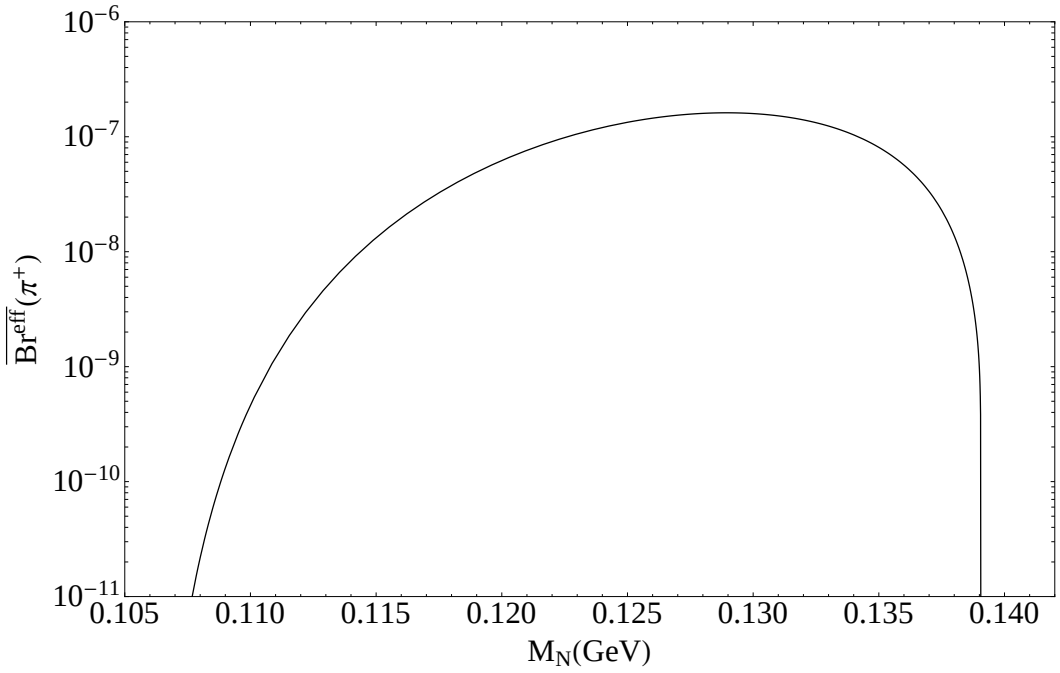

FIGURE 3.7: *The canonical effective branching ratio* $\overline{\mathrm{Br}^{\mathrm{eff}}}(\pi^+)$ *for on-shell* M_{N1} *mass range.*

In order to get an estimate of the magnitude of the effective branching ratios $\mathrm{Br}^{(X)}(\pi^+)^{(eff)}$, we can take into account the limits for $|B_{eN_1}|^2 \leq 10^{-8}$ and $|B_{\mu N_1}|^2 \leq 10^{-6}$ given in [45], and draw a plot for these in Fig. 3.8.

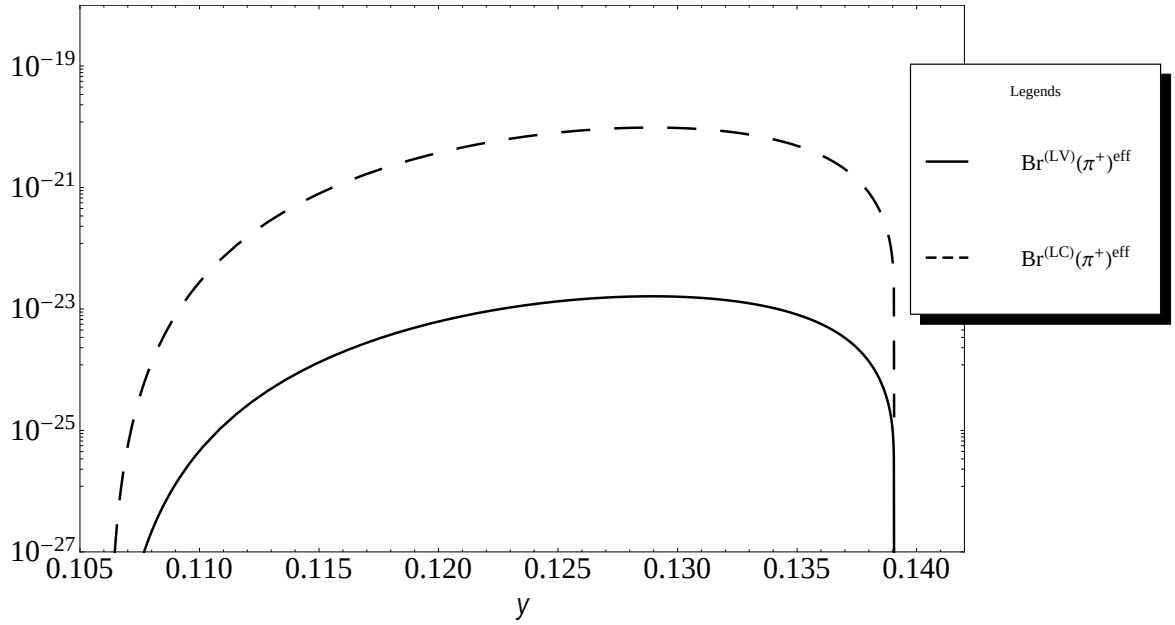

FIGURE 3.8: *The LV and LC canonical effective branching ratios for on-shell* M_{N1} *mass range.*

3.2.2 $\pi^+ \to e^+e^+\mu^-\nu_e$ via one off-shell neutrino

In the off-shell M_{N1} mass region the same expressions (3.16) as in the on-shell mass region are valid, however this time, the identities (3.10) are not valid. Then, all the integrations over the final particle phase space must be performed numerically. There is no on-shell "amplification" factor $(1/\widetilde{\mathcal{K}}_1)$ anymore. Once having implemented and finished the numerical calculations, we have clear indication of:

- There is no dependence of the neutrino decay width (Γ_N) in the off-shell mass regions, in contrast with $1/\Gamma_N$ $(\propto 1/\widetilde{\mathcal{K}}_1)$ dependence in the on-shell case.
- The D-C interference terms are not negligible, these contributions even have the same order of magnitude as DD and CC contributions.

All the numerical calculation was implemented by two differents codes, one of them in Mathematica and the other one in Vegas (Fortran).

The results of $\overline{\text{Br}^{\text{eff}}}(\pi^+)$ in the complete mass range (including the on-shell and off-shell mass region), are presented in Fig.3.9:

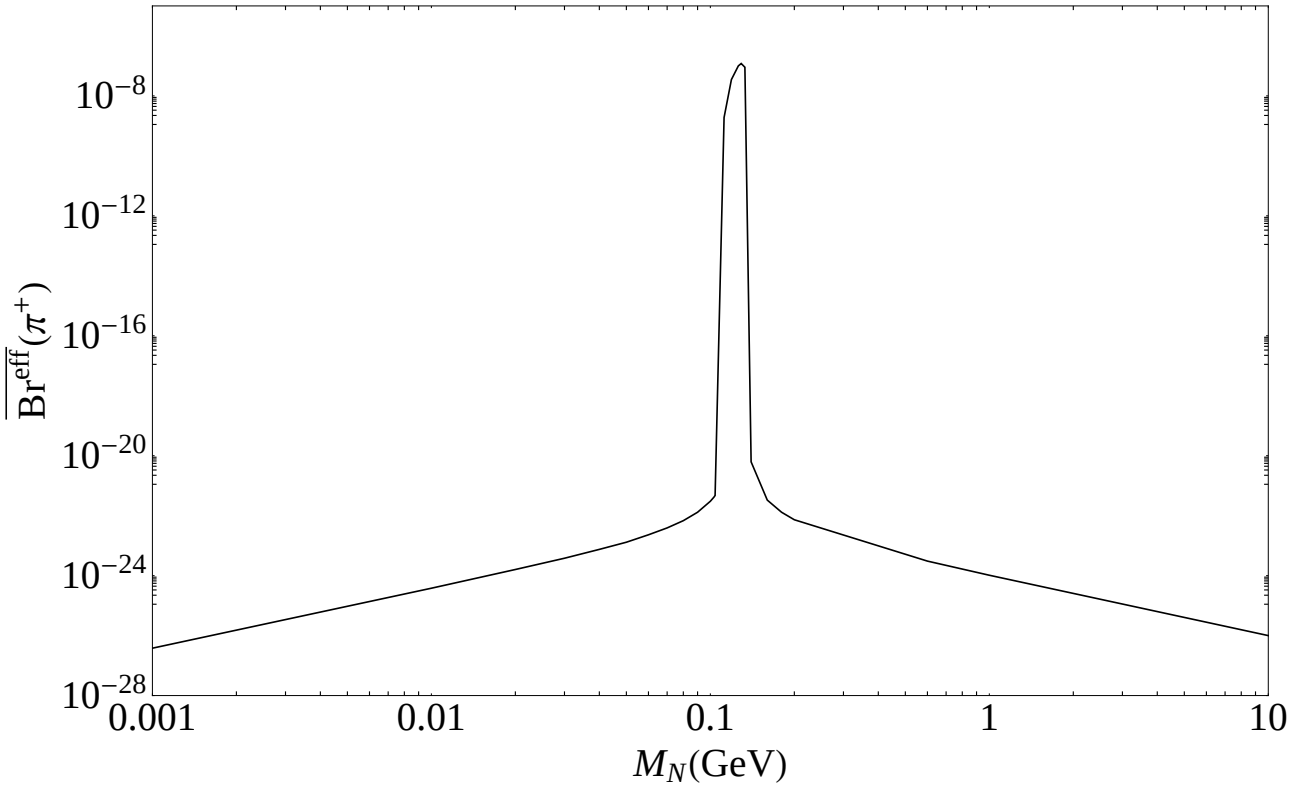

Figure 3.9: *The effective branching ratio, when one intermediate Majorana neutrino is exchanged.*

In Fig.3.9 we can distinguish clearly the two mass regions. While the on-shell mass region corresponds to a big peak around $106-139$ MeV $\overline{\text{Br}^{\text{eff}}}(\pi^+)$ decreases very quickly and by many orders of magnitude as we move away from the on-shell region.

3.3 The branching ratio and CP asymmetry of $\pi^{\pm} \to e^{\pm}e^{\pm}\mu^{\mp}\nu$ through two on-shell intermediate neutrinos.

This section is based mainly in our work [42] and we shall use the results of the previous Section to obtain the results for the branching ratios $\mathrm{Br}_{\pm}^{(X)}$ $(X = LV, LC)$ and the CP asymmetries $A_{CP}^{(Y)}$ $(Y = Di, Ma)$ of $(\pi^+ \to e^+ N_j \to e^+\mu^-\nu)$ through two on-shell intermediate neutrinos $(j = 2)$.

$$\mathrm{Br}_{\pm}^{(X)} = \frac{S_{\pm}^{(X)}(\pi)}{\Gamma(\pi^- \to \mathrm{all}) + \Gamma(\pi^+ \to \mathrm{all})} \approx \frac{\Gamma^{(X)}(\pi^-) \pm \Gamma^{(X)}(\pi^+)}{2\,\Gamma(\pi^+ \to \mathrm{all})}\ , \tag{3.29a}$$

$$\mathcal{A}_{\mathrm{CP}}^{(\mathrm{Y})} = \frac{\mathrm{Br}_{-}^{(\mathrm{Y})}}{\mathrm{Br}_{+}^{(\mathrm{Y})}} \equiv \frac{\Gamma^{(Y)}(\pi^-) - \Gamma^{(Y)}(\pi^+)}{\Gamma^{(Y)}(\pi^-) + \Gamma^{(Y)}(\pi^+)}, \tag{3.29b}$$

where we note that $\Gamma^{Di}(\pi^{\pm}) = \Gamma^{LC}(\pi^{\pm})$ and $\Gamma^{Ma}(\pi^{\pm}) = \Gamma^{LC}(\pi^{\pm}) + \Gamma^{LV}(\pi^{\pm})$.

The total branching ratio and the total asymmetry are $\mathrm{Br} = \mathrm{Br}^{(LV)} + \mathrm{Br}^{(LC)}$ and $A = A^{(\mathrm{LV})} + A^{(LC)}$ when N_j are Majorana neutrinos, and $\mathrm{Br} = \mathrm{Br}^{(LC)}$ and $A = A^{(LC)}$ when N_j are Dirac neutrinos. As we shall see, for $\mathcal{A}_{\mathrm{CP}}^{(\mathrm{Y})}$ to be appreciable nonzero, we shall need at least two on-shell neutrinos N_j $(j = 1, 2)$ which should be almost mass degenerate. From now on, we assume that have two on-shell neutrinos. It is useful to introduce the phase conventions of the book Ref. [39] related with the heavy-light neutrino mixing elements B_{eN_j} and $B_{\mu N_j}$. Furthermore, we adopt the convention $M_{N_2} > M_{N_1}$:

$$\kappa_e = \frac{|B_{eN_2}|}{|B_{eN_1}|}\ , \qquad \kappa_\mu = \frac{|B_{\mu N_2}|}{|B_{\mu N_1}|}\ , \tag{3.30a}$$

$$B_{eN_j} = |B_{eN_j}|e^{i\theta_{ej}}\ , \qquad B_{\mu N_j} = |B_{\mu N_j}|e^{i\theta_{\mu j}}\ , \tag{3.30b}$$

$$\theta^{(LV)} = 2(\theta_{e2} - \theta_{e1})\ , \quad \theta^{(LC)} = (\theta_{e2} - \theta_{e1}) - (\theta_{\mu 2} - \theta_{\mu 1})\ . \tag{3.30c}$$

It turns out (see later) that in our cases of interest the D-C interference contributions are negligible. Using Eqs. (3.8), we then obtain the resulting (sums) $S_{+}^{(X)}(\pi)$ of the decay widths are:

$$
\begin{aligned}
S_{+}^{(LV)}(\pi) &\equiv \left(\Gamma^{(LV)}(\pi^-) + \Gamma^{(LV)}(\pi^+)\right) \\
&= 4|B_{eN_1}|^4 \widetilde{\Gamma}^{(LV)}(DD^*)_{11} \\
&\quad \times \left[1 + \kappa_e^4 \frac{\widetilde{\Gamma}^{(LV)}(DD^*)_{22}}{\widetilde{\Gamma}^{(LV)}(DD^*)_{11}} + 2\kappa_e^2 \left(\cos\theta^{(LV)}\right) \delta_1^{(LV)}\right] \,, \qquad (3.31a)
\end{aligned}
$$

$$
\begin{aligned}
S_{+}^{(LC)}(\pi) &\equiv \left(\Gamma^{(LC)}(\pi^-) + \Gamma^{(LC)}(\pi^+)\right) \\
&= 4|B_{eN_1}|^2 |B_{\mu N_1}|^2 \widetilde{\Gamma}^{(LC)}(DD^*)_{11} \\
&\quad \times \left[1 + \kappa_e^2 \kappa_\mu^2 \frac{\widetilde{\Gamma}^{(LC)}(DD^*)_{22}}{\widetilde{\Gamma}^{(LC)}(DD^*)_{11}} + 2\kappa_e\kappa_\mu \left(\cos\theta^{(LC)}\right) \delta_1^{(LC)}\right] \,, \qquad (3.31b)
\end{aligned}
$$

where $\delta_j^{(X)}$ in the above quantities represent the relative contribution, due to the overlaping between N_1-N_2 in the interference channel.

$$
\delta_j^{(X)} \equiv \frac{\mathrm{Re}\widetilde{\Gamma}^{(X)}(DD^*)_{12}}{\widetilde{\Gamma}^{(X)}(DD^*)_{jj}} \,, \quad (X = LV, LC;\ j = 1, 2) \,. \qquad (3.32)
$$

On the other hand, the difference $S_{-}^{(X)}(\pi)$ of the π^- and π^+ rare decays is (again using Eqs. (3.8)):

$$
\begin{aligned}
S_{-}^{(LV)}(\pi) &\equiv \left(\Gamma^{(LV)}(\pi^-) - \Gamma^{(LV)}(\pi^+)\right) \\
&= 8|B_{eN_1}|^4 \kappa_e^2 \left(\sin\theta^{(LV)}\right) \mathrm{Im}\widetilde{\Gamma}^{(LV)}(DD^*)_{12} \,, \qquad (3.33a)
\end{aligned}
$$

$$
\begin{aligned}
S_{-}^{(LC)}(\pi) &\equiv \left(\Gamma^{(LC)}(\pi^-) - \Gamma^{(LC)}(\pi^+)\right) \\
&= 8|B_{eN_1}|^2 |B_{\mu N_1}|^2 \kappa_e\kappa_\mu \left(\sin\theta^{(LC)}\right) \mathrm{Im}\widetilde{\Gamma}^{(LC)}(DD^*)_{12} \,. \qquad (3.33b)
\end{aligned}
$$

Nonzero value of $S_{-}^{(X)}(\pi)$ signals CP violation in the neutrino sector N_1-N_2. In the above expressions we have neglected the D-C terms. Furthermore, we can recognize (a posteriori) the difference of the CP-odd phases as $\theta^{(X)}$ $(X = LV, LC)$ coming from the PMNS mixing matrix elements, cf. Eqs. (3.30b)-(3.30c); while (sinus of) the difference of the CP-even phases is contained in the imaginary part of the product of propagators, $\mathrm{Im}\Gamma^{(X)}(DD^*)_{12} \propto \mathrm{Im}P_1^{(X)}(D)P_2^{(X)}(D)^*$, cf. Eqs. (3.35) later.

In the limit of $\Gamma_{N_j} \to +0$ ($\Gamma_{N_j} \ll M_{N_j}$), the expression for the "diagonal" decay width $\Gamma^{(X)}(DD^*)_{11}$ (and thus also for $\Gamma^{(X)}(DD^*)_{22}$) can be calculated analytically, see Eqs. (3.20),(3.21).

Furthermore, we can also calculate, analogously as $\Gamma^{(X)}(DD^*)_{jj}$, the analytic expression for the CP asymmetric difference $S_{-}^{(X)}$ in the limit $\Gamma_{N_j} \to +0$ ($\Gamma_{N_j} \ll M_{N_2} - M_{N_1}$). In order to explain this analogy, we note that in the limit $\Gamma_{N_j} \to +0$ it was crucial to use in the analytic calculation of $\Gamma^{(X)}(DD^*)_{jj}$ the identity:

$$|P_j^{(LC)}(D)|^2 = \left|\frac{1}{(p_\pi - p_1)^2 - M_{N_j}^2 + i\Gamma_{N_j}M_{N_j}}\right|^2$$
$$\approx \frac{\pi}{M_{N_j}\Gamma_{N_j}}\delta((p_\pi - p_1)^2 - M_{N_j}^2)\ ; \quad (j = 1, 2;\ \Gamma_{N_j} \ll M_{N_j})\ . \tag{3.34}$$

On the other hand, in the difference $S_-^{(X)} \propto \mathrm{Im}\Gamma^{(X)}(DD^*)_{12}$ we have in the integrand of $\mathrm{Im}\Gamma^{(X)}(DD^*)_{12}$ as a factor the following combination of propagators:

$$\mathrm{Im}\left(P_1(D)P_2(D)^*\right) = \frac{\left(p_N^2 - M_{N_1}^2\right)\Gamma_{N_2}M_{N_2} - \Gamma_{N_1}M_{N_1}\left(p_N^2 - M_{N_2}^2\right)}{\left[\left(p_N^2 - M_{N_1}^2\right)^2 + \Gamma_{N_1}^2M_{N_1}^2\right]\left[\left(p_N^2 - M_{N_2}^2\right)^2 + \Gamma_{N_2}^2M_{N_2}^2\right]} \tag{3.35a}$$
$$= \eta \times \frac{\pi}{M_{N_2}^2 - M_{N_1}^2}\left[\delta(p_N^2 - M_{N_2}^2) + \delta(p_N^2 - M_{N_1}^2)\right]\ , \tag{3.35b}$$

where $p_N = (p_\pi - p_1)$ in the direct channel, and we assumed that $\Gamma_{N_j} \ll |\Delta M_N| \equiv M_{N_2} - M_{N_1}$ in Eq. (3.35b). The parameter η was introduced in Eq. 3.35b which parametrizes any deviation from the naive expectation $\eta = 1$. We expect $\eta \approx 1$ when $\Delta M_N^2 \gg \Gamma_{N_j}$. There is a detailed explanation about the validity of (3.35) in Appendix D where it is argued that when $\Delta M_N \ll M_{N1}$ $(\equiv M_N)$ $\eta(y) = \frac{y^2}{y^2+1}$, with $y = \Delta M_N/\Gamma_N$ and $\Gamma_N = \frac{1}{2}(\Gamma_{N1} + \Gamma_{N2})$. When $X = LV$, the corresponding combination of propagators is the same as in Eq. (3.35) but with the additional factor $M_{N_1}M_{N_2}$. The expression (3.35b) has formally the same structure as the expression (3.34), except for the factors in front of the Dirac delta(s). Therefore, integration over the final phase space can be performed formally in the same way. This then results in the expressions:

$$\mathrm{Im}\widetilde{\Gamma}^{(LV)}(DD^*)_{12} = \eta(y)\ \frac{K_\pi^2}{192(2\pi)^4}\frac{1}{M_\pi^3}\frac{M_{N_1}M_{N_2}}{(M_{N_2} + M_{N_1})(M_{N_2} - M_{N_1})} \tag{3.36a}$$
$$\times \sum_{j=1}^{2} M_{N_j}^{10}\lambda^{1/2}(x_{\pi j}, 1, x_{ej})\left[x_{\pi j} - 1 + x_{ej}(x_{\pi j} + 2 - x_{ej})\right]\mathcal{F}(x_j, x_{ej})\ ,$$

$$\mathrm{Im}\widetilde{\Gamma}^{(LC)}(DD^*)_{12} = \eta(y)\ \frac{K_\pi^2}{192(2\pi)^4}\frac{1}{M_\pi^3}\frac{1}{(M_{N_2} + M_{N_1})(M_{N_2} - M_{N_1})}$$
$$\times \sum_{j=1}^{2} M_{N_j}^{12}\lambda^{1/2}(x_{\pi j}, 1, x_{ej})\left[x_{\pi j} - 1 + x_{ej}(x_{\pi j} + 2 - x_{ej})\right]\mathcal{F}(x_j, x_{ej})\ , \tag{3.36b}$$

where the overall factor $\eta(y)$ is equal to unity $(\eta(y) = 1)$ when $\Gamma_{N_j} \ll |\Delta M_N|$.

We note that there is no such overall correction factor in the expression (3.21) for $\overline{\Gamma}(DD^*)_{jj}$, because in our considered cases $\Gamma_{N_j} \ll M_{N_j}$ always, and Eq. (3.21) is the correct expression then.

All these quantities presented above, can be evaluated also via numerical integrations over the final phase space, with finite widths Γ_{N_j} in the propagators.

Once the numerical evaluation has been performed, we have clear indications of :

- The scalings $\widetilde{\Gamma}^{(X)}(DD^*)_{jj} \propto 1/\Gamma_{N_j}$ and $\mathrm{Im}\widetilde{\Gamma}^{(X)}(DD^*)_{12} \propto 1/\Delta M_N$, as suggested by Eqs. (3.21) and (3.36), are confirmed numerically (when $\Gamma_{N_j} \ll M_{N_j}$, and $\Gamma_{N_j} \ll \Delta M_N$, respectively).

- When the two intermediate neutrino are on-shell, the direct-crossed (DC^* and CD^*) interference contributions to $S_{\pm}^{(X)}(\pi)$ are negligible in all considered cases, in comparison with the corresponding direct (DD^*) and crossed channel (CC^*) contributions.

- In the sum $S_{+}^{(X)}(\pi)$, the interference contributions $\mathrm{Re}\widetilde{\Gamma}^{(X)}(DC^*)_{ij} \sim 10^{-37}$ GeV are approximately independent of Γ_{N_j}. On the other hand, $\widetilde{\Gamma}^{(X)}(DD^*)_{jj} = \widetilde{\Gamma}^{(X)}(CC^*)_{jj}$ is at $\Gamma_N = 10^{-4}$ GeV about two orders of magnitude larger than $\mathrm{Re}\widetilde{\Gamma}^{(X)}(DC^*)_{ij}$.
$\widetilde{\Gamma}^{(X)}(DD^*)_{jj}$ grows at decreasing Γ_N as $1/\Gamma_N$ [Eq. (3.21)], while $\mathrm{Re}\widetilde{\Gamma}^{(X)}(DC^*)_{ij}$ does not decrease and becomes thus at $\Gamma_N < 10^{-4}$ GeV relatively negligible.

- In the difference (asymmetry) $S_{-}^{(X)}(\pi)$, the DC^* interference contribution $\mathrm{Im}\widetilde{\Gamma}^{(X)}(DC^*)_{12} \sim 10^{-38}$ GeV is approximately independent of ΔM_N. On the other hand, $\mathrm{Im}\widetilde{\Gamma}^{(X)}(DD^*)_{12} = \mathrm{Im}\widetilde{\Gamma}^{(X)}(CC^*)_{12}$ is at $\Delta M_N = 10^{-3}$ GeV about two orders of magnitude larger than $\mathrm{Im}\widetilde{\Gamma}^{(X)}(DC^*)_{12}$. $\mathrm{Im}\widetilde{\Gamma}^{(X)}(DD^*)_{12}$ grows at decreasing ΔM_N as $1/\Delta M_N$ [Eq. (3.36)], while $\mathrm{Im}\widetilde{\Gamma}^{(X)}(DC^*)_{12}$ does not decrease and becomes thus at $\Delta M_N < 10^{-3}$ GeV relatively negligible.

Furthermore, the numerical evaluations with $\Gamma_{N_j} \ll \Delta M_N$ give us the values of the $\delta_j^{(X)}$ (Eqs. (3.32) and (3.31)) and $\eta^{(X)}$ correction factors, due to non-negligible overlap of the N_1 with N_2 resonance. It turns out that these functions are independent of X ($= LV, LC$), and that η and $\delta \equiv (1/2)(\delta_1 + \delta_2)$ are effectively functions of only one parameter, $y \equiv \Delta M_N/\Gamma_N$, where $\Delta M_N \equiv M_{N_2} - M_{N_1}$ (> 0), and $\Gamma_N = (1/2)(\Gamma_{N_1} + \Gamma_{N_2})$. Then, we can write:

$$\eta = \eta(y) \ , \quad y \equiv \frac{\Delta M_N}{\Gamma_N} \ , \quad \Gamma_N \equiv \frac{1}{2}(\Gamma_{N_1} + \Gamma_{N_2}) \ , \tag{3.37a}$$

$$\delta = \delta(y) \ , \quad \delta \equiv \frac{1}{2}(\delta_1 + \delta_2) \ , \quad \frac{\delta_1}{\delta_2} = \frac{\overline{\Gamma}(DD^*)_{22}}{\overline{\Gamma}(DD^*)_{11}} = \frac{\widetilde{\mathcal{K}}_2}{\widetilde{\mathcal{K}}_1} \ . \tag{3.37b}$$

The values of δ ($= \delta^{(X)}$) and η ($= \eta^{(X)}$) as functions of $\Delta M_N/\Gamma_N$ can be obtained by numerical integrations over the four-particle finite phase space, and are tabulated in Table 3.2 and Table 3.1, respectively (with their estimated uncertainties due to numerical integrations).

Table 3.1: *Values of $\eta(y)/y$ correction factors for various values of $y \equiv \Delta M_N/\Gamma_N$.*

$y \equiv \frac{\Delta M_N}{\Gamma_N}$	$\log_{10} y$	$\eta(y)$	$\frac{\eta(y)}{y}$
10.0	1.000	0.984 ± 0.003	$0.0984 \pm 3 \times 10^{-4}$
5.00	0.699	0.957 ± 0.003	0.191 ± 0.001
2.50	0.398	0.854 ± 0.003	0.342 ± 0.001
1.67	0.222	0.730 ± 0.005	0.438 ± 0.003
1.25	0.097	0.610 ± 0.007	0.488 ± 0.006
1.00	0.000	0.498 ± 0.005	0.498 ± 0.005
0.70	-0.155	0.333 ± 0.005	0.476 ± 0.005
0.50	-0.301	0.199 ± 0.004	0.399 ± 0.004
0.33	-0.481	0.099 ± 0.003	0.300 ± 0.003
0.10	-1.000	0.009 ± 0.001	0.098 ± 0.001

In order to give a better presentation of the values of Tables 3.1 and 3.2, this information is depicted in figures 3.10 and 3.11.

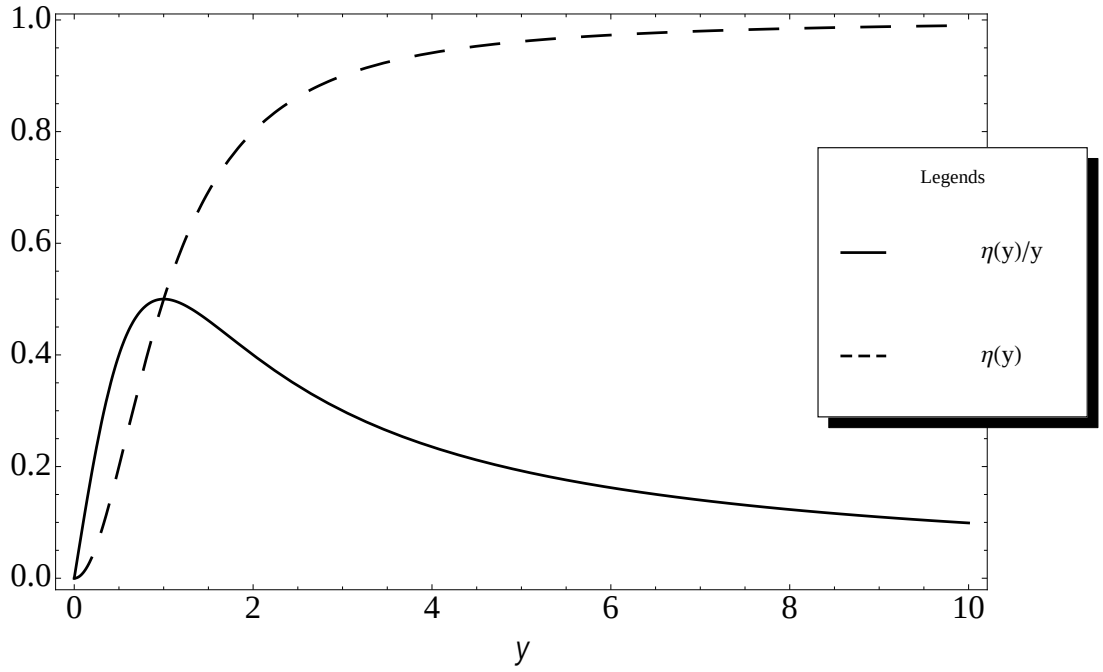

Figure 3.10: *The functions $\frac{\eta(y)}{y}$ and $\eta(y)$, as a function of $y = \frac{\Delta M_N}{\Gamma_N}$. The interception point occurs when $y = 1$ and matches to the maximum value of $\frac{\eta(y)}{y}$, this value ($\Delta M_N = \Gamma_N$) being the necessary condition for get maximum CP violation.*

Table 3.2: *Values of $\delta(y)$ correction terms for various values of $y \equiv \Delta M_N/\Gamma_N$.*

$y \equiv \frac{\Delta M_N}{\Gamma_N}$	$\log_{10} y$	$\delta(y)$
10.0	1.000	$(993.4 \pm 6.25) \cdot 10^{-5}$
9.00	1.000	$(122.3 \pm 0.57) \cdot 10^{-4}$
8.00	1.000	$(154.6 \pm 0.64) \cdot 10^{-4}$
7.00	1.000	$(200.8 \pm 0.61) \cdot 10^{-4}$
6.00	0.699	$(270.8 \pm 0.69) \cdot 10^{-4}$
5.00	0.398	$(385.7 \pm 0.79) \cdot 10^{-4}$
4.00	1.000	$(589.2 \pm 0.90) \cdot 10^{-4}$
3.00	1.000	$(100.0 \pm 0.11) \cdot 10^{-3}$
2.00	0.222	$(199.5 \pm 0.12) \cdot 10^{-3}$
1.00	0.000	$(500.7 \pm 0.18) \cdot 10^{-3}$
0.90	-0.046	$(552.2 \pm 0.21) \cdot 10^{-3}$
0.80	-0.097	$(610.3 \pm 0.22) \cdot 10^{-3}$
0.70	-0.155	$(671.1 \pm 0.23) \cdot 10^{-3}$
0.60	-0.222	$(735.8 \pm 0.26) \cdot 10^{-3}$
0.50	-0.301	$(800.5 \pm 0.30) \cdot 10^{-3}$
0.40	-0.398	$(862.6 \pm 0.29) \cdot 10^{-3}$
0.30	-0.523	$(918.1 \pm 0.32) \cdot 10^{-3}$
0.20	-0.699	$(961.7 \pm 0.34) \cdot 10^{-3}$
0.10	-1.000	$(990.8 \pm 0.36) \cdot 10^{-3}$

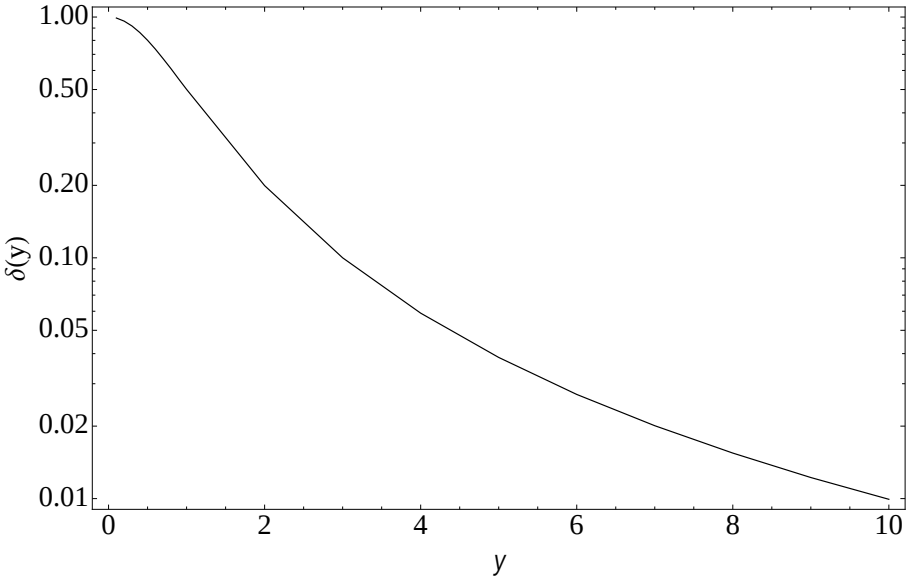

Figure 3.11: *The function $\delta(y)$ as a function of $y = \frac{\Delta M_N}{\Gamma_N}$, on a logarithmic scale.*

We note that the rare process decay widths $S_+^{(X)}(\pi)$, Eqs. (3.31), are formally quartic in the heavy-light mixing elements $|B_{\ell N}|$, i.e., very small. Nonetheless, they are proportional to the expressions $\widetilde{\Gamma}(DD^*)_{jj}$, Eqs. (3.20) and (3.21), which in turn is proportional to $1/\Gamma_{N_j}$ due to the on-shellness of the intermediate N_j's. This $1/\Gamma_{N_j}$ is proportional to $1/\widetilde{\mathcal{K}}_j \sim 1/|B_{\ell N_j}|^2$ according to Eqs. (3.13)-(3.15). Therefore, the on-shellness of N_j's makes the rare process decay widths significantly less suppressed by the mixings:

$$\widetilde{\Gamma}(DD^*)_{jj} \;\propto\; 1/\Gamma_{N_j} \propto 1/\widetilde{\mathcal{K}}_j \propto 1/|B_{\ell N_j}|^2 \;, \tag{3.38a}$$

$$S_+^{(X)}(\pi) \;\propto\; |B_{\ell N_j}|^2 \;. \tag{3.38b}$$

On the other hand, comparing the expressions (3.36) relevant for the CP asymmetries $S_-^{(X)}(\pi)$ (3.33), with the expression (3.20) relevant for the decay widths $S_+^{(X)}(\pi)$ (3.31), we see that the asymmetries $S_-^{(X)}(\pi)$ are suppressed by mixings as $\sim |B_{\ell N}|^4$, making them in general much smaller than the decay widths $S_+^{(X)}(\pi) \propto |B_{\ell N_j}|^2$. However, the asymmetries are proportional to $1/\Delta M_N$ (where $\Delta M_N = M_{N_2} - M_{N_1} > 0$). In general, $\Delta M_N \gg \Gamma_{N_j}$. Nonetheless, in a scenario where ΔM_N becomes comparable with Γ_{N_j} ($y = \frac{\Delta M_N}{\Gamma_N} \approx 1$, very degenerate neutrinos), the asymmetries $S_-^{(X)}(\pi)$ can become comparable with the decay widths $S_+^{(X)}(\pi)$.

Our analysis works in general low-scale seesaw scenarios. However, we shall pay special attention to the νMSM model [29, 30], because it includes two almost degenerate neutrinos N_j in the mass range of $\sim 10^2$ GeV and a dark matter (DM) candidate.

In particular, in this limit of two almost degenerate neutrinos N_j, where now $M_{N_1} \approx M_{N_2} \equiv M_N$, the formulas (3.21), (3.32) and (3.36) get simplified. In this case, it is convenient to introduce a "canonical" branching ratio $\overline{\rm Br}$

$$\begin{aligned}\overline{\rm Br}(M_N) \;\equiv\; & \frac{1}{4\pi}\frac{K_\pi^2 M_\pi^3}{G_F^2 2\,\Gamma(\pi^+ \to \text{all})}\frac{1}{x_\pi^6}\lambda^{1/2}(x_\pi,1,x_e) \\ & \times\left[x_\pi - 1 + x_e(x_\pi + 2 - x_e)\right]\mathcal{F}(x,x_e) \;,\end{aligned} \tag{3.39}$$

where we use the notations

$$x_\pi \;=\; \frac{M_\pi^2}{M_N^2} \;,\quad x_e = \frac{M_e^2}{M_N^2} \;,\quad x = \frac{M_\mu^2}{M_N^2} \;. \tag{3.40}$$

In terms of the canonical branching ratio, the formulas (3.21), (3.32) and (3.36) can be rewritten, in the mentioned almost degenerate scenario, as

$$\frac{\widetilde{\Gamma}(DD^*)_{jj}}{\Gamma(\pi^+ \to \text{all})} \;=\; \frac{1}{4\widetilde{\mathcal{K}}_j^{(T)}}\overline{\rm Br} \;, \tag{3.41a}$$

$$\frac{{\rm Re}\widetilde{\Gamma}(DD^*)_{12}}{\Gamma(\pi^+ \to \text{all})} \;=\; \frac{\delta(y)}{2(\widetilde{\mathcal{K}}_1^{(T)} + \widetilde{\mathcal{K}}_2^{(T)})}\overline{\rm Br} \;, \tag{3.41b}$$

$$\frac{{\rm Im}\widetilde{\Gamma}(DD^*)_{12}}{\Gamma(\pi^+ \to \text{all})} \;=\; \frac{\eta(y)/y}{2(\widetilde{\mathcal{K}}_1^{(T)} + \widetilde{\mathcal{K}}_2^{(T)})}\overline{\rm Br} \;, \tag{3.41c}$$

where $y \equiv \Delta M_N/\Gamma_N$ and $T = Di,\ Ma$ (there is no difference between $\widetilde{\mathcal{K}}^{(Di)}$ and $\widetilde{\mathcal{K}}^{(Ma)}$ in the on-shell mass range, cf. Eq. (3.25)). Similarly, after some algebra, we can rewrite in this scenario ($M_{N_1} \approx M_{N_2} \equiv M_N$) the obtained branching ratios for the considered rare decays and CP asymmetries, in terms of $\overline{\text{Br}}$ and of the heavy-light mixing parameters. Below we present the results for the case when the neutrinos N_j are Dirac (Di), and when they are Majorana (Ma) neutrinos. The branching ratio for the considered rare processes are:

$$\begin{aligned}
\text{Br}_{+}^{(\text{Di})} &\equiv \frac{S_{+}^{(LC)}(\pi)}{2\,\Gamma(\pi^+ \to \text{all})} = \Bigg[\sum_{j=1}^{2} \frac{|B_{eN_j}|^2 |B_{\mu N_j}|^2}{\widetilde{\mathcal{K}}_j^{Di}} \\
&\quad + 4\delta(y) \frac{|B_{eN_1}||B_{eN_2}||B_{\mu N_1}||B_{\mu N_2}|}{(\widetilde{\mathcal{K}}_1^{Di} + \widetilde{\mathcal{K}}_2^{Di})} \cos\theta^{(LC)} \Bigg] \overline{\text{Br}}(M_N) \qquad (3.42a) \\
&= \frac{|B_{eN_1}|^2 |B_{\mu N_1}|^2}{\widetilde{\mathcal{K}}_1^{Di}} \left[1 + \frac{\widetilde{\mathcal{K}}_1^{Di}}{\widetilde{\mathcal{K}}_2^{Di}} \kappa_e^2 \kappa_\mu^2 + 4\delta(y) \frac{\widetilde{\mathcal{K}}_1^{Di}}{(\widetilde{\mathcal{K}}_1^{Di} + \widetilde{\mathcal{K}}_2^{Di})} \kappa_e^2 \kappa_\mu^2 \cos\theta^{(LC)}\right] \overline{\text{Br}}(M_N)
\end{aligned}$$

$$\begin{aligned}
\text{Br}_{+}^{(\text{Ma})} &\equiv \frac{S_{+}^{(LV)}(\pi) + S_{+}^{(LC)}(\pi)}{2\,\Gamma(\pi^+ \to \text{all})} \\
&= \Bigg[\sum_{j=1}^{2} \frac{|B_{eN_j}|^2 (|B_{eN_j}|^2 + |B_{\mu N_j}|^2)}{\widetilde{\mathcal{K}}_j^{Ma}} + 4\delta(y) \frac{|B_{eN_1}||B_{eN_2}|}{(\widetilde{\mathcal{K}}_1^{Ma} + \widetilde{\mathcal{K}}_2^{Ma})} \\
&\quad \times \left(|B_{eN_1}||B_{eN_2}| \cos\theta^{(LV)} + |B_{\mu N_1}||B_{\mu N_2}| \cos\theta^{(LC)}\right) \Bigg] \overline{\text{Br}}(M_N) \qquad (3.42b) \\
&= \frac{|B_{eN_1}|^2 (|B_{eN_1}|^2 + |B_{\mu N_1}|^2)}{\widetilde{\mathcal{K}}_1^{Ma}} \Bigg[1 + \frac{\widetilde{\mathcal{K}}_1^{Ma}}{\widetilde{\mathcal{K}}_2^{Ma}} \kappa_e^2 \left(\frac{\kappa_e^2 |B_{eN_1}|^2 + \kappa_\mu^2 |B_{\mu N_1}|^2}{|B_{eN_1}|^2 + |B_{\mu N_1}|^2}\right) \\
&\quad + 4\delta(y) \frac{\widetilde{\mathcal{K}}_1^{Ma}}{(\widetilde{\mathcal{K}}_1^{Ma} + \widetilde{\mathcal{K}}_2^{Ma})} \kappa_e \Bigg(\frac{\kappa_e |B_{eN_1}|^2}{(|B_{eN_1}|^2 + |B_{\mu N_1}|^2)} \cos\theta^{(LV)} \\
&\quad + \frac{\kappa_\mu |B_{\mu N_1}|^2}{(|B_{eN_1}|^2 + |B_{\mu N_1}|^2)} \cos\theta^{(LC)} \Bigg) \Bigg] \overline{\text{Br}}(M_N)\ .
\end{aligned}$$

Here we took into account that in the Dirac case only the LC process constributes, while in the Majorana case both the lepton number violating (LV) and conserving (LC) processes contribute. The mixing parameters $\widetilde{\mathcal{K}}_j$ are given in Eq. (3.25). The contributions of the N_1-N_2 overlap effects give the relative corrections of $\mathcal{O}(\delta)$ and are negligible when $\Delta M_N > 10\Gamma_N$, cf. Table 3.2.

The CP violating branching ratios Br_- for these considered rare processes are:

$$\begin{aligned}
\mathrm{Br}_-^{(\mathrm{Di})} &\equiv \frac{S_-^{(LC)}(\pi)}{2\,\Gamma(\pi^+ \to \mathrm{all})} = \frac{\Gamma^{(LC)}(\pi^-) - \Gamma^{(LC)}(\pi^+)}{2\,\Gamma(\pi^+ \to \mathrm{all})} \\
&= \frac{4|B_{eN_1}||B_{eN_2}||B_{\mu N_1}||B_{\mu N_2}|}{(\widetilde{\mathcal{K}}_1^{Di} + \widetilde{\mathcal{K}}_2^{Di})} \sin\theta^{(LC)} \frac{\eta(y)}{y} \overline{\mathrm{Br}}(M_N) \qquad (3.43a) \\
&= \frac{4|B_{eN_1}|^2|B_{eN_2}|^2\kappa_e\kappa_\mu}{(\widetilde{\mathcal{K}}_1^{Di} + \widetilde{\mathcal{K}}_2^{Di})} \sin\theta^{(LC)} \frac{\eta(y)}{y} \overline{\mathrm{Br}}(M_N)
\end{aligned}$$

$$\begin{aligned}
\mathrm{Br}_-^{(\mathrm{Ma})} &\equiv \frac{(S_-^{(LV)}(\pi) + S_-^{(LC)}(\pi))}{2\,\Gamma(\pi^+ \to \mathrm{all})} \\
&= \frac{\Gamma^{(LV)}(\pi^-) + \Gamma^{(LC)}(\pi^-) - \Gamma^{(LV)}(\pi^+) - \Gamma^{(LC)}(\pi^+)}{2\,\Gamma(\pi^+ \to \mathrm{all})} = \frac{4|B_{eN_1}||B_{eN_2}|}{(\widetilde{\mathcal{K}}_1^{Ma} + \widetilde{\mathcal{K}}_2^{Ma})} \\
&\quad \times \left(|B_{eN_1}||B_{eN_2}| \sin\theta^{(LV)} + |B_{\mu N_1}||B_{\mu N_2}| \sin\theta^{(LC)}\right) \frac{\eta(y)}{y} \overline{\mathrm{Br}}(M_N) \qquad (3.43b) \\
&= \frac{4\kappa_e|B_{eN_1}|^2}{(\widetilde{\mathcal{K}}_1^{Ma} + \widetilde{\mathcal{K}}_2^{Ma})} \left(\kappa_e|B_{eN_1}|^2 \sin\theta^{(LV)} + \kappa_\mu|B_{\mu N_1}|^2 \sin\theta^{(LC)}\right) \frac{\eta(y)}{y} \overline{\mathrm{Br}}(M_N).
\end{aligned}$$

Consequently, the CP asymmetry ratios $\mathcal{A}_{\mathrm{CP}}^{(X)}$ are obtained from Eqs. (3.42)-(3.43) and are presented in Eqs. (3.44a) and (3.44b).

$$\mathcal{A}_{\rm CP}^{\rm (Di)} \equiv \frac{{\rm Br}_{-}^{\rm (Di)}}{{\rm Br}_{+}^{\rm (Di)}} = \frac{\Gamma^{\rm (LC)}(\pi^-) - \Gamma^{\rm (LC)}(\pi^+)}{\Gamma^{\rm (LC)}(\pi^-) + \Gamma^{\rm (LC)}(\pi^+)}$$

$$= \frac{\sin\theta^{\rm (LC)}}{\left[\frac{1}{4}\frac{|B_{eN_1}|}{|B_{eN_2}|}\frac{|B_{\mu N_1}|}{|B_{\mu N_2}|}\left(1+\frac{\widetilde{\mathcal{K}}_2^{Di}}{\widetilde{\mathcal{K}}_1^{Di}}\right) + \frac{1}{4}\frac{|B_{eN_2}|}{|B_{eN_1}|}\frac{|B_{\mu N_2}|}{|B_{\mu N_1}|}\left(1+\frac{\widetilde{\mathcal{K}}_1^{Di}}{\widetilde{\mathcal{K}}_2^{Di}}\right) + \delta(y)\cos\theta^{\rm (LC)}\right]}\,\frac{\eta(y)}{y}\,, \tag{3.44a}$$

$$\mathcal{A}_{\rm CP}^{\rm (Ma)} \equiv \frac{{\rm Br}_{-}^{\rm (Ma)}}{{\rm Br}_{+}^{\rm (Ma)}} = \frac{\Gamma^{\rm (LV)}(\pi^-) + \Gamma^{\rm (LC)}(\pi^-) - \Gamma^{\rm (LV)}(\pi^+) - \Gamma^{\rm (LC)}(\pi^+)}{\Gamma^{\rm (LV)}(\pi^-) + \Gamma^{\rm (LC)}(\pi^-) + \Gamma^{\rm (LV)}(\pi^+) + \Gamma^{\rm (LC)}(\pi^+)}$$

$$= \frac{\left(\sin\theta^{\rm (LV)} + \frac{|B_{\mu N_1}||B_{\mu N_2}|}{|B_{eN_1}||B_{eN_2}|}\sin\theta^{\rm (LC)}\right)}{\left[\frac{1}{4}\frac{(|B_{eN_1}|^2+|B_{\mu N_1}|^2)}{|B_{eN_2}|^2}\left(1+\frac{\widetilde{\mathcal{K}}_2^{Ma}}{\widetilde{\mathcal{K}}_1^{Ma}}\right) + \frac{1}{4}\frac{(|B_{eN_2}|^2+|B_{\mu N_2}|^2)}{|B_{eN_1}|^2}\left(1+\frac{\widetilde{\mathcal{K}}_1^{Ma}}{\widetilde{\mathcal{K}}_2^{Ma}}\right) + \delta(y)\left(\cos\theta^{\rm (LV)} + \frac{|B_{\mu N_1}||B_{\mu N_2}|}{|B_{eN_1}||B_{eN_2}|}\cos\theta^{\rm (LC)}\right)\right]} \times \frac{\eta(y)}{y}\,. \tag{3.44b}$$

When y ($\equiv \Delta M_N/\Gamma_N$) becomes large ($y > 10$), i.e., when $\Delta M_N > 10\Gamma_N$, Table 3.1 implies that the CP asymmetries (3.44a)-(3.44b) become suppressed by the $\eta(y)/y$ factor. On the other hand, when $y \approx 1$ and $|\theta^{(X)}| \sim 1$, the factor $\eta(y)/y$ is ~ 1 and the CP asymmetry ratio $\mathcal{A}_{\rm CP}^{(X)}$ is maximal and becomes ~ 1, while all $\mathrm{Br}_{\pm}$ become $\sim |B_{\ell N_j}|^2 \overline{\mathrm{Br}}(M_N)$ ($\ell = e, \mu$).

If we also assume that $|B_{\ell N_2}| \approx |B_{\ell N_1}|$ (for $\ell = e, \mu, \tau$), then also $\widetilde{\mathcal{K}}_1^{(T)} = \widetilde{\mathcal{K}}_2^{(T)} \equiv \widetilde{\mathcal{K}}^{(T)}$, and the expressions for $\mathcal{A}_{\rm CP}$ become particularly simple

$$\mathcal{A}_{\rm CP}^{(\rm Di)} = \frac{\sin\theta^{(\rm LC)}}{(1+\delta(y)\cos\theta^{(\rm LC)})}\,\frac{\eta(y)}{y} = \sin\theta^{(\rm LC)}\,\frac{\eta(y)}{y}\,(1+\mathcal{O}(\delta))\ ,$$

$$\mathcal{A}_{\rm CP}^{(\rm Ma)} = \left(\frac{|B_{eN_1}|^2\sin\theta^{(\rm LV)} + |B_{\mu N_1}|^2\sin\theta^{(\rm LC)}}{|B_{eN_1}|^2 + |B_{\mu N_1}|^2}\right)\frac{\eta(y)}{y}\,(1+\mathcal{O}(\delta))\ .$$

We present in Fig. 3.12 the normalized quantity $\overline{\mathrm{Br}}$ as a function of M_N in the on-shell kinematic interval; and in Fig. 3.13 the same curve near the lower end point $M_N \approx M_\mu + M_e$ ($= 0.1062$ GeV), where the effects of $M_e \neq 0$ are relatively appreciable. On the other hand, the (CP asymmetry) branching ratio Br_- in the case of mixing one and maximal CP phases (i.e., when $|B_{\ell N_j}| = 1$ for all ℓ, and $\sin\theta^{(X)} = 1$; $\mathrm{Br}_-^{(\rm Di)} = \mathrm{Br}_-^{(\rm Ma)} \equiv \mathrm{Br}_-$ then), as a function of ΔM_N, is presented in Fig. 3.14. In that Figure, no overlap effects are taken into account, i.e., $\eta = 1$.

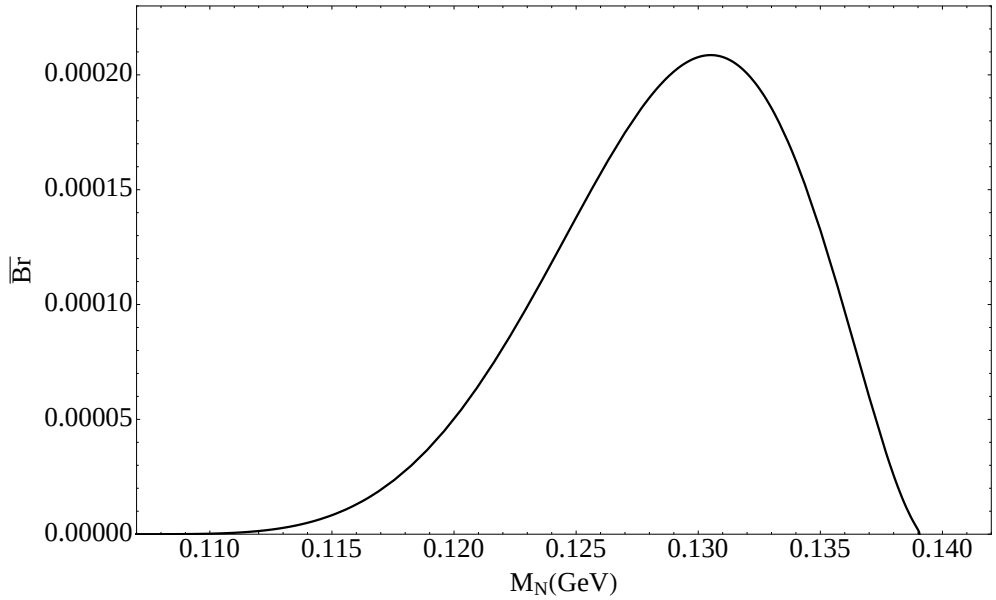

Figure 3.12: *The normalized branching ratio* $\overline{\mathrm{Br}}$, *Eq. (3.39), as a function of the mass* $M_{N_1} \approx M_{N_2} \equiv M_N$. *The full formula was used (with* $M_e = 0.511 \times 10^{-3}$ *GeV). The formula for* $M_e = 0$ *case gives a line which is in this Figure indistinguishable from the depicted line.*

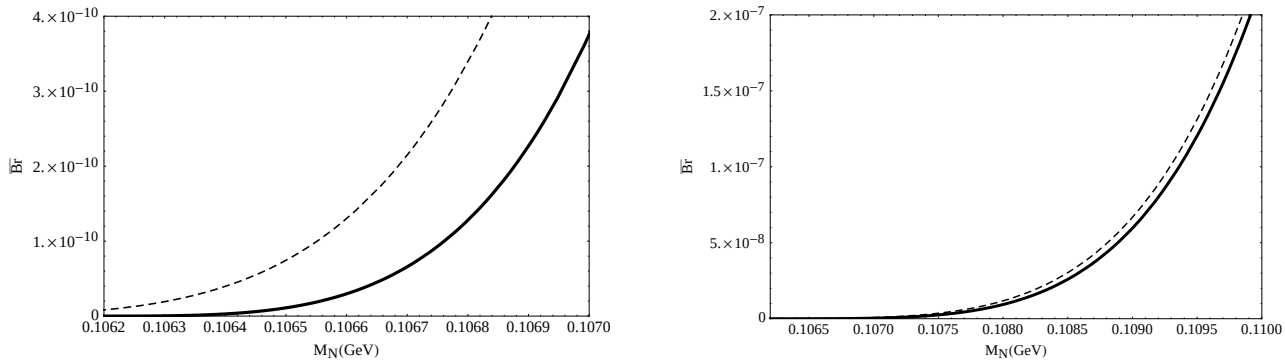

FIGURE 3.13: *The normalized branching ratio* $\overline{\mathrm{Br}}$ *near the lower end point* $M_\mu + M_e$ $(= 0.1062\ GeV)$*: (a) in the interval below* $0.107\ GeV$*; (b) in the interval below* $0.110\ GeV$*. The dashed line is for* $M_e = 0$*, the full line includes the effects of* $M_e = 0.511 \times 10^{-3}\ GeV$*.*

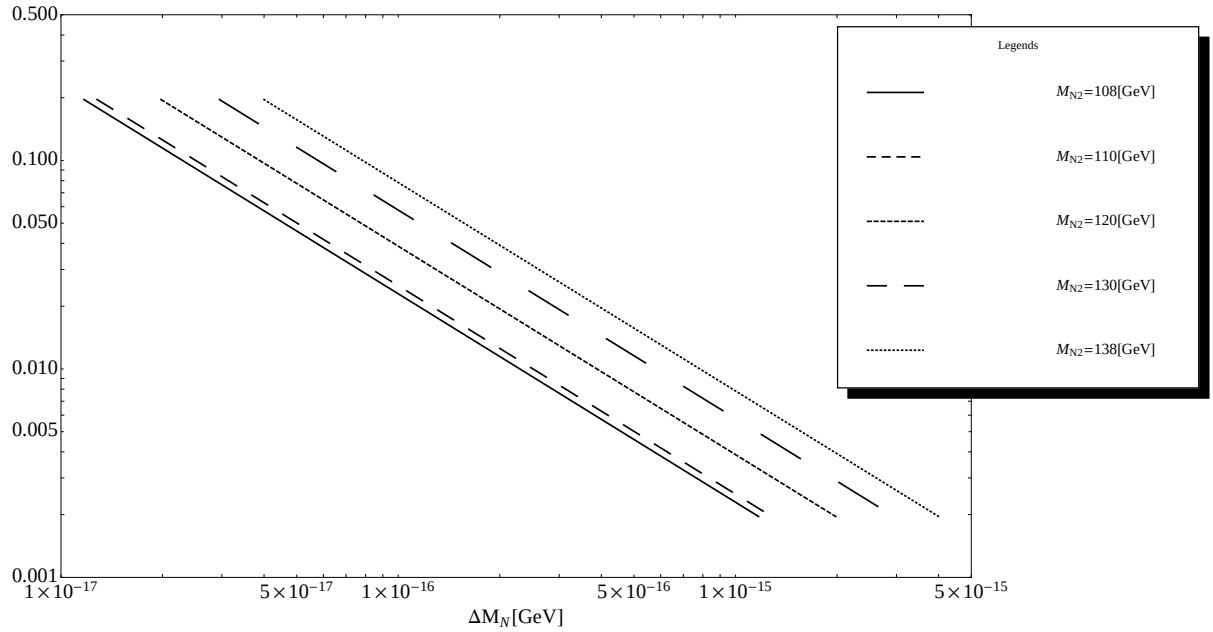

FIGURE 3.14: *The CP asymmetry* A *as a function of* $\Delta M_N = M_{N_2} - M_{N_1}$*, for mixing one* ($|B_{\ell N_j}| = 1$) *and large CP-violating phases* ($\sin\theta^{(X)} = 1$)*, for four different values of* M_{N_2}*. No suppression effects from the overlap of the* N_1 *and* N_2 *resonances are accounted for here* ($\eta = 1$)*.*

Therefore, when $0.33 < y \equiv \Delta M_N/\Gamma_N < 5$, i.e., in the almost degenerate case of two on-shell neutrinos N_j, we can expect in general the CP asymmetry ratio $\mathcal{A}_{\mathrm{CP}}$ of the considered rare process to be ~ 1. The branching ratio for this process, in the case of one N neutrino and in the $M_e = 0$ limit, was considered in Ref. [43], however, the general conclusions remain unchanged with respect to the $M_e = 0.511$ MeV case. All the conclusions about the measurability of this branching ratio Br_+ can be translated into the conclusions about the measurability of the (CP asymmetry) branching ratio Br_- in the described almost degenerate scenario, provided that $|\theta^{(\mathrm{LC})}|, |\theta^{(\mathrm{LV})}| \sim 1$.

This means that the CP asymmetries could be measured in the future pion factories in the described scenarios, provided that the heavy-light mixing parameters $|B_{\ell N_j}|^2$ $(\ell = e, \mu)$ are not many orders of magnitude below the present experimental upper bounds. The present experimental bounds [45] of the mixing parameters $|B_{\ell N_j}|^2$ $(\ell = e, \mu, \tau)$ in the considered mass range, are: $|B_{eN_j}|^2 \lesssim 10^{-8}$; $|B_{\mu N_j}|^2 \lesssim 10^{-6}$; $|B_{\tau N_j}|^2 \lesssim 10^{-4}$.

In order to take into account the acceptance factor (C.2) which is the probability of the on-shell neutrino to decay within the detector, we should multiply the obtained branching ratios $\mathrm{Br}_{\pm}$ by such acceptance factors P_N to obtain the effective branching ratios $\mathrm{Br}_{\pm}^{(\mathrm{eff})}$.

If the largest among the mixing elements $|B_{\ell N_j}|^2$ $(\ell = e, \mu)$ are $|B_{\mu N_j}|^2$ $(\sim |B_{\mu N}|^2)$ $(j = 1, 2)$, i.e., if we have $|B_{\mu N}|^2 \gg |B_{eN_j}|^2$ $(\sim |B_{eN}|^2)$, the formulas (C.2) with (3.42) and (3.43) give:

$$P_N \mathrm{Br}_{+}^{(\mathrm{Di,Ma})} \sim 10^{-3} |B_{eN}|^2 |B_{\mu N}|^2 \overline{\mathrm{Br}}(M_N) \sim |B_{eN}|^2 |B_{\mu N}|^2 10^{-7} \,, \tag{3.45a}$$

$$P_N \mathrm{Br}_{-}^{(\mathrm{Di,Ma})} \sim 10^{-3} |B_{eN}|^2 |B_{\mu N}|^2 \sin\theta^{(X)} \overline{\mathrm{Br}}(M_N) \sim |B_{eN}|^2 |B_{\mu N_j}|^2 \sin\theta^{(\mathrm{LC})} 10^{-7} \tag{3.45b}$$

In these relations, we took into account that the LC process dominates over the LV process in the considered case, and that $\overline{\mathrm{Br}} \sim 10^{-4}$ in most of the on-shell interval for the masses $M_{N_1} \approx M_{N_2} \equiv M_N$, cf. Fig. 3.12. If in this case, in addition, $|B_{\ell N_j}|^2$ $(\ell = e, \mu)$ are close to their present upper bounds $|B_{eN_j}|^2 \sim 10^{-8}$ and $|B_{\mu N_j}|^2 \sim 10^{-6}$, this implies that:

$P_N \mathrm{Br}_{+} \sim 10^{-21}$ and $P_N \mathrm{Br}_{-} \sim 10^{-21}$ (the latter provided $\sin\theta^{(X)} \sim 1$), implying that $\sim 10^8$ events can be detected per year, with the difference between π^- and π^+ decays also of the order $\sim 10^8$. This number decreases in proportionality with the factor $|B_{eN}|^2 |B_{\mu N}|^2$ when this factor decreases. In this scenario there is almost no difference between the case when N_j are Dirac and the case when N_j are Majorana.

If the largest among the mixing elements $|B_{\ell N_j}|^2$ $(\ell = e, \mu)$ are $|B_{eN_j}|^2$ $(\sim |B_{eN}|^2)$ $(j = 1, 2)$, i.e., if we have $|B_{eN}|^2 \gg |B_{\mu N_j}|^2$ $(\sim |B_{\mu N}|^2)$, the formulas (C.2) with (3.42) and (3.43) give:

$$P_N \mathrm{Br}_{+}^{(\mathrm{Di})} \sim 10^{-3} |B_{eN}|^2 |B_{\mu N}|^2 \overline{\mathrm{Br}}(M_N) \sim |B_{eN}|^2 |B_{\mu N}|^2 10^{-7} \,. \tag{3.46a}$$

$$P_N \mathrm{Br}_{+}^{(\mathrm{Ma})} \sim 10^{-3} |B_{eN}|^4 \overline{\mathrm{Br}}(M_N) \sim |B_{eN}|^4 10^{-7} \,. \tag{3.46b}$$

$$P_N \mathrm{Br}_{-}^{(\mathrm{Di})} \sim 10^{-3} |B_{eN}|^2 |B_{\mu N}|^2 \sin\theta^{(\mathrm{LC})} \overline{\mathrm{Br}}(M_N) \sim |B_{eN}|^2 |B_{\mu N}|^2 \sin\theta^{(\mathrm{LC})} 10^{-7} \,. \tag{3.46c}$$

$$P_N \mathrm{Br}_{-}^{(\mathrm{Ma})} \sim 10^{-3} |B_{eN}|^4 \sin\theta^{(\mathrm{LV})} \overline{\mathrm{Br}}(M_N) \sim |B_{eN}|^4 \sin\theta^{(\mathrm{LV})} 10^{-7} \,. \tag{3.46d}$$

In this considered case, the LV process dominates over the LC process. If in this case, in addition, $|B_{eN_j}|^2$ are close to their present upper bounds, $|B_{eN_j}|^2 \sim 10^{-8}$ (and $|B_{\mu N}|^2 \ll |B_{eN_j}|^2$), this implies that:

$P_N \mathrm{Br}_{+}^{(\mathrm{Ma})} \sim 10^{-23}$ ($\gg P_N \mathrm{Br}_{+}^{(\mathrm{Di})}$) and $P_N \mathrm{Br}_{-}^{(\mathrm{Ma})} \sim 10^{-23}$ ($\gg P_N \mathrm{Br}_{-}^{(\mathrm{Di})}$), assuming that $\sin\theta^{(\mathrm{LV})} \sim 1$. This implies that $\sim 10^6$ events can be detected per year, with the difference between π^- and π^+ decays also of the order $\sim 10^6$, if N_j are Majorana neutrinos (and less events if N_j are Dirac neutrinos). This number decreases in proportionality with the factor $|B_{eN}|^4$ when this factor decreases. In this scenario there is a clear difference between the case when N_j are Dirac and the case when N_j are Majorana.

The mentioned present experimental upper bounds on the mixings ($|B_{eN_j}|^2 \lesssim 10^{-8}$; $|B_{\mu N_j}|^2 \lesssim 10^{-6}$) suggest that the first of the mentioned two scenarios is more likely, i.e., that the LC processes dominate over the LV processes. Then, the measurement of the CP asymmetries alone cannot distinguish between the Dirac and the Majorana character of intermediate neutrinos N_j's. However, as argued in Ref. [43], the neutrino character could be determined from the measured differential decay rates ($d\Gamma/dE_\mu$) of these processes with respect to the muon energy E_μ in the N_j rest frame.

Chapter 4

The Rare $M^+ \to e^+e^+M'^-$ Semi-Hadronic Decay

In this Section we pay our atention to the rare semihadronic decays $M^+ \to e^+e^+M'^-$, where M and M' are pseudoscalar mesons: $M = K, D, D_s, B, B_c$ and $M^{'} = \pi, K, D, D_s$. The dominant contribution to this decay is presented in figure 4.1; and is given by exchanges of on-shell neutrinos N_j.

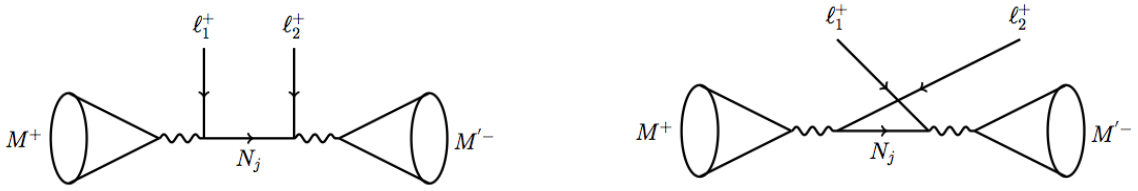

FIGURE 4.1: *The lepton number violating decay $M^+ \to \ell_1^+\ell_2^+M^{'-}$: the direct (D) channel (the left-hand figure); the crossed (C) channel (the right-hand figure).*

As we can see in Fig. 4.1 the intermediate neutrinos (N_j) must to be Majorana, because the process violates the lepton number (by two units). Again we shall consider the scenario of two on-shell neutrinos with similar masses. This Section is based mainly on our work [46] and [43], see also [47] for a similar approach.

4.1 The process and formalism for the LV semihadronic decays of pseudoscalars

As we seen in the previous Section 3, the off-shell condition in the neutrino propagator produce a strong suppresion in the decay width. Therefore, in this Section we only concentrate on the on-shell mass region.
The topology of these tree level processes is like "s-channel." The processes with (two-loop) "t-channel" topology are strongly suppressed [48]. The type of processes of Fig. 4.1, within the models with sterile neutrinos N in the mass range of mesons, have been studied in several works, among them Refs. [20, 21, 23–26, 45, 48].
We have to remember that we denote the heavy-light mixing elements Eq.(2.7) for the heavy neutrinos as $B_{\ell N_j}$ $(j = 1, 2)$. We shall use the phase conventions of the book Ref. [39], i.e., all the CP-violating phases are incorporated in the PMNS matrix of mixing elements. The sum and difference of the decay widths, $S_{\pm}(M) \equiv [\Gamma(M^- \to \ell_1^-\ell_2^-M^{'+}) \pm \Gamma(M^+ \to \ell_1^-\ell_2^-M^{'+})]$, of the processes of Fig. 4.1 will be appreciable only if the two intermediate neutrinos N_j are

on-shell

$$\begin{aligned}(M_{M'} + M_{\ell_2}) &< M_{N_j} < (M_M - M_{\ell_1}) \ , \ \text{or/and} \\ (M_{M'} + M_{\ell_1}) &< M_{N_j} < (M_M - M_{\ell_2}) \ . \end{aligned} \tag{4.1}$$

We shall use the same short-hand notation as in the previous Section 3 for the decay widths of these rare processes:

$$\Gamma(M^\pm) \equiv \Gamma(M^\pm \to \ell_1^\pm \ell_2^\pm M'^\mp) \ . \tag{4.2}$$

These decay widths can be written in the form

$$\Gamma(M^\pm) = (2 - \delta_{\ell_1\ell_2}) \frac{1}{2!} \frac{1}{2M_M} \frac{1}{(2\pi)^5} \int d_3 \, |\mathcal{T}(M^\pm)|^2 \ , \tag{4.3}$$

where $1/2!$ is the symmetry factor when the two charged leptons are equal. Here, $|\mathcal{T}(M^\pm)|^2$ is the absolute square (summed over the final helicities) of the sum of amplitudes from N_1 and N_2 neutrinos in the two channels D (direct) and C (crossed). We refer to Appendix E for details. In Eq. (4.3), d_3 denotes the integration over the three-particle final phase space

$$d_3 \equiv \frac{d^3\vec{p}_1}{2E_{\ell_1}(\vec{p}_1)} \frac{d^3\vec{p}_2}{2E_{\ell_2}(\vec{p}_2)} \frac{d^3\vec{p}_{M'}}{2E_{M'}(\vec{p}_{M'})} \delta^{(4)}\left(p_M - p_1 - p_2 - p_{M'}\right) \ . \tag{4.4}$$

We denoted by p_1 and p_2 the momenta of ℓ_1 and ℓ_2 charged leptons from the left and the right vertex of the direct channels, respectively (in the crossed channel ℓ_2 couples to the left vertex), cf. Fig. 4.1. The decay widths Eq.(4.3) can then be written as a double sum over the contributions of N_i and N_j exchanges ($i, j = 1, 2$), with the explict mixing factors factored out

$$\begin{aligned}\Gamma(M^\pm) = (2 - \delta_{\ell_1\ell_2}) &\sum_{i=1}^{2} \sum_{j=1}^{2} k_i^{(\pm)} k_j^{(\pm)*} \\ &\times \left[\widetilde{\Gamma}_M (DD^*)_{ij} + \widetilde{\Gamma}_M (CC^*)_{ij} + \widetilde{\Gamma}_{M\pm} (DC^*)_{ij} + \widetilde{\Gamma}_{M\pm} (CD^*)_{ij}\right] \ , \end{aligned} \tag{4.5}$$

where $k_j^{(\pm)}$ are the corresponding mixing factors

$$k_j^{(-)} = B_{\ell_1 N_j} B_{\ell_2 N_j} \ , \qquad k_j^{(+)} = (k_j^{(-)})^* \ , \tag{4.6}$$

Since $|T_{M+}(D)|^2 = |T_{M-}(D)|^2$ and $|T_{M+}(C)|^2 = |T_{M-}(C)|^2$, we omitted the subscripts $\pm$ from the DD^* and CC^* contribution terms $\widetilde{\Gamma}_M(DD^*)_{ij}$ and $\widetilde{\Gamma}_M(CC^*)_{ij}$ in Eq. (4.5).

$\widetilde{\Gamma}_{M\pm}(XY^*)_{ij}$ are the normalized contributions (without the mixing factor) of N_i exchange in the X channel and complex-conjugate of the N_j exchange in the Y channel ($X, Y = C, D$)

$$\widetilde{\Gamma}_{M\pm}(XY^*)_{ij} \equiv K_M^2 \ \frac{1}{2!} \frac{1}{2M_M} \frac{1}{(2\pi)^5} \int d_3 \ P_i(X) P_j(Y)^* M_{N_i} M_{N_j} T_{M\pm}(X) T_{M\pm}(Y)^* \ . \tag{4.7}$$

Here, $T_{M\pm}(X)$ ($X = D, C$) are the relevant parts of the amplitude in the X channel which appear also in the total decay amplitudes $\mathcal{T}_{M\pm}$ (see Appendix E) and $P_j(X)$ ($X = D, C$) are

the propagators of the intermediate neutrinos N_j in the two channels

$$P_j(D) = \frac{1}{\left[(p_M - p_1)^2 - M_{N_j}^2 + i\Gamma_{N_j} M_{N_j}\right]} , \tag{4.8a}$$

$$P_j(C) = \frac{1}{\left[(p_M - p_2)^2 - M_{N_j}^2 + i\Gamma_{N_j} M_{N_j}\right]} . \tag{4.8b}$$

The overall constant K_M^2 appearing in Eqs. (4.7) is

$$K_M^2 = G_F^4 f_M^2 f_{M'}^2 |V_{Q_u Q_d} V_{q_u q_d}|^2 , \tag{4.9}$$

where f_M and $f_{M'}$ are the decay constants of $M^{\pm}$ and $M'^{\mp}$, and $V_{Q_u Q_d}$ and $V_{q_u q_d}$ are the CKM elements corresponding to $M^{\pm}$ and $M'^{\mp}$ (the valence quark content of M^+ is $Q_u \bar{Q}_d$; of M'^+ is $q_u \bar{q}_d$).

Several symmetry relations exist among the normalized decay widths $\widetilde{\Gamma}_{\pm}(XY^*)_{ij}$, as given in Eqs. (E.6)-(E.7) in Appendix E. The most important symmetry property is that the (2×2) matrices $\widetilde{\Gamma}_M(DD^*)$ and $\widetilde{\Gamma}_M(CC^*)$ are self-adjoint (and even equal if $\ell_1 = \ell_2$). The matrices $\widetilde{\Gamma}_{M\pm}(DC^*)$ and $\widetilde{\Gamma}_{M\pm}(CD^*)$, which represent the (canonical) D-C channel interference contributions to the decay widths $\Gamma(M^{\pm})$, will turn out to be several orders of magnitude smaller than the $\widetilde{\Gamma}_M(DD^*)$ and $\widetilde{\Gamma}_M(CC^*)$ matrices.

In our calculations we shall also need to know the total decay width $\Gamma(N_j^{(Ma)} \to \text{all}) \equiv \Gamma_{N_j}^{(Ma)}$ [Eq.3.13] of the two Majorana neutrinos N_j as a function of the mass M_{N_j}, or more specifically, the corresponding mixing factor $\widetilde{\mathcal{K}}_j^{(Ma)}$ [Eq.3.15] in our relevant on-shell mass range $[0.14 - 6.3](GeV)$ of the neutrino mass. The mixing factor in our relevant mass range is given in figure B.2 in Appendix B.

On the other hand, the present upper bounds for the squares $|B_{\ell N}|^2$ of the heavy-light mixing matrix elements, in our range of interest 0.14 GeV $< M_N <$ 6.3 GeV, can be inferred from Ref. [45]. The present upper bounds for $|B_{eN}|^2$, in the mentioned range of M_N, are largely determined by the neutrinoless double beta decay experiments [49, 50] $(0\nu\beta\beta)$. The upper bounds for $|B_{\mu N}|^2$ come from searches of peaks in the spectrum of μ in pion and kaon decays [51] and from decay searches [51–56]. The upper bounds for $|B_{\tau N}|^2$ come from CC interactions (if τ is produced) and from NC interactions [56–58]. In Table 4.1 we present the present upper bounds on $|B_{\ell N}|^2$ for specific chosen values of M_N within the mentioned interval.

Table 4.1: *Present upper bounds for the squares $|B_{\ell N}|^2$ of the heavy-light mixing matrix elements, for various specific values of M_N.*

$M_N[GeV]$	$\lvert B_{eN}\rvert^2$	$\lvert B_{\mu N}\rvert^2$	$\lvert B_{\tau N}\rvert^2$
0.1	$(1.5 \pm 0.5) \times 10^{-8}$	$(6.0 \pm 0.5) \times 10^{-6}$	$(8.0 \pm 0.5) \times 10^{-4}$
0.3	$(2.5 \pm 0.5) \times 10^{-9}$	$(3.0 \pm 0.5) \times 10^{-9}$	$(1.5 \pm 0.5) \times 10^{-1}$
0.5	$(2.0 \pm 0.5) \times 10^{-8}$	$(6.5 \pm 0.5) \times 10^{-7}$	$(2.5 \pm 0.5) \times 10^{-2}$
0.7	$(3.5 \pm 0.5) \times 10^{-8}$	$(2.5 \pm 0.5) \times 10^{-7}$	$(9.0 \pm 0.5) \times 10^{-3}$
1.0	$(4.5 \pm 0.5) \times 10^{-8}$	$(1.5 \pm 0.5) \times 10^{-7}$	$(3.0 \pm 0.5) \times 10^{-3}$
2.0	$(1.0 \pm 0.5) \times 10^{-7}$	$(2.5 \pm 0.5) \times 10^{-5}$	$(3.0 \pm 0.5) \times 10^{-4}$
3.0	$(1.5 \pm 0.5) \times 10^{-7}$	$(2.5 \pm 0.5) \times 10^{-5}$	$(4.5 \pm 0.5) \times 10^{-5}$
4.0	$(2.5 \pm 0.5) \times 10^{-7}$	$(1.5 \pm 0.5) \times 10^{-5}$	$(1.5 \pm 0.5) \times 10^{-5}$
5.0	$(3.0 \pm 0.5) \times 10^{-7}$	$(1.5 \pm 0.5) \times 10^{-5}$	$(1.5 \pm 0.5) \times 10^{-5}$
6.0	$(3.5 \pm 0.5) \times 10^{-7}$	$(1.5 \pm 0.5) \times 10^{-5}$	$(1.5 \pm 0.5) \times 10^{-5}$

The upper bounds have in some cases strong dependence on the precise values of M_N, and for further details we refer to the corresponding figures in Ref. [45].

4.2 The decay widths and CP asymmetry for the LV semihadronic decays of pseudoscalars

Here we shall use the results of Sec. 4.1, and a combination of analytic and numerical evaluations, in order to obtain the results for the decay widths $S_\pm$ and the CP asymmetry ratios $\mathcal{A}_{\rm CP}$ of the discussed semihadronic LV decays of pseudoscalar mesons $M^\pm$:

$$S_\pm(M) \equiv \Gamma(M^-) \pm \Gamma(M^+) \ , \tag{4.10}$$

$$\mathcal{A}_{\rm CP}(M) \equiv \frac{S_-(M)}{S_+(M)} \equiv \frac{\Gamma(M^-) - \Gamma(M^+)}{\Gamma(M^-) + \Gamma(M^+)} \ , \tag{4.11}$$

where we use the notations of Eq. (4.2). $S_+(M)$ represents the total (sum) of the decay widths of M^+ and M^- for these rare LV decays, while $S_-(M)$ is the corresponding (CP-violating) difference. The ratio $\mathcal{A}_{\rm CP}(M)$ in Eq. (4.11) is the usual measure of the relative CP violation effect. We adopt again the convention $M_{N_2} > M_{N_1}$, and we reintroduce the following notations related with the heavy-light neutrino mixing elements $B_{\ell_1 N_j}$ and $B_{\ell_2 N_j}$ and their phases:

$$\kappa_{\ell_1} = \frac{|B_{\ell_1 N_2}|}{|B_{\ell_1 N_1}|} \ , \quad \kappa_{\ell_2} = \frac{|B_{\ell_2 N_2}|}{|B_{\ell_2 N_1}|} \ , \tag{4.12a}$$

$$B_{\ell_k N_j} \equiv |B_{\ell_k N_j}| e^{i\phi_{kj}} \qquad (k, j = 1, 2) \ , \tag{4.12b}$$

$$\theta_{ij} = (\phi_{1i} + \phi_{2i} - \phi_{1j} - \phi_{2j}) \quad (i, j = 1, 2) \ . \tag{4.12c}$$

For example, if $\ell_1 = \ell_2 = \mu$, then $\theta_{21} = 2(\phi_{\mu 2} - \phi_{\mu 1}) = 2(\arg(B_{\mu N_2}) - \arg(B_{\mu N_1}))$. Here we shall

not write explicitly the D-C channel interference contributions to the quantities Eqs.(4.10)-(4.11), as our numerical calculations give us for them contributions which are several orders of magnitude smaller that the contributions from the D channel and from the C channel.

The resulting sums $S_+(M) \equiv \left(\Gamma(M^-) + \Gamma(M^+)\right)$ of the decay widths can then be written only in terms of the normalized decay widths $\widetilde{\Gamma}_M(XX^*)_{11}$, $\widetilde{\Gamma}_M(XX^*)_{22}$ and $\mathrm{Re}\widetilde{\Gamma}_M(XX^*)_{12}$ (where $X = D; C$), and in terms of the phase difference θ_{21}

$$\begin{aligned} S_+(M) &\equiv \left(\Gamma(M^-) + \Gamma(M^+)\right) \\ &= 2(2-\delta_{\ell_1\ell_2})|B_{\ell_1 N_1}|^2|B_{\ell_2 N_1}|^2\Bigg\{\widetilde{\Gamma}_M(DD^*)_{11}\left[1+\kappa_{\ell_1}^2\kappa_{\ell_2}^2\frac{\widetilde{\Gamma}_M(DD^*)_{22}}{\widetilde{\Gamma}_M(DD^*)_{11}}+2\kappa_{\ell_1}\kappa_{\ell_2}\cos\theta_{21}\delta_1\right] \\ &+\widetilde{\Gamma}_M(CC^*)_{11}\left[1+\kappa_{\ell_1}^2\kappa_{\ell_2}^2\frac{\widetilde{\Gamma}_M(CC^*)_{22}}{\widetilde{\Gamma}_M(CC^*)_{11}}+2\kappa_{\ell_1}\kappa_{\ell_2}\cos\theta_{21}\delta_1\right]+(D-C\text{ terms})\Bigg\}\,, \end{aligned} \tag{4.13}$$

where we used the notations Eq.(4.12), and the quantity δ_1 measures the effect of N_1-N_2 overlap contributions

$$\delta_j \equiv \frac{\mathrm{Re}\widetilde{\Gamma}_M(XX^*)_{12}}{\widetilde{\Gamma}_M(XX^*)_{jj}}\,, \quad (X = D; C; \quad j = 1; 2)\,. \tag{4.14}$$

It is expected that $\delta_j \approx 0$ when $\Delta M_N \gg \Gamma_{N_j}$ because in such a case the overlap (interference) effects of the N_1 and N_2 exchanges are expected to be absent due to a large distance between the two "bumps" of the neutrino propagators.

The (CP-violating) difference $S_-(M) \equiv (\Gamma(M^-) - \Gamma(M^+))$ of the LV rare decays is:

$$\begin{aligned} S_-(M) &\equiv \left(\Gamma(M^-) - \Gamma(M^+)\right) = 4(2-\delta_{\ell_1\ell_2})|B_{\ell_1 N_1}||B_{\ell_2 N_1}||B_{\ell_1 N_2}||B_{\ell_2 N_2}| \\ &\times \Bigg\{\sin\theta_{21}\left[\mathrm{Im}\widetilde{\Gamma}_M(DD^*)_{12}+\mathrm{Im}\widetilde{\Gamma}_M(CC^*)_{12}\right]+(D-C\text{ terms})\Bigg\}\,. \end{aligned} \tag{4.15}$$

We can see that CP violation in these decays is proportional to the CP-odd phase difference θ_{21} defined in Eq. (4.12c). The other factor in this CP violation is the imaginary part of $\widetilde{\Gamma}_M(DD^*)_{12} + \widetilde{\Gamma}_M(CC^*)_{12}$. This factor contains $\mathrm{Im}P_1(D)P_2(D)^*$ and $\mathrm{Im}P_1(C)P_2(C)^*$ which was investigated in Eq. (3.35) and given in detail in appendix D.

The decay widths Γ_{N_j} are very small in comparison with the masses M_{N_j}, due to the mixing suppression (in general $\Gamma_{N_j} \ll 1$ eV). Therefore, the absolute value of the square of the intermediate neutrino propagator can be approximated to a high degree of accuracy by the delta function as in Eq.(3.34)

$$\begin{aligned} |P_j(D)|^2 &= \left|\frac{1}{(p_M-p_1)^2 - M_{N_j}^2 + i\Gamma_{N_j}M_{N_j}}\right|^2 \\ &\approx \frac{\pi}{M_{N_j}\Gamma_{N_j}}\delta((p_M-p_1)^2 - M_{N_j}^2)\,; \quad (j=1,2;\ \Gamma_{N_j} \ll M_{N_j})\,, \end{aligned} \tag{4.16}$$

and analogous equation for $|P_j(C)|^2$. Therefore, in the integration d_3, the part of integration dp_N^2 ($p_N = p_M - p_1$ in D channel; $p_N = p_M - p_2$ in C channel) becomes a trivial integration over

a delta function, and the expressions for the diagonal elements $\widetilde{\Gamma}_M(DD^*)_{jj}$ and $\widetilde{\Gamma}_M(CC^*)_{jj}$ can be calculated analytically, cf. Appendix E

$$\widetilde{\Gamma}_M(DD^*)_{jj} = \frac{K_M^2 M_M^5}{128\pi^2}\frac{M_{N_j}}{\Gamma_{N_j}}\lambda^{1/2}(1,x_j,x_{\ell_1})\lambda^{1/2}\left(1,\frac{x^{'}}{x_j},\frac{x_{\ell_2}}{x_j}\right)\times$$
$$Q(x_j;x_{\ell_1},x_{\ell_2},x^{'}) \qquad (j=1 \text{ or } j=2)\ , \tag{4.17}$$

and $\widetilde{\Gamma}_M(CC^*)_{jj}$ is obtained from the expression (4.17) by the simple exchange $x_{\ell_1} \leftrightarrow x_{\ell_2}$

$$\widetilde{\Gamma}_M(CC^*)_{jj} = \widetilde{\Gamma}_M(DD^*)_{jj}(x_{\ell_1} \leftrightarrow x_{\ell_2})\ . \tag{4.18}$$

In Eq. (4.17) we used the notations

$$\lambda(y_1,y_2,y_3) = y_1^2+y_2^2+y_3^2-2y_1y_2-2y_2y_3-2y_3y_1\ , \tag{4.19a}$$

$$x_j = \frac{M_{N_j}^2}{M_M^2}\ ,\quad x_{\ell_s}=\frac{M_{\ell_s}^2}{M_M^2}\ ,\quad x^{'}=\frac{M_{M'}^2}{M_M^2}\ ,\quad (j=1,2;\ \ell_s=\ell_1,\ell_2)\ , \tag{4.19b}$$

and the function $Q(x_j;x_{\ell_1},x_{\ell_2},x^{'})$ is given in Appendix E. In the special case $\ell_1=\ell_2$, the expression for $\widetilde{\Gamma}_M(DD^*)_{jj}$ is somewhat simpler and can be deduced, e.g., from Ref. [25]. The expressions (4.17) and (4.18) are used in the evaluation of the sum $S_+(M)$, Eq. (4.13), of the rare decay widths of $M^\pm$. In Eq. (4.13), the contributions of the N_1-N_2 overlap effects are parametrized in the function δ_1 defined in Eq. (4.14), and it was evaluated in figure 3.11 and Table 3.2 of Sec.3. It is interesting that the numerical results for $\delta(y)$ for the considered decay are indistinguishable from those of the decay $\pi^\pm \to e^\pm e^\pm \mu^\mp \nu$ in Sec.3. Further, $\delta(y)$ ($y \equiv \frac{\Delta M_N}{\Gamma_N}$, see Sec.3 Eqs. 3.37) is independent of $M^\pm$ and $M'^\mp$, as long as $\ell_1,\ell_2 = e,\mu$.

In order to evaluate the CP-violating difference $S_-(M)$, Eq. (4.15), of the rare decay widths $M^\pm$, the evaluation of the quantity $\mathrm{Im}\overline{\Gamma}_M(XX^*)_{12}$ ($X=D;C$) is of central importance. In the integrand of $\mathrm{Im}\overline{\Gamma}_M(XX^*)_{12}$ we have to take into account equations (4.7) and (3.35) and these lead to the result:

$$\mathrm{Im}\widetilde{\Gamma}_M(DD^*)_{12} = \eta\ \frac{K_M^2 M_M^5}{128\pi^2}\frac{M_{N_1}M_{N_2}}{(M_{N_2}+M_{N_1})\Delta M_N}$$
$$\times\sum_{j=1}^{2}\lambda^{1/2}(1,x_j,x_{\ell_1})\ ,\lambda^{1/2}\left(1,\frac{x^{'}}{x_j},\frac{x_{\ell_2}}{x_j}\right)Q(x_j;x_{\ell_1},x_{\ell_2},x^{'})\ , \tag{4.20a}$$

$$\mathrm{Im}\widetilde{\Gamma}_M(CC^*)_{12} = \mathrm{Im}\widetilde{\Gamma}_M(DD^*)_{12}(x_{\ell_1} \leftrightarrow x_{\ell_2})\ , \tag{4.20b}$$

where we denoted $\Delta M_N \equiv M_{N_2}-M_{N_1} > 0$. In Eqs. (4.20) we introduced an overall factor η which accounts for the N_1-N_2 overlap effects when $\Delta M_N \not\gg \Gamma_N$, i.e., for the situation when the naive approximation for $\mathrm{ImP_1(D)P_2(D)^*}$ in Eq.(3.35b) with $\eta=1$, is not justified.

The canonical decay matrix elements $\widetilde{\Gamma}_M(XY^*)_{ij}$, Eq. (4.7), were evaluated numerically, by means of two differents codes (Vegas and Mathematica), using finite (small) widths Γ_{N_j} in the propagators.
The numerical simulation gave for $\delta(y)$ and $\eta(y)$ equal results for $(\pi^\pm \to e^\pm e^\pm \mu^\mp \nu)$ leptonic decay (3.10), (3.1) and for $(M^\pm \to \ell_1^\pm \ell_2^\pm M'^\mp)$ semihadronic decay (3.11),(3.2). For the results, see Tables 3.1, 3.2 and Figs. 3.10 and 3.11.

The numerical simulations gave us the following results:

- The analytic expression (4.17) for $\widetilde{\Gamma}_M^{(X)}(DD^*)_{jj}$ $(\propto 1/\Gamma_{N_j})$ is valid.
- The analytic expression (4.20) with $\eta = 1$ for $\mathrm{Im}\widetilde{\Gamma}_M(DD^*)_{12}$ $(\propto 1/\Delta M_N)$ is valid when $\Delta M_N \gg \Gamma_{N_j}$, and $\eta = \frac{y^2}{y^2+1}$ for $\Delta M_N \sim \Gamma_{Nj}$ (see Eq. 3.36, Sec.3)
- The direct-crossed channel (DC^* and CD^*) interference contributions to the sum and the difference of the rare decay widths $S_\pm(M)$ of $M^\pm$ are by several orders of magnitude smaller that the corresponding direct (DD^*) and crossed (CC^*) channel contributions to these quantities, in all cases.[1]

The rare LV semihadronic decay widths of $M^\pm$, cf. $S_+(M)$ of Eq. (4.13), at first sight appear to be quartic in the heavy-light mixing elements $|B_{\ell N}|$ and thus very suppressed.
However, they are proportional to the expressions $\widetilde{\Gamma}_M(DD^*)_{jj}$, Eq. (4.17), which are proportional to $1/\Gamma_{N_j}$ due to the on-shellness of the intermediate N_j's. This $1/\Gamma_{N_j}$ is proportional to $1/\widetilde{\mathcal{K}}_j \sim 1/|B_{\ell N_j}|^2$ according to Eqs. (3.13)-(3.15). Hence this on-shellness of N_j's makes these rare process decay widths significantly less suppressed

$$\widetilde{\Gamma}_M(DD^*)_{jj} \propto 1/\Gamma_{N_j} \propto 1/\widetilde{\mathcal{K}}_j \propto 1/|B_{\ell N_j}|^2 \;\Rightarrow\; S_+(M) \propto |B_{\ell N_j}|^2 \,. \tag{4.21}$$

However, the expressions (4.20), which appear in the CP-violating decay width difference $S_-(M)$ (4.15), are suppressed by mixings as $\sim |B_{\ell N}|^4$. This means that in general $S_-(M)$ is much smaller than the decay width $S_+(M) \propto |B_{\ell N_j}|^2$. Nonetheless, Eqs. (4.20) show that $S_-(M)$ is proportional to $1/\Delta M_N$, and it is this aspect that represents the opportunity to detect appreciable CP violation in such decays when ΔM_N is sufficiently small. While in general we expect $\Delta M_N \gg \Gamma_{N_j}$, there exists a well-motivated model νMSM [29–34] with two heavy sterile almost degenerate neutrinos (where the relation $\Delta M_N \not\gg \Gamma_{N_j}$ is possible) in the mass range $0.1 \text{ GeV} \lesssim M_{N_j} \lesssim 10^1 \text{ GeV}$. Our calculations thus suggest that in such a model the CP violation effects may be appreciable, namely for $\Delta M_N \sim \Gamma_N$ we obtain $S_-(M) \sim S_+(M)$ and thus $\mathcal{A}_{\mathrm{CP}}(M) \sim 1$. These conclusions are similar to those of CP violation in $\pi^\pm \to e^\pm e^\pm \mu^\mp \nu$ decays of Sec.3.

For these reasons, from now on we consider the case of near degeneracy: $\Delta M_N \not\gg \Gamma_N$ $(\frac{\Delta M_N}{\Gamma_N} = y \approx 1)$. In this case, several formulas written by now in this Section get even more

[1] For example, when $M^\pm = K^\pm$ and $M'^\mp = \pi^\mp$, and we choose in numerical calculation $\Gamma_N \sim 10^{-3}$ GeV $\sim \Delta M_N$, the $\widetilde{\Gamma}(DD^*)_{ij}$ and $\widetilde{\Gamma}(CC^*)_{ij}$ contributions are by about two orders of magnitude larger than the D-C interference contributions $\widetilde{\Gamma}_\pm(DC^*)_{ij}$. When Γ_N and ΔM_N are decreased further ($\Gamma_N \sim \Delta M_N$), the $\widetilde{\Gamma}(DD^*)_{ij}$ and $\widetilde{\Gamma}(CC^*)_{ij}$ contributions increase (they are $\propto 1/\Gamma_N$), while the D-C interference contributions $\widetilde{\Gamma}_\pm(DC^*)_{ij}$ remain approximately unchanged and become thus relatively insignificant.

simplified, in particular the expressions (4.17), (4.14), (4.20). Namely, they can be written in terms of the common canonical decay width $\overline{S}$ ratio[2]

$$\overline{S}(x;x_{\ell_1},x_{\ell_2},x') \equiv \frac{3\pi}{4}\frac{K_M^2 M_M}{G_F^2}\frac{1}{x^2}\lambda^{1/2}(1,x,x_{\ell_1})\lambda^{1/2}\left(1,\frac{x'}{x},\frac{x_{\ell_2}}{x}\right)Q(x;x_{\ell_1},x_{\ell_2},x') \ , \quad (4.22)$$

where we use the notations (4.19) and

$$x \equiv \frac{M_N^2}{M_M^2} \equiv x_2 \approx x_1 \ , \quad (4.23)$$

where we denoted by $M_N \equiv M_{N_2} \approx M_{N_1}$. The function Q is the same as in Eqs. (4.17) and (4.20), and is given explicitly in Appendix E. In practice we will need two variants of this function $\overline{S}$, namely the one for the DD^* contributions ($\overline{S}^{(D)}$) and the one of the CC^* contributions ($\overline{S}^{(C)}$)

$$\overline{S}^{(D)}(x) \equiv \overline{S}(x;x_{\ell_1},x_{\ell_2},x') \ , \quad (4.24a)$$
$$\overline{S}^{(C)}(x) \equiv \overline{S}(x;x_{\ell_2},x_{\ell_1},x') \ . \quad (4.24b)$$

When $\ell_1 = \ell_2$ (e.g., when both final leptons are electrons; or both are muons), the two functions $\overline{S}^{(D)}$ and $\overline{S}^{(C)}$ coincide. It is straightforward to check that the expressions of Eqs. (4.17), (4.14), (4.20) can then be rewritten in the considered case of nearly degenerate N_1 and N_2 in terms of these common functions $\overline{S}^{(X)}$ ($X = D, C$) and of the heavy-light mixing expressions $\widetilde{\mathcal{K}}_j^{Ma}$.

$$\widetilde{\Gamma}_M(DD^*)_{jj} = \frac{1}{\widetilde{\mathcal{K}}_j^{Ma}}\overline{S}^{(D)}(x) \quad ; \qquad \widetilde{\Gamma}_M(CC^*)_{jj} = \frac{1}{\widetilde{\mathcal{K}}_j^{Ma}}\overline{S}^{(C)}(x) \quad (4.25a)$$

$$\mathrm{Re}\widetilde{\Gamma}_M(DD^*)_{12} = \delta(y)\frac{2}{(\widetilde{\mathcal{K}}_1^{Ma}+\widetilde{\mathcal{K}}_2^{Ma})}\overline{S}^{(D)}(x) \quad ; \quad \mathrm{Re}\widetilde{\Gamma}_M(CC^*)_{12} = \delta(y)\frac{2}{(\widetilde{\mathcal{K}}_1^{Ma}+\widetilde{\mathcal{K}}_2^{Ma})}\overline{S}^{(C)}(x) \quad (4.25b)$$

$$\mathrm{Im}\widetilde{\Gamma}_M(DD^*)_{12} = \frac{\eta(y)}{y}\frac{2}{(\widetilde{\mathcal{K}}_1^{Ma}+\widetilde{\mathcal{K}}_2^{Ma})}\overline{S}^{(D)}(x) \quad ; \quad \mathrm{Im}\widetilde{\Gamma}_M(CC^*)_{12} = \frac{\eta(y)}{y}\frac{2}{(\widetilde{\mathcal{K}}_1^{Ma}+\widetilde{\mathcal{K}}_2^{Ma})}\overline{S}^{(C)}(x) \quad (4.25c)$$

where the definition $y \equiv \Delta M_N/\Gamma_N$ is kept (we recall: $\Gamma_N \equiv \frac{1}{2}(\Gamma_{N1}+\Gamma_{N2})$).

After some straightforward algebra, we can rewrite the sum and difference $S_\pm(M)$ of decay widths, Eqs. (4.10), as expressions proportional to these canonical decay widths $\overline{S}^{(X)}$ ($X = D, C$). The proportionality factors involve the heavy-light mixing factors $|B_{\ell N_j}|$ and $\widetilde{\mathcal{K}}_j^{Ma}$, and the overlap functions $\delta(y)$ and $\eta(y)/y$ tabulated in Tables 3.2 and 3.1. The resulting expressions are:

[2]Canonical: in these sense that it has no dependence on mixings.

$$S_+(M) \equiv \Gamma(M^- \to \ell_1^- \ell_2^- M'^+) + \Gamma(M^+ \to \ell_1^+ \ell_2^+ M'^-) = 2(2-\delta_{\ell_1\ell_2}) \times \tag{4.26a}$$

$$\times \left[\sum_{j=1}^{2} \frac{|B_{\ell_1 N_j}|^2 |B_{\ell_2 N_j}|^2}{\widetilde{\mathcal{K}}_j^{Ma}} + 4\delta(y) \frac{|B_{\ell_1 N_1}||B_{\ell_2 N_1}||B_{\ell_1 N_2}||B_{\ell_2 N_2}|}{(\widetilde{\mathcal{K}}_1^{Ma} + \widetilde{\mathcal{K}}_2^{Ma})} \cos\theta_{21}\right] \left(\overline{S}^{(D)}(x) + \overline{S}^{(C)}(x)\right)$$

$$S_-(M) \equiv \Gamma(M^- \to \ell_1^- \ell_2^- M'^+) - \Gamma(M^+ \to \ell_1^+ \ell_2^+ M'^-)$$

$$= 8(2-\delta_{\ell_1\ell_2}) \frac{|B_{\ell_1 N_1}||B_{\ell_2 N_1}||B_{\ell_1 N_2}||B_{\ell_2 N_2}|}{(\widetilde{\mathcal{K}}_1^{Ma} + \widetilde{\mathcal{K}}_2^{Ma})} \sin\theta_{21} \frac{\eta(y)}{y} \left(\overline{S}^{(D)}(x) + \overline{S}^{(C)}(x)\right) . \tag{4.26b}$$

The resulting CP violation ratio $\mathcal{A}_{\rm CP}(M)$, Eq. (4.11), can then be written in a form involving only the heavy-light mixing factors $|B_{\ell N_j}|$ and $\widetilde{\mathcal{K}}_j^{Ma}$, and the overlap functions $\delta(y)$ and $\eta(y)/y$ tabulated in Tables 3.2 and 3.1:

$$\mathcal{A}_{\rm CP}(M) \equiv \frac{S_-(M)}{S_+(M)} \equiv \frac{\Gamma(M^- \to \ell_1^- \ell_2^- M'^+) - \Gamma(M^+ \to \ell_1^+ \ell_2^+ M'^-)}{\Gamma(M^- \to \ell_1^- \ell_2^- M'^+) + \Gamma(M^+ \to \ell_1^+ \ell_2^+ M'^-)}$$

$$= \frac{\sin\theta_{21}}{\left[\frac{1}{4}\sum_{j=1}^{2} \frac{|B_{\ell_1 N_j}|^2 |B_{\ell_2 N_j}|^2}{|B_{\ell_1 N_1}||B_{\ell_2 N_1}||B_{\ell_1 N_2}||B_{\ell_2 N_2}|} \frac{(\widetilde{\mathcal{K}}_1^{Ma} + \widetilde{\mathcal{K}}_2^{Ma})}{\widetilde{\mathcal{K}}_j^{Ma}} + \delta(y)\cos\theta_{21}\right]} \frac{\eta(y)}{y} \tag{4.27a}$$

$$= \frac{\sin\theta_{21}}{\left\{\frac{1}{4}\left[\kappa_{\ell_1}\kappa_{\ell_2}\left(1 + \frac{\widetilde{\mathcal{K}}_1^{Ma}}{\widetilde{\mathcal{K}}_2^{Ma}}\right) + \frac{1}{\kappa_{\ell_1}\kappa_{\ell_2}}\left(1 + \frac{\widetilde{\mathcal{K}}_2^{Ma}}{\widetilde{\mathcal{K}}_1^{Ma}}\right)\right] + \delta(y)\cos\theta_{21}\right\}} \frac{\eta(y)}{y} . \tag{4.27b}$$

In Eq. (4.27b) we used the notations (4.12a).

When $\ell_1 = \ell_2$ ($\equiv \ell$), the formulas (4.26)-(4.27) simplify because then $\overline{S}^{(D)} = \overline{S}^{(C)} = \overline{S}$, and $B_{\ell_1 N_j} = B_{\ell_2 N_j} = B_{\ell N_j}$, $\kappa_{\ell_1} = \kappa_{\ell_2} = \kappa_\ell$.

$$S_+(M) = = 4\left[\sum_{j=1}^{2} \frac{|B_{\ell N_j}|^4}{\widetilde{\mathcal{K}}_j^{Ma}} + 4\delta(y) \frac{|B_{\ell N_1}|^2 |B_{\ell N_2}|^2}{(\widetilde{\mathcal{K}}_1^{Ma} + \widetilde{\mathcal{K}}_2^{Ma})} \cos\theta_{21}\right] \overline{S}(x) , \tag{4.28a}$$

$$S_-(M) = 16 \frac{|B_{\ell N_1}|^2 |B_{\ell N_2}|^2}{(\widetilde{\mathcal{K}}_1^{Ma} + \widetilde{\mathcal{K}}_2^{Ma})} \sin\theta_{21} \frac{\eta(y)}{y} \overline{S}(x) , \tag{4.28b}$$

$$\mathcal{A}_{\rm CP}(M) = \frac{\sin\theta_{21}}{\left\{\frac{1}{4}\left[\kappa_\ell^2\left(1 + \frac{\widetilde{\mathcal{K}}_1^{Ma}}{\widetilde{\mathcal{K}}_2^{Ma}}\right) + \frac{1}{\kappa_\ell^2}\left(1 + \frac{\widetilde{\mathcal{K}}_2^{Ma}}{\widetilde{\mathcal{K}}_1^{Ma}}\right)\right] + \delta(y)\cos\theta_{21}\right\}} \frac{\eta(y)}{y} . \tag{4.28c}$$

From these expressions and Table 3.1 we can deduce:

1. When y becomes large ($y > 10$, i.e., $\Delta M_N > 10\Gamma_N$), the CP asymmetries (4.26b)-(4.27) become suppressed by the small $\eta(y)/y$ factor.
2. When y is smaller ($y < 10$, e.g., $0.33\ \Gamma_N < \Delta M_N < 5\ \Gamma_N$), then the factor $\eta(y)/y$ is comparable with unity, the expressions $S_\pm(M)$ become $\sim |B_{\ell N_j}|^2 \overline{S}^{(D)}(x)$ (where $x \equiv M_N^2/M_M^2$; $\ell = e, \mu$; note that $\widetilde{\mathcal{K}}_j^{Ma} \sim |B_{\ell N_j}|^2$); and the CP violation ratio $\mathcal{A}_{\rm CP}(M)$ becomes ~ 1.

In Ref. [25], the decay widths for these processes, in the case of one (on-shell) neutrino N, $\Gamma(M^+) \equiv \Gamma(M^+ \to \ell^+\ell^+M'^-)$, were considered. Since in our case $S_+(M) \approx 2\Gamma(M^+)$,[3] the conclusions in Ref. [25] on the size and measurability of $\Gamma(M^+)$ can be taken over as the conclusions on the size and measurability of $S_+(M)$ here. If, in addition, $\Delta M_N \not\gg \Gamma_N$ (say: $0.33 < y \equiv \Delta M_N/\Gamma_N < 5$), these conclusions are valid also for the measurability of the CP-violating decay width difference $S_-(M)$ provided that the phase difference $|\theta_{21}| \sim 1$.[4]

4.3 The effective branching ratios

The branching ratios of experimental significance for the LV decays $M^\pm \to \ell_1^\pm \ell_2^\pm M'^\mp$ are:

$$\mathrm{Br}(M) \equiv \frac{S_+(M)}{[\Gamma(M^- \to \mathrm{all}) + \Gamma(M^+ \to \mathrm{all})]} \approx \frac{S_+(M)}{2\Gamma(M^- \to \mathrm{all})}\ , \tag{4.29a}$$

$$\mathcal{A}_{\rm CP}(M)\mathrm{Br}(M) = \frac{S_-(M)}{[\Gamma(M^- \to \mathrm{all}) + \Gamma(M^+ \to \mathrm{all})]} \approx \frac{S_-(M)}{2\Gamma(M^- \to \mathrm{all})}\ , \tag{4.29b}$$

where we use the notation of Eqs. (4.10)-(4.11) and (4.2). We also used the fact that in the considered cases of pseudoscalar mesons $M^\pm$ the total decay widths $\Gamma(M^- \to \mathrm{all})$ and $\Gamma(M^+ \to \mathrm{all})$ are practically equal. $\mathrm{Br}(M)$ represents the average of the branching ratios of M^+ and M^- for these LV decays, while $\mathcal{A}_{\rm CP}(M)\mathrm{Br}(M)$ is the corresponding branching ratio for the (CP-violating) difference. The corresponding canonical branching fraction $\overline{\mathrm{Br}}(M)$ is obtained by dividing the canonical decay width (4.22) by $2\Gamma(M^- \to \mathrm{all})$

$$\begin{aligned}\overline{\mathrm{Br}}(x; x_{\ell_1}, x_{\ell_2}, x') &\equiv \frac{\overline{S}(x; x_{\ell_1}, x_{\ell_2}, x')}{2\Gamma(M^- \to \mathrm{all})} \\ &= \frac{3\pi}{8}\frac{K_M^2 M_M}{G_F^2 \Gamma(M^- \to \mathrm{all})}\frac{1}{x^2}\lambda^{1/2}(1, x, x_{\ell_1})\lambda^{1/2}\left(1, \frac{x'}{x}, \frac{x_{\ell_2}}{x}\right) Q(x; x_{\ell_1}, x_{\ell_2}, x')\ ,\end{aligned} \tag{4.30}$$

[3] when neglecting the N_1-N_2 overlap effects $\propto \delta(y)$ in $S_+(M)$
[4] We recall that if $0.33 < y < 5$, we have $\mathcal{A}_{\rm CP}(M) \sim 1$ and thus $S_-(M) \sim S_+(M)$.

where the notations (4.19) and (4.23) are used. We have two variants of this function: the one for the DD^* contributions ($\overline{\text{Br}}^{(D)}$) and the other one of the CC^* contributions ($\overline{\text{Br}}^{(C)}$), which are obtained by dividing by $2\Gamma(M^- \to \text{all})$ the expressions $\overline{S}^{(D)}$ and $\overline{S}^{(C)}$ of Eqs. (4.24), respectively. When $\ell_1 = \ell_2$, the two functions $\overline{\text{Br}}^{(D)}$ and $\overline{\text{Br}}^{(C)}$ coincide ($\equiv \overline{\text{Br}}$).

Nonetheless, in experiments we must also take into account the acceptance (suppression) factor in the detection of these decays, which appears due to the small length of the detector in comparison to the relatively large lifetime of the (on-shell) sterile neutrinos N_j.

In Appendix C we obtained for the acceptance factor P_{N_j} the following estimates and upper bounds relevant for the K decays ($M_N \approx 0.25$ GeV), D and D_s decays ($M_N \approx 1$ GeV), and B and B_c decays ($M_N \approx 3$ GeV), see Eqs. (C.4).

The upper bounds for P_{N_j} in Eqs. (C.4) are written as a sum of the contributions of upper bounds from $|B_{eN_j}|^2$, $|B_{\mu N_j}|^2$ and $|B_{\tau N_j}|^2$ separately. Further, the contributions of $|B_{\tau N_j}|^2$ are included in Eqs. (C.4) optionally, in the parentheses, because the upper bounds of the mixings $|B_{\tau N_j}|^2$ are still very high and are expected to be reduced significantly in the foreseeable future. The upper bounds which give results higher than one are replaced by one (10^0), because the acceptance (decay probability) P_{N_j} can never be higher than one by definition.

From now on in this Section, we shall assume the following:

$$|B_{\ell N_1}|^2 \;\sim\; |B_{\ell N_2}|^2 \equiv |B_{\ell N}|^2 \tag{4.31a}$$

$$\Rightarrow\; \widetilde{\mathcal{K}}_1^{Ma} \;\sim\; \widetilde{\mathcal{K}}_2^{Ma} \equiv \widetilde{\mathcal{K}}^{Ma}\ . \tag{4.31b}$$

In addition, we consider that it is the flavor ℓ which has the dominant (largest) mixing $|B_{\ell N}|^2$. Then we have:

$$\widetilde{\mathcal{K}}^{Ma} \approx \mathcal{N}_{\ell N} |B_{\ell N}|^2 \sim 10\ |B_{\ell N}|^2\ . \tag{4.32}$$

The dominant branching ratios $\text{Br}(M)$ and $\mathcal{A}_{\text{CP}}(M)\text{Br}(M)$ will then be, according to the obtained expressions (4.26) and (4.28) (together with the definitions (4.29)-(4.30)), those which have in the final state two equal charged leptons ℓ with dominant mixing: $M^\pm \to \ell^\pm \ell^\pm M'^\mp$.

The theoretical branching ratios $\text{Br}(M)$ and $\mathcal{A}_{\text{CP}}(M)\text{Br}(M)$, Eqs. (4.29), can be obtained by dividing Eqs. (4.28a)-(4.28b) by $2\Gamma(M^- \to \text{all})$. Using in addition Eqs. (4.31)-(4.32) and the definition (4.30), this gives:

$$\text{Br}(M) \;\approx\; 8\frac{|B_{\ell N}|^4}{\widetilde{\mathcal{K}}}\overline{\text{Br}}(x) \sim \overline{\text{Br}}(x)|B_{\ell N}|^2\ , \tag{4.33a}$$

$$\mathcal{A}_{\text{CP}}(M)\text{Br}(M) \;\approx\; 8\frac{|B_{\ell N}|^4}{\widetilde{\mathcal{K}}}\sin\theta_{21}\frac{\eta(y)}{y}\overline{\text{Br}}(x) \sim \overline{\text{Br}}(x)|B_{\ell N}|^2\sin\theta_{21}\ , \tag{4.33b}$$

where in the last relation we took into account that $\eta(y)/y \sim 1$ (since $\Delta M_N \not\gg \Gamma_N$ in our considered cases).

The effective (i.e., experimental) branching ratios $\mathrm{Br}^{(\mathrm{eff})}(M) = P_N \mathrm{Br}(M)$ and $\mathcal{A}_{\mathrm{CP}}(M)\mathrm{Br}^{(\mathrm{eff})}(M)$ can be estimated, in the considered case of Eqs. (4.31)-(4.32), in the following way (using Eqs. (C.2) and (4.33)):

$$\begin{aligned} \mathrm{Br}^{(\mathrm{eff})}(M) &\equiv P_N \mathrm{Br}(M) = \overline{A}(M_N)\widetilde{\mathcal{K}}\mathrm{Br}(M) \approx \overline{A}(M_N)\widetilde{\mathcal{K}}\left(\frac{8|B_{\ell N}|^4}{\widetilde{\mathcal{K}}}\overline{\mathrm{Br}}(x)\right) \\ &= \left[8\overline{A}(M_N)\overline{\mathrm{Br}}(x)\right]|B_{\ell N}|^4 \,, \end{aligned} \tag{4.34a}$$

$$\begin{aligned} \mathcal{A}_{\mathrm{CP}}(M)\mathrm{Br}^{(\mathrm{eff})}(M) &\equiv P_N \mathcal{A}_{\mathrm{CP}}(M)\mathrm{Br}(M) \approx \overline{A}(M_N)\widetilde{\mathcal{K}}\left(\frac{8|B_{\ell N}|^4}{\widetilde{\mathcal{K}}}\sin\theta_{21}\frac{\eta(y)}{y}\overline{\mathrm{Br}}(x)\right) \\ &= 8\overline{A}(M_N)|B_{\ell N}|^4\sin\theta_{21}\frac{\eta(y)}{y}\overline{\mathrm{Br}}(x) \sim \left[4\overline{A}(M_N)\overline{\mathrm{Br}}(x)\right]|B_{\ell N}|^4\sin\theta_{21} \,, \end{aligned} \tag{4.34b}$$

where in the last line of Eq. (4.34b) we took into account that $\eta(y)/y \equiv \frac{y^2}{y^2+1} \leq \frac{1}{2}$ (the maximun achieved at $y = 1$, i.e. when $\Delta M_N = \Gamma_N$). Furthermore, since $\ell_1 = \ell_2 = \ell$ in the considered case, the canonical branching fractions are equal: $\overline{\mathrm{Br}}^{(C)}(x) = \overline{\mathrm{Br}}^{(D)}(x) \equiv \overline{\mathrm{Br}}(x)$; and we recall that $x \equiv (M_N/M_M)^2$. We see that in Eqs. (4.34) the most important factor at $|B_{\ell N}|^4$ is the "effective" canonical branching ratio:

$$\overline{\mathrm{Br}}_{\mathrm{eff}}(M_N) \equiv 8\overline{A}(M_N)\overline{\mathrm{Br}}(x) \,. \tag{4.35}$$

Only in the case of $B^\pm$ and $B_c^\pm$ LV decays we could have $P_N \sim 1$, Eq. (C.4d), and in such a case Eqs. (4.34) do not apply, but rather Eqs. (4.33).

In Figs. 4.2,4.3,4.4,4.5 and 4.7 we present the effective canonical branching ratios Eq.(4.35) as a function of the neutrino mass M_N, for various considered LV decays of the type $M^\pm \to \ell^\pm\ell^\pm M'^\mp$, where: $M = K$ in Fig. 4.2; $M = D$ in Fig. 4.3; $M = D_s$ in Fig. 4.4; $M = B$ in Fig. 4.5 and $M = B_C$ in Fig. 4.7. In general $\ell = e, \mu$. We took $L = 1$ m and $\gamma_N = 2$. In addition, for the case when $P_N \sim 1$ and consequently the estimates Eqs. (4.33) apply, we present in Figs. 4.6 and 4.8 the theoretical branching ratios $\overline{\mathrm{Br}}(x)$ as a function of M_N for $B^\pm$ and $B_c^\pm$ decays, respectively.

On other hand, our formulas permit also evaluation of $\overline{\mathrm{Br}}_{\mathrm{eff}}$ and $\overline{\mathrm{Br}}(x)$ for the decays $M^\pm \to \ell_1^\pm\ell_2^\pm M'^\mp$ when $\ell_1 \neq \ell_2$. And also when the final leptons are τ leptons (and $M^\pm = B^\pm$ or $B_c^\pm$), with the values similar to those in Figs. 4.5, 4.6, 4.7 and 4.8, except that the range of M_N is now significantly shorter: $M_{M'} + M_\tau < M_N < M_M - M_\tau$.

For the CKM matrix elements and the meson decay constants, appearing in K_M^2 factor defined in Eq. (4.9), and for masses and lifetimes of the mesons, we used the values of Ref. [59]; and for the decay constants f_B and f_{B_c} we used the values of Ref. [60]: $f_B = 0.196$ GeV, $f_{B_c} = 0.322$ GeV. We note that CKM suppresion is significantly stronger in the case of B meson ($|V_{ub}| = 0.004$) than in the case of B_C meson ($|V_{cb}| = 0.04$). D_S and π mesons have no CKM suppresion ($|V_{cs}| \approx |V_{ud}| \approx 0.98$), while K and D have minor CKM suppresion

($|V_{us}| \approx |V_{cd}| \approx 0.225$). We should also keep in mind that if $M^{\pm}$ is more massive, the final particle phase space is larger and thus $\Gamma(M^{\pm})$ is larger (but $\overline{B_r}$ is lower); M_N can be for such $M^{\pm}$ larger, too (and thus P_N).

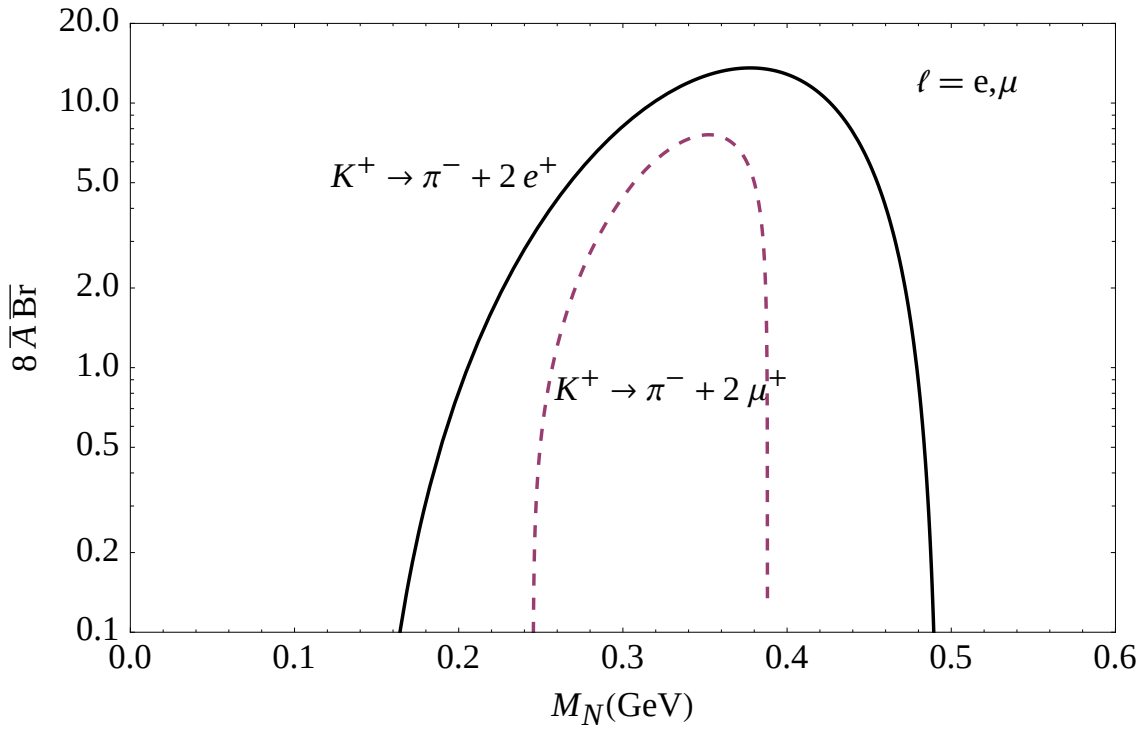

FIGURE 4.2: *The effective canonical branching ratio (4.35) for the $K^{\pm} \to \ell^{\pm}\ell^{\pm}\pi'^{\mp}$ decays ($\ell = e, \mu$) as a function of the Majorana neutrino mass M_N.*

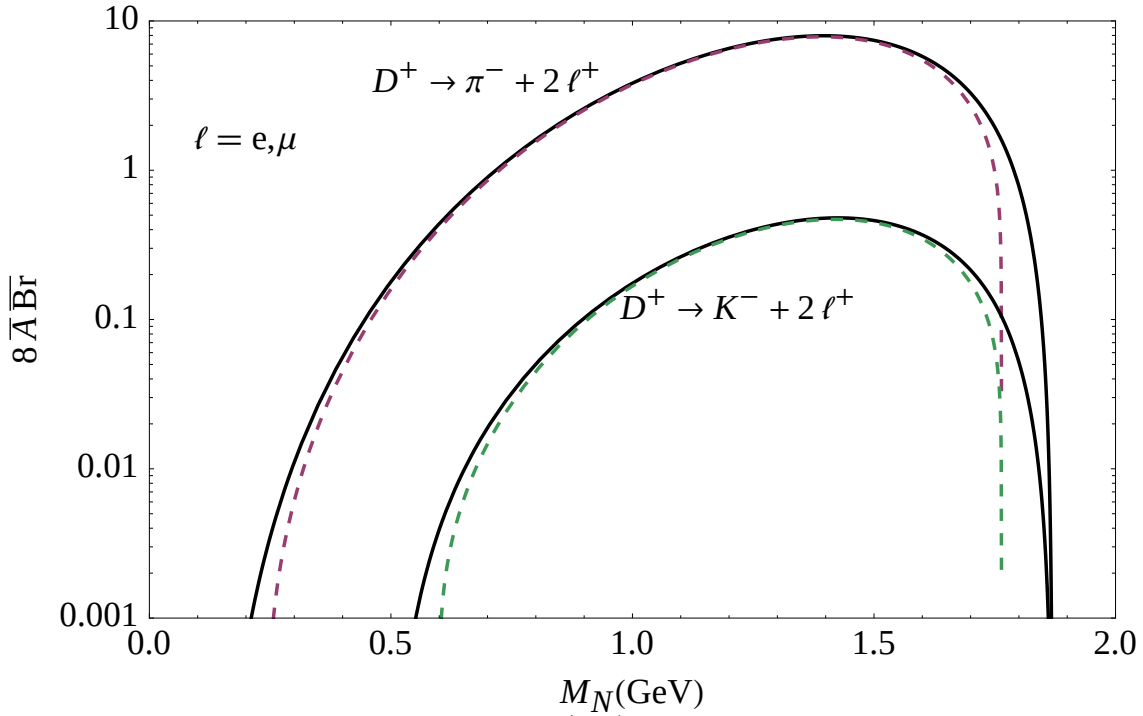

Figure 4.3: *The effective canonical branching ratio (4.35) as a function of the Majorana neutrino mass M_N for the LV decays of $D^\pm$ mesons. The solid lines are for $\ell = e$, and the dashed lines for $\ell = \mu$.*

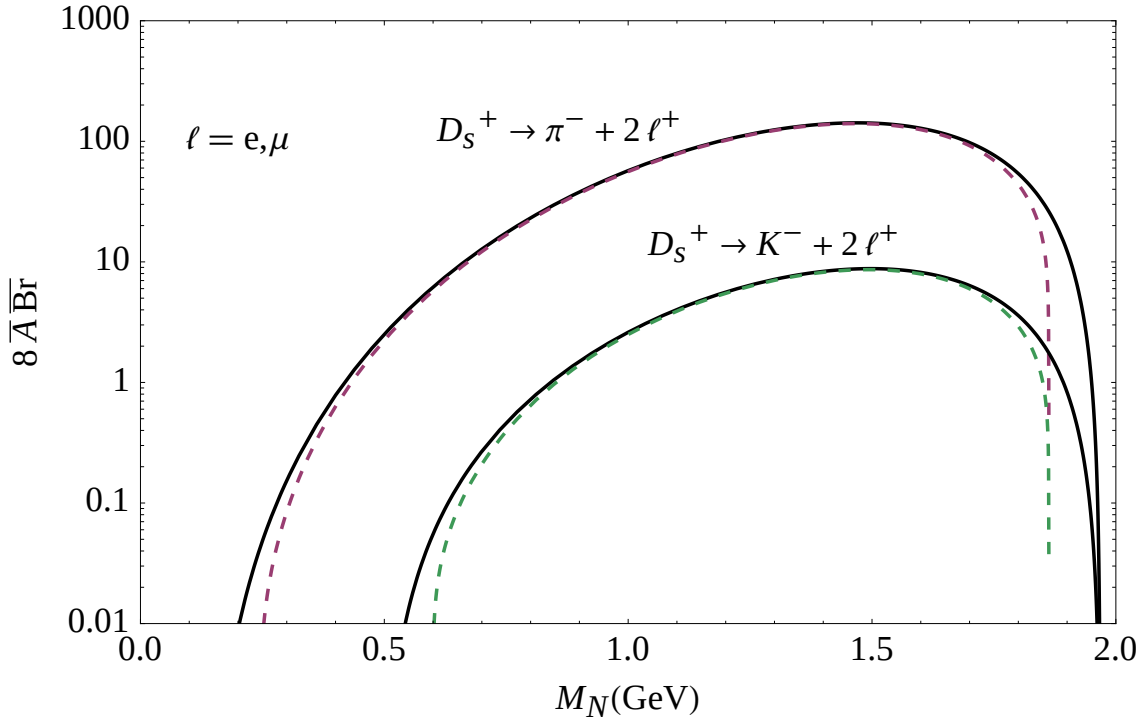

Figure 4.4: *The effective canonical branching ratio (4.35) as a function of the Majorana neutrino mass M_N for the LV decays of $D_s^\pm$ mesons.The solid lines are for $\ell = e$, and the dashed lines for $\ell = \mu$.*

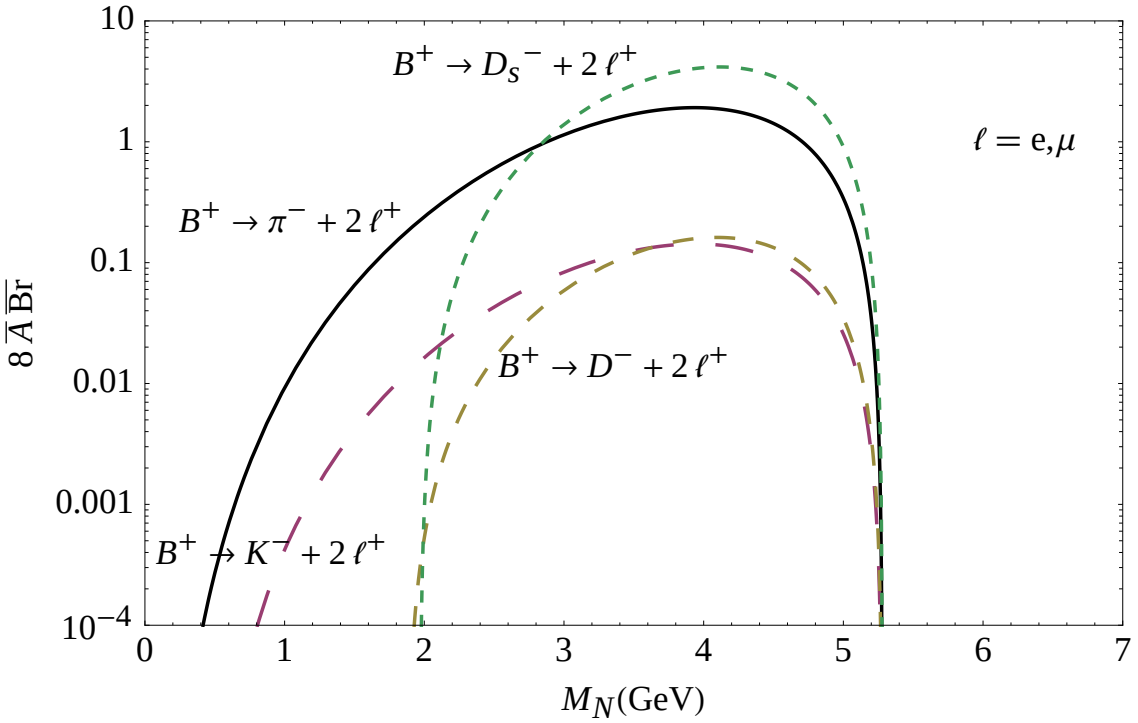

FIGURE 4.5: *The effective canonical branching ratio (4.35) as a function of the Majorana neutrino mass M_N for the LV decays of $B^{\pm}$ mesons. Here is not possible distinguish between $\ell = e, \mu$.*

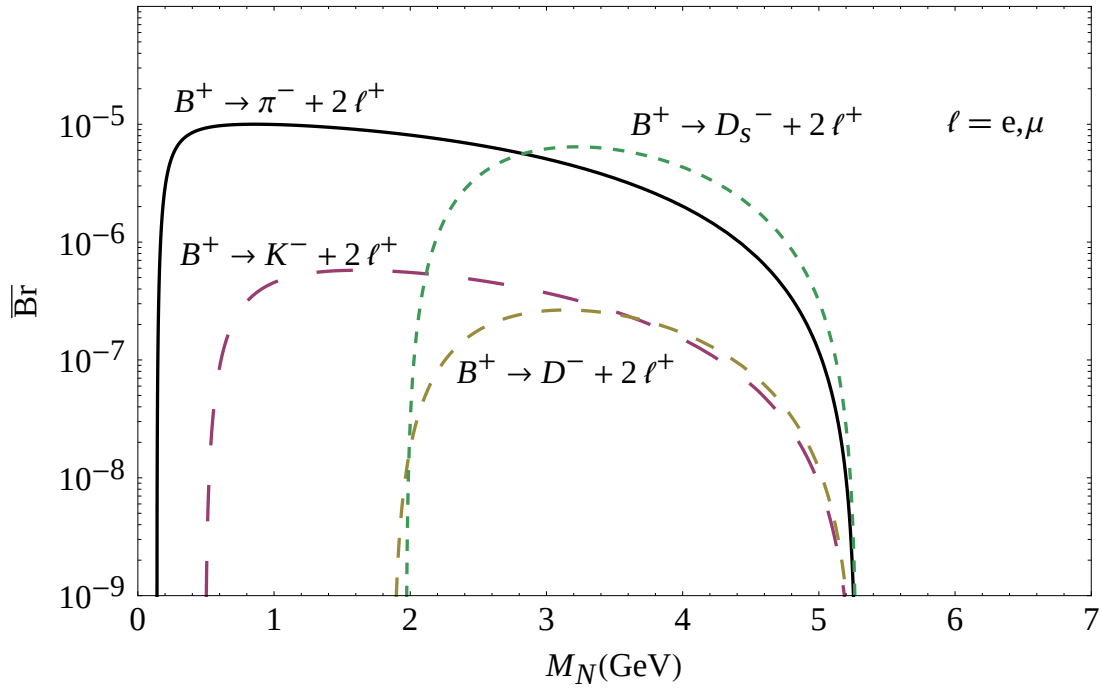

FIGURE 4.6: *The theoretical canonical branching ratios (4.30) for the $B^{\pm}$ mesons decays, where $\ell = e, \mu$ (no discernible difference between the two cases).*

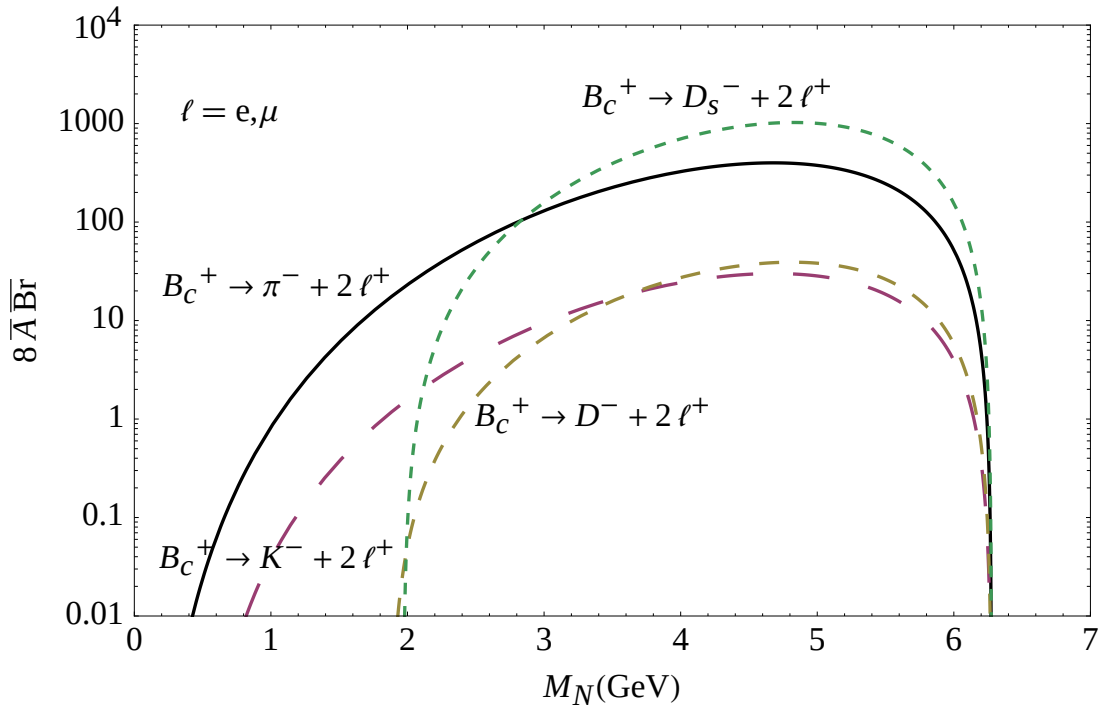

Figure 4.7: *The effective canonical branching ratio (4.35) as a function of the Majorana neutrino mass M_N for the LV decays of the charmed mesons $B_c^{\pm}$. The solid lines are for $\ell = e$, and the dashed lines for $\ell = \mu$ (no discernible difference between the two cases).*

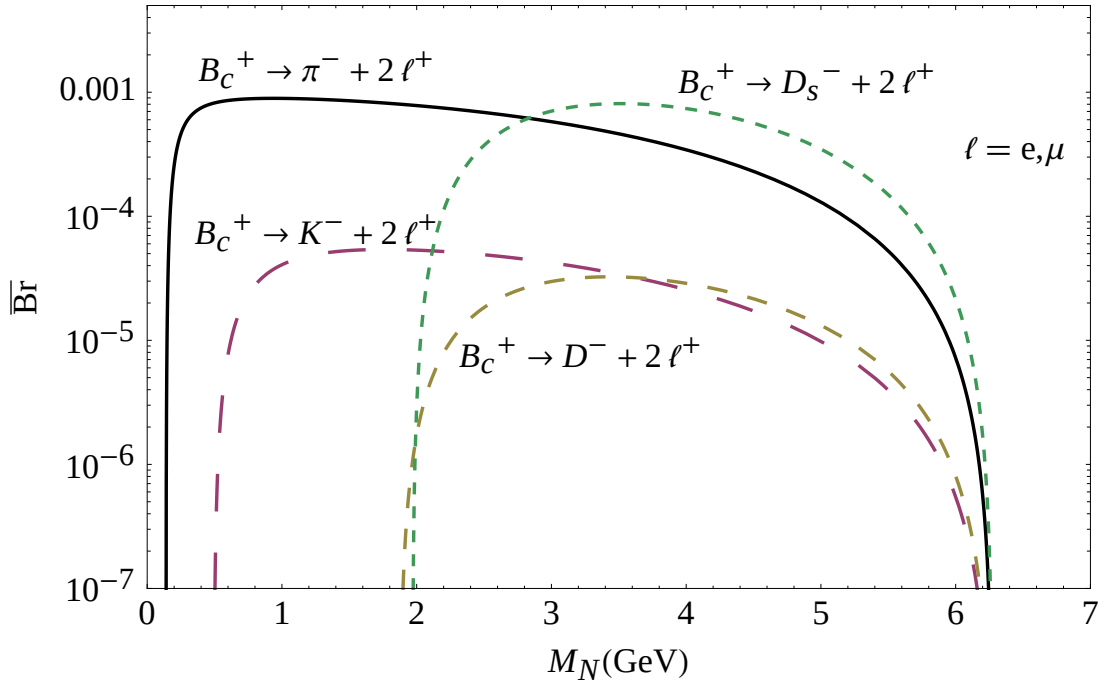

Figure 4.8: *The theoretical canonical branching ratio (4.30) for the $B_c^{\pm}$ mesons decays, where $\ell = e, \mu$ (no discernible difference between the two cases).*

In Table 4.2 we display some values of the factor $\overline{\text{Br}}_{\text{eff}}$, for the representative values of M_N in the decays $M^\pm \to \ell^\pm \ell^\pm M'^\mp$.

TABLE 4.2: *Values of the factor $8\overline{A}(M_N)\overline{\text{Br}}(x)$ (with $L = 1$ m and $\gamma_N = 2$) for some of the considered LV decays: $M^\pm \to \ell^\pm \ell^\pm \pi'^\mp$. We chose M_N such that the maximal value is obtained (this value of M_N is given in parentheses, in GeV). For the K decay, the two different values are given for $\ell = e$ and $\ell = \mu$. For all other decays $\ell = \mu$ is chosen (the values for $\ell = e$ are similar).*

$M^\pm$:	$K^\pm$ $(\ell = e)$	$K^\pm$ $(\ell = \mu)$	$D^\pm$	$D_s^\pm$	$B^\pm$	$B_c^\pm$
$8\overline{A}\overline{\text{Br}}$:	13.5 (0.38)	7.5 (0.35)	8. (1.39)	159. (1.47)	1.93 (3.9)	395. (4.7)

Let us now take, as an example, the decays $D_s^\pm \to \mu^\pm \mu^\pm \pi^\mp$,[5] and let us assume that $|B_{\mu N}|^2$ is the dominant mixing (i.e., $\ell = \mu$). Then Eqs. (4.34) and Table 4.2 imply that the effective (experimentally measurable) sum $P_N \text{Br}(D_s)$ and difference $P_N \mathcal{A}_{\text{CP}}(D_s)\text{Br}(D_s)$ of the branching ratios for these decays are

$$\text{Br}^{(\text{eff})}(D_s) \equiv P_N \text{Br}(D_s) \sim 10^2 |B_{\mu N}|^4 , \tag{4.36a}$$

$$\mathcal{A}_{\text{CP}}(D_s)\text{Br}^{(\text{eff})}(D_s) \equiv P_N \mathcal{A}_{\text{CP}}(D_s)\text{Br}(D_s) \sim 10^2 |B_{\ell N}|^4 \sin\theta_{21} \frac{\eta(y)}{y} \sim 10^2 |B_{\ell N}|^4 \sin\theta_{21} . \tag{4.36b}$$

Taking into account that in such decays the present rough upper bound on the mixing is $|B_{\mu N}|^2 \lesssim 10^{-7}$, Eqs. (4.36) imply that $P_N \text{Br}(D_s) \lesssim 10^{-12}$. The proposed experiment at CERN-SPS [35] would produce the numbers of D and D_s mesons by several orders higher than 10^{12} and would thus be able to explore whether there is a production of the sterile Majorana neutrinos N_j. Furthermore, if there are two almost degenerate neutrinos (as is the case in the νMSM model [29–31]), then in such a case it is possible that $y(\equiv \Delta M_N/\Gamma_N) \not\ll 1$, and thus $\eta(y)/y \sim 1$. Then the estimate (4.36b) would imply that the CP-violating difference of effective branching ratios $P_N \mathcal{A}_{\text{CP}}(D_s)\text{Br}(D_s)$ is of the same order as the sum $P_N \text{Br}(D_s)$ (provided that the phase difference $|\theta_{21}| \not\ll 1$). This means that if experiments discover the aforementioned νMSM-type Majorana neutrinos, they will possibly discover also CP violation in the Majorana neutrino sector.

4.4 The Future searches of semihadronic decays of K, D, D_s, B, B_c

In this section we analyze the oportunity to detect the CP violation in future experiments, as SHiP (Search for Hidden Particles) [36]. Although SHiP at this moment is just a proposal, however, the scientific community is hopeful that SHiP starts to run in 2021. In the particular case of semihadronic meson decays, SHiP in the original version cannot detect the primary decay ($M^+ \to \ell^+ N_j$), because SHiP will not have a particle detector in the primary collision region. Therefore, SHIP could only detect the secondary decay ($N_j \to \ell_2^+ M'^-$). However, there are hopes that an upgrade of the experiment can be performed, where the principal vertex can be detected [61].

[5] This is one of the preferred decay modes proposed at CERN-SPS [35].

Here we shall estimate the region of neutrino mixing $|B_{\ell N}|^2$, where the CP violation could be detected (when $\eta(y)/y \sim 1$) in the decays $M^+ \to \ell_1^+ \ell_2^+ M'^-$ mediated by two almost degenerate Majorana neutrinos N_1 and N_2. To date, the experiments provide less restrictive upper bounds for $|B_{\mu N}|$; therefore, we are interested in the CP violation in the decays $B_C^\pm \to \mu^\pm \mu^\pm \pi^\mp$ where the branching ratios can be larger, and we shall considers.

$$|B_{\mu N}| \gg |B_{eN}|, |B_{\tau N}| \ . \tag{4.37}$$

In addition we shall assume $|B_{\mu N_1}|^2 \approx |B_{\mu N_2}|^2 \equiv |B_{\mu N}|^2$.

In order to detect at least one event, we have to satisfy the next two conditions:

1. The quantity $|\mathcal{A}_{\rm CP}(M)|{\rm Br}^{\rm (eff)}(M)$ times N_M have to be greater than 1 (where N_M is the number of $M^\pm$ produces):

$$|\mathcal{A}_{\rm CP}(M)|{\rm Br}^{\rm (eff)}(M) \geq \frac{1}{N_M} \tag{4.38}$$

2. The mixing elements $|B_{\mu N}|^2$ cannot be bigger than experimental limits (EL) given in [45].

In Eq. (4.38) N_M is the number of mesons produced in the experiment in a large period of time.
The left-hand side of Eq. (4.38) is given by Eqs. (4.34)

$$|\mathcal{A}_{\rm CP}(M)|{\rm Br}^{\rm (eff)}(M) \leq \left[4\overline{A}(M_N)\overline{\rm Br}(x)\right] |B_{\mu N}|^4 \sin\theta_{21}$$

Both aforementioned conditions, have to be fulfilled simultaneously and can be summarized in one inequality, this inequality leads to found a restriction over the mixing $|B_{\mu N}|^2$:

$$EL \quad \geq \quad |B_{\mu N}|^2 \quad \geq \quad \left(\frac{1}{4\ N_M\ \overline{A}(M_N)\ \overline{\rm Br}(x) \sin\theta_{21}}\right)^{\frac{1}{2}}, \tag{4.39}$$

where EL is the present upper bound on $|B_{\mu N}|^2$.

The number of mesons B_c and B expected in SHiP is bigger than 10^{12} in five years, and the number of mesons D_s is around 10^{17} in five years [61].

In Figs. 4.9-4.14 we show the mixing region (MRS) that satisfies the inequality given in Eq. (4.39) for decays of mesons B_c, B and D_s , where we used $\sin\theta_{21} = 1$.

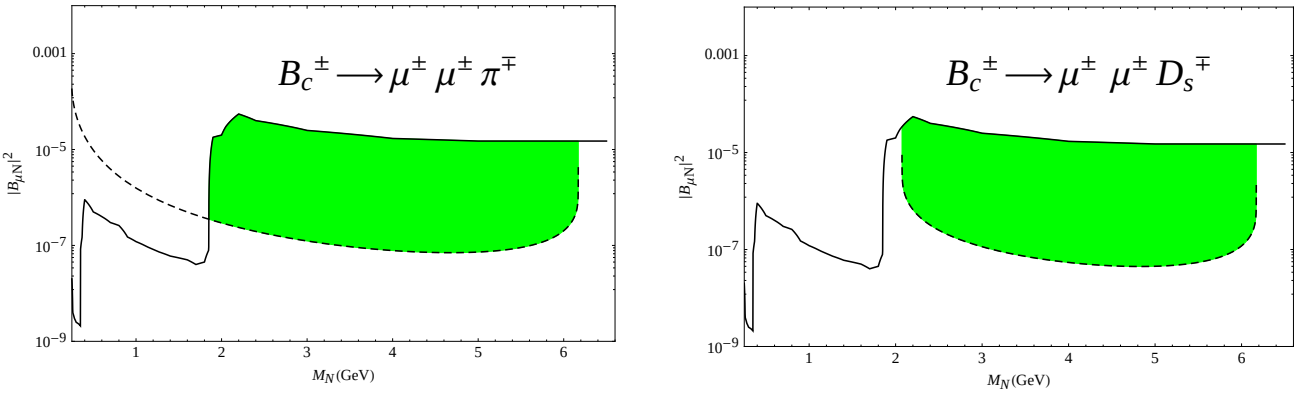

FIGURE 4.9: *Here the light grey (online green) region represents the values for which CP violation can be observed at SHiP. Left-hand: $B_c^{\pm} \to \mu^{\pm}\mu^{\pm}\pi^{\mp}$. Right-hand: $B_c^{\pm} \to \mu^{\pm}\mu^{\pm}D_s^{\mp}$. The dashed line correspond to $|\mathcal{A}_{\rm CP}(M)|{\rm Br}^{(\rm eff)}(M)$ and Black line correspond to experimental limits. Here we used $N_M = 10^{12}$, $\Delta M_N = \Gamma_N$ and $sin\theta_{21} = 1$.*

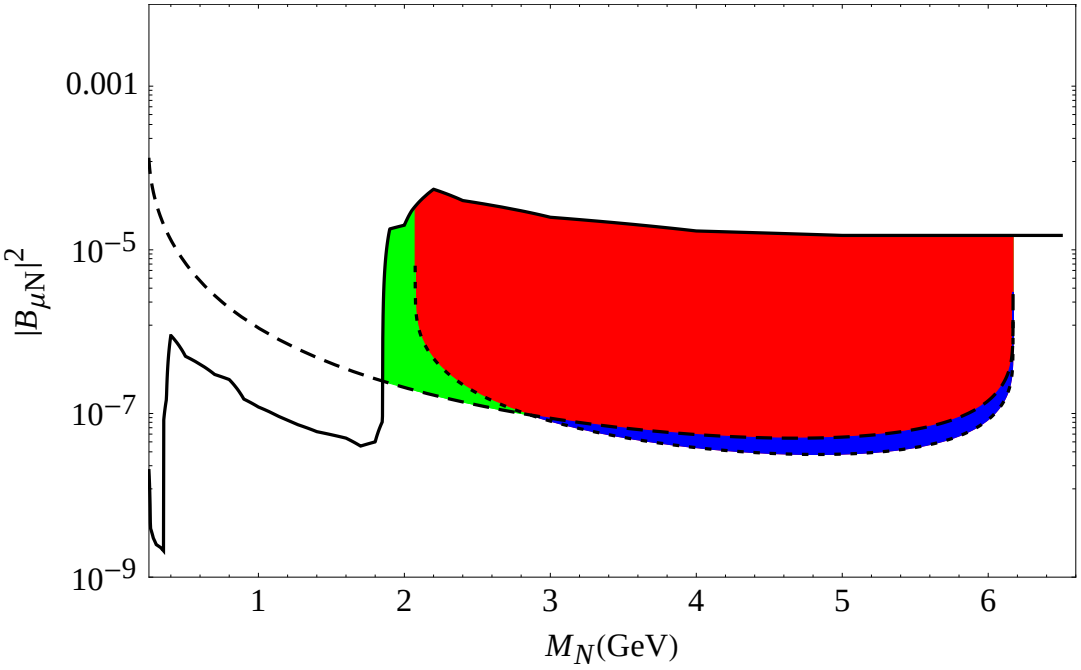

FIGURE 4.10: *The superposition of figures in 4.9.*

In Fig. 4.10 we can see three different regions. The region in grey (online: red) corresponds to MRS covered for $B_c^{\pm} \to \mu^{\pm}\mu^{\pm}\pi^{\mp}$ and $B_c^{\pm} \to \mu^{\pm}\mu^{\pm}D_s^{\mp}$ simultaneously, the light grey (online: green) region is covered only for $B_c^{\pm} \to \mu^{\pm}\mu^{\pm}\pi^{\mp}$, and the dark grey (online: blue) is covered only for $B_c^{\pm} \to \mu^{\pm}\mu^{\pm}D_s^{\mp}$.

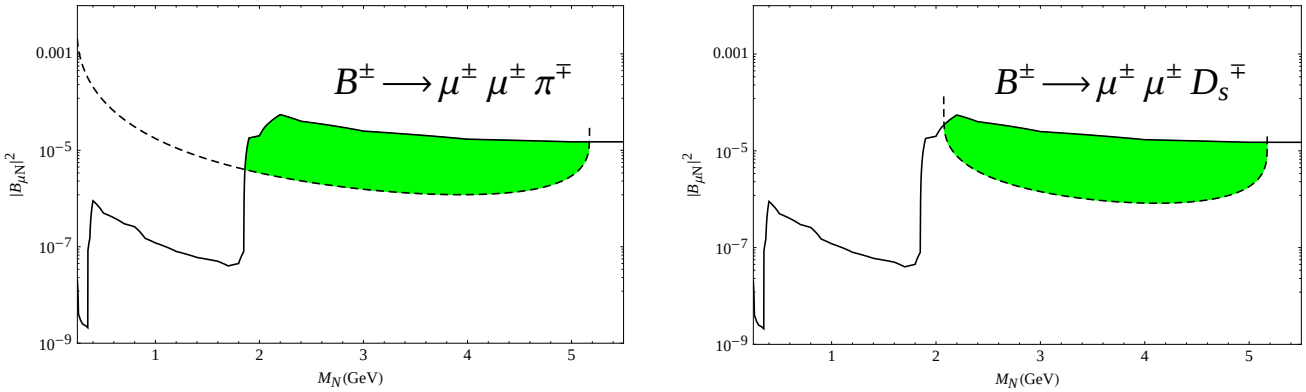

FIGURE 4.11: *The same as in Fig. 4.9, but for decays of $B^\pm$ instead of $B_C^\pm$.*

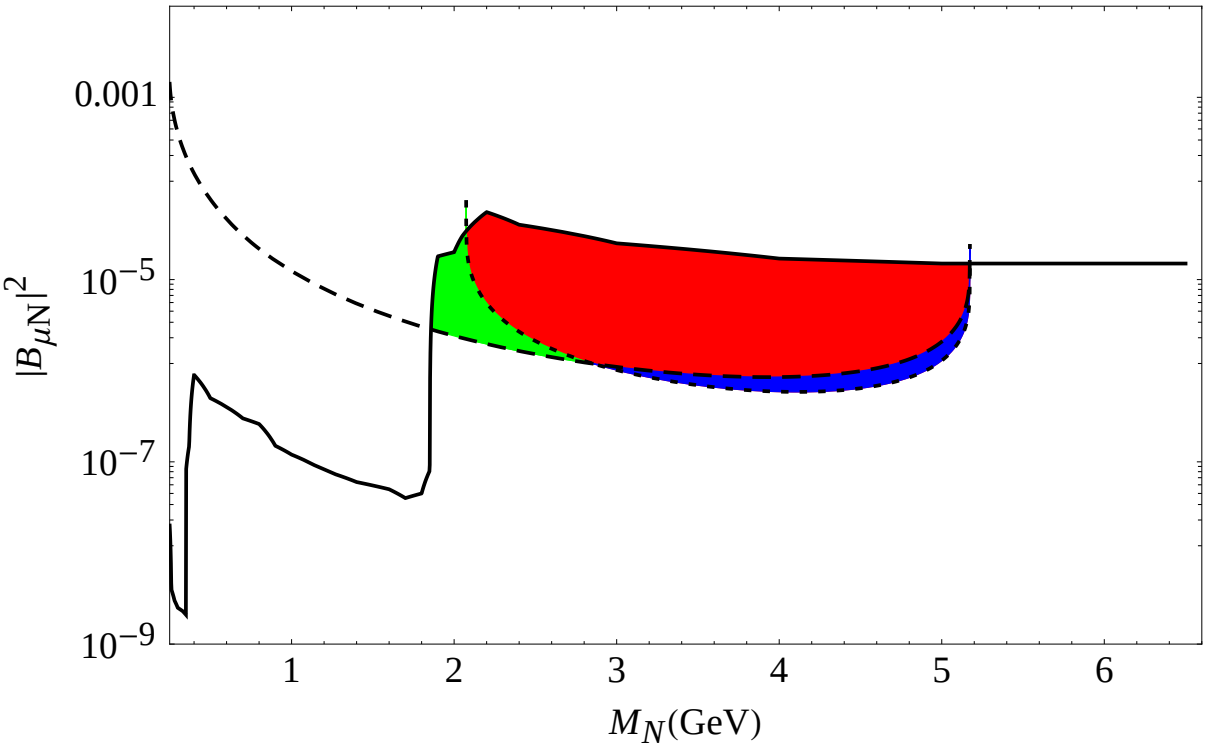

FIGURE 4.12: *The superposition of figures in 4.11.*

Figure 4.12 give analogous results, but now for $B^\pm$ decays (instead of B_C). In comparison with Fig. 4.10, these regions are significantly smaller now, due to strong CKM suppresion factor of B ($|V_{ub}| \approx 0.004$, while in B_C: $|V_{cb}| \approx 0.04$).

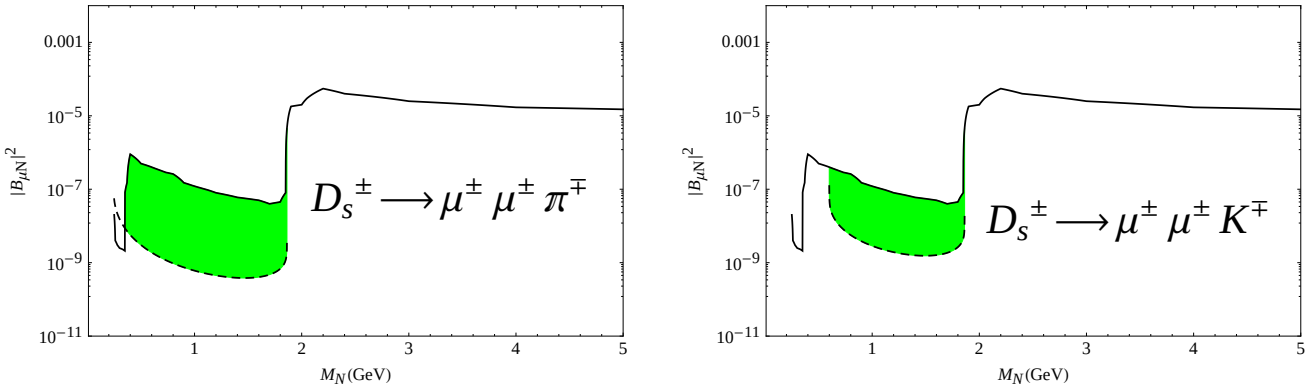

FIGURE 4.13: *The same as in Figs. 4.9, but for the decays of Left-hand:* $D_s^{\pm} \to \mu^{\pm}\mu^{\pm}\pi^{\mp}$. *Right-hand:* $D_s^{\pm} \to \mu^{\pm}\mu^{\pm}K^{\mp}$. *Here we used* $N_M = 10^{17}$.

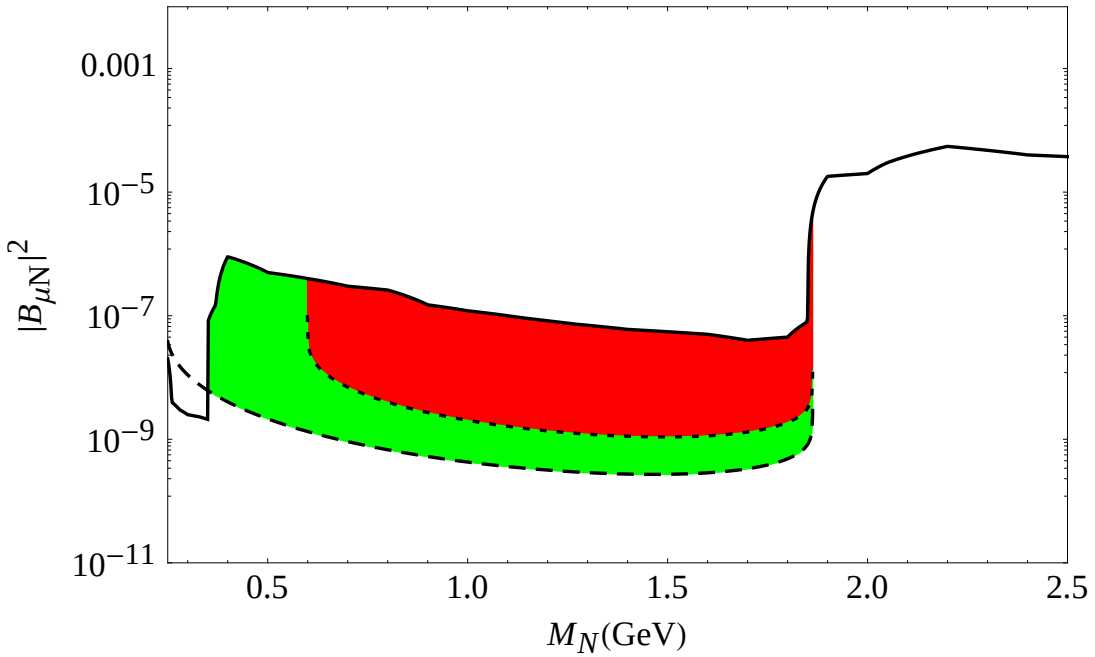

FIGURE 4.14: *The superposition of figures in 4.13.*

Fig. 4.14 gives analogous results for $D_s^{\pm} \to \mu^{\pm}\mu^{\pm}\pi^{\mp}$ and $D_s^{\pm} \to \mu^{\pm}\mu^{\pm}K^{\mp}$. In comparison with $B_C^{\pm}$ and $B^{\pm}$ decays the present upper bounds on $|B_{\mu N}|^2$ in the relevant M_N-mass range ($M_N < 2$ GeV) are significantly lower, and therefore a larger number N_M (of produced D_s) is needed.

In all considered cases, we took into account that the experiment can detect both primary and secondary decays.

Chapter 5

Oscillation of heavy sterile neutrino in decay of $B \to \mu e \pi$

In this Section we discuss neutrino oscillations in semihadronic decays (as presented in Section. 4) of heavy pseudoscalar mesons (such as B, B_c, D_s) mediated by two on-shell Majorana neutrinos N_j $(j = 1, 2)$ which are almost mass degenerate. Similar effects have been investigated recently in leptonic decays of such mesons, in the work [62], where a quantum field theoretical generalization of the Wigner-Weisskopf approach [63–65] was implemented and used. Our approach is simpler, and the results obtained are hopefully easier to interpret. This Section is based mainly in our work [66].

5.1 The decay width expression

In this Section we present formulas for the LV and LC semileptonic decays of charged B mesons, of the type $B \to \mu e \pi$, mediated by heavy sterile on-shell neutrinos. The formulas for the decay width of the LV decays of this type, $B^{\pm} \to \mu^{\pm} e^{\pm} \pi^{\mp}$, in the case one heavy neutrino, were presented in Ref. [25]. They were extended to the case of two almost degenerate heavy on-shell neutrinos in Section. 4, in the context of CP violation. For a review we refer to [43].

The two flavor neutrinos ν_e and ν_μ $(\ell = e, \mu, \tau)$ can be represented as

$$\nu_e = \sum_{j=1}^{3} B_{ej}\nu_j + B_{eN_1}N_1 + B_{eN_2}N_2 + \ldots, \tag{5.1a}$$

$$\nu_\mu = \sum_{j=1}^{3} B_{\mu j}\nu_j + B_{\mu N_1}N_1 + B_{\mu N_2}N_2 + \ldots. \tag{5.1b}$$

The coupling of these two flavor neutrinos to the corresponding charged leptons $e^{\pm}$ and $\mu^{\pm}$ has a part which contains the coupling to the heavy almost mass-degenerate neutrinos N_1 and N_2

$$\mathcal{L}_{eWN} = \frac{g}{2\sqrt{2}}\left[\overline{\psi}_{(e)} \not{W}_L \left(B_{eN_1}N_1 + B_{eN_2}N_2\right) + \text{h.c.}\right] = K_1 \frac{g}{2\sqrt{2}} \overline{\psi}_{(e)} \not{W}_L \mathcal{N}_1 + \text{h.c.} \tag{5.2a}$$

$$\mathcal{L}_{\mu WN} = \frac{g}{2\sqrt{2}}\left[\overline{\psi}_{(\mu)} \not{W}_L \left(B_{\mu N_1}N_1 + B_{\mu N_2}N_2\right) + \text{h.c.}\right] = K_2 \frac{g}{2\sqrt{2}} \overline{\psi}_{(\mu)} \not{W}_L \mathcal{N}_2 + \text{h.c.}, \tag{5.2b}$$

where we denoted by $\mathcal{N}_1$ and $\mathcal{N}_2$ the e- and μ-flavor analogs of the heavy neutrino mass eigenfields N_j $(j = 1, 2)$

$$\begin{aligned} \mathcal{N}_1 &= \mathcal{B}_{11}N_1 + \mathcal{B}_{12}N_2 \\ \mathcal{N}_2 &= \mathcal{B}_{21}N_1 + \mathcal{B}_{22}N_2 \end{aligned} \tag{5.3a}$$

$$\mathcal{B}_{\alpha k} \equiv \frac{1}{K_\alpha} B_{\alpha k}, \qquad K_\alpha \equiv \sqrt{|B_{\alpha 1}|^2 + |B_{\alpha 2}|^2} \qquad (\alpha, k = 1, 2), \tag{5.3b}$$

where in $B_{\alpha k}$ the coefficients $\alpha = 1, 2$ stand for e, μ, respectively; and $k = 1, 2$ for N_1, N_2, respectively. The considered process for the LV decays $B^{\pm} \to \mu^{\pm} e^{\pm} \pi^{\mp}$, with on-shell N_j's ($j = 1, 2$), are those of Fig. 5.1; and for the LC decays, $B^{\pm} \to \mu^{\pm} e^{\mp} \pi^{\pm}$ are those of Fig. 5.2.

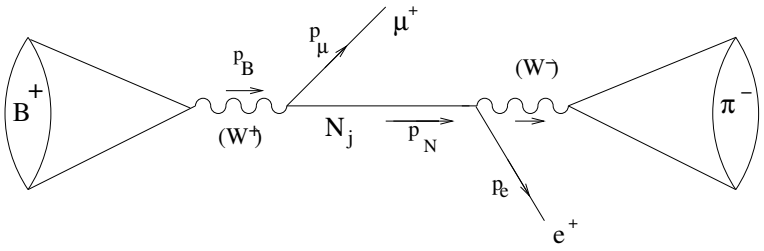

Figure 5.1: *The LV decay $B^+ \to \mu^+ e^+ \pi^-$ via exchange of an on-shell neutrinos N_j ($j = 1, 2$).*

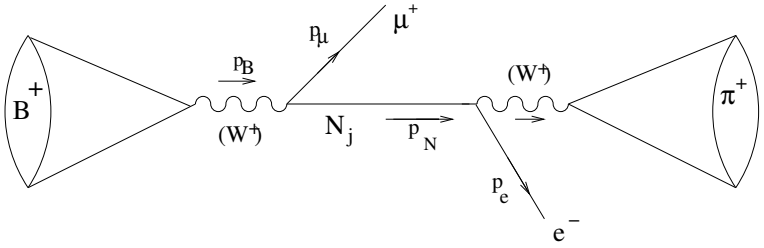

Figure 5.2: *The LC decay $B^+ \to \mu^+ e^- \pi^+$ via exchange of an on-shell neutrinos N_j ($j = 1, 2$).*

Although the LV decays have also the crossed channel (i.e., the ones where the vertices of μ and e are exchanged), we assume here that the measurements can distinguish these two channels (since $\mu \neq e$), by reconstructing invariant masses from the detected final state particles.

For these processes, we shall consider the scenarios where the two heavy neutrinos N_1 and N_2 are almost mass-degenerate ($\Delta M_N \ll M_N \equiv M_{N_1}$) and are on-shell. We shall consider only the neutrino couplings (5.2), with no components of the other mass eigenfields (thus no light mass eigenfields ν_1, ν_2, ν_3), because we shall assume that N_1 and N_2 are the only neutrinos which are on-shell in these processes. This is then reflected in our definition of "hevay" flavor states $\mathcal{N}_j$, Eq. (5.3a). We stress that neutrinos which are off-shell in these processes give, in relative terms, completely negligible contributions and will thus be ignored.

In the more general case of the LV decay $M^{\pm} \to \ell_1^{\pm} N \to \ell_1^{\pm} \ell_2^{\pm} M'^{\mp}$ ($\ell_j = e, \mu, \tau$; M and M' pseudoscalars), with $\ell_1 \neq \ell_2$ and neutrino N on-shell, can be written as

$$\Gamma(M^{\pm} \to \ell_1^{\pm} N \to \ell_1^{\pm} \ell_2^{\pm} M'^{\mp}) = |B_{\ell_1 N}|^2 |B_{\ell_2 N}|^2 \, \overline{\Gamma} \qquad (\ell_1 \neq \ell_2), \tag{5.4}$$

where

$$\overline{\Gamma} \;=\; \frac{K_M^2 M_M^5}{64\pi^2} \frac{M_N}{\Gamma_N} \, \lambda^{1/2}(1, y_N, y_{\ell_1}) \, \lambda^{1/2}\left(1, \frac{y'}{y_N}, \frac{y_{\ell_2}}{y_N}\right) Q(y_N; y_{\ell_1}, y_{\ell_2}, y') \;, \tag{5.5}$$

and the notations used in Eq. (5.5) (the same used in Section. 4) are

$$K_M^2 = G_F^4 f_M^2 f_{M'}^2 |V_{Q_u Q_d} V_{q_u q_d}|^2 \,, \tag{5.6a}$$

$$\lambda(y_1, y_2, y_3) = y_1^2 + y_2^2 + y_3^2 - 2y_1 y_2 - 2y_2 y_3 - 2y_3 y_1 \,, \tag{5.6b}$$

$$y_N = \frac{M_N^2}{M_M^2} \,, \quad y_{\ell_s} = \frac{M_{\ell_s}^2}{M_M^2} \,, \quad y^{'} = \frac{M_{M'}^2}{M_M^2} \,, \quad (\ell_s = \ell_1, \ell_2) \,, \tag{5.6c}$$

and the function $Q(y_N; y_{\ell_1}, y_{\ell_2}, y^{'})$ is given in Appendix E.

In Eq. (5.6a), f_M and $f_{M'}$ are the decay constants, and $V_{Q_u Q_d}$ and $V_{q_u q_d}$ are the CKM matrix elements of pseudoscalars $M^{\pm}$ and $M^{'\mp}$.

We notice that in the considered specific case ($\ell_1 = \mu$ and $\ell_2 = e$) we have $y_{\ell_1} \approx y_{\ell_2} \approx 0$, and the expression (E.9) simplifies i.e.,

$$Q(y_N; y_{\ell_1}, y_{\ell_2}, y') \approx Q(y_N; 0, 0, y') = \frac{1}{2} \left[y_N (1 - y_N) \right] \left[y_N - y' \right] . \tag{5.7}$$

The result (5.4), (5.5), (5.6) and (E.9) can be written in an equivalent form

$$\Gamma(M^{\pm} \to \ell_1^{\pm} N \to \ell_1^{\pm} \ell_2^{\pm} M^{'\mp}) = \frac{1}{\Gamma_N} \Gamma(M^{\pm} \to \ell_1^{\pm} N) \Gamma(N \to \ell_2^{\pm} M^{'\mp}) \qquad (\ell_1 \neq \ell_2), \tag{5.8}$$

where the widths of the two decays are

$$\Gamma(M^{\pm} \to \ell_1^{\pm} N) = |B_{\ell_1 N}|^2 \overline{\Gamma}(M^{\pm} \to \ell_1^{\pm} N), \tag{5.9a}$$

$$\Gamma(N \to \ell_2^{\pm} M^{'\mp}) = |B_{\ell_2 N}|^2 \overline{\Gamma}(N \to \ell_2^{\pm} M^{'\mp}), \tag{5.9b}$$

and the expressions for the corresponding canonical widths $\overline{\Gamma}$ (i.e., widths without the mixing factors) are

$$\begin{aligned} \overline{\Gamma}(M^{\pm} \to \ell_1^{\pm} N) &= \frac{1}{8\pi} G_F^2 f_M^2 |V_{Q_u Q_d}|^2 M_M^3 \, \lambda^{1/2}(1, y_N, y_{\ell_1}) \\ &\times \left[(1 - y_N) y_N + y_{\ell_1} (1 + 2y_N - y_{\ell_1}) \right] , \end{aligned} \tag{5.10a}$$

$$\begin{aligned} \overline{\Gamma}(N \to \ell_2^{\pm} M^{'\mp}) &= \frac{1}{16\pi} G_F^2 f_{M'}^2 |V_{q_u q_d}|^2 \frac{1}{M_N} \, \lambda^{1/2} \left(1, \frac{y^{'}}{y_N}, \frac{y_{\ell_2}}{y_N} \right) \times \\ &\left[(M_N^2 + M_{\ell_2}^2)(M_N^2 - M_{M'}^2 + M_{\ell_2}^2) - 4 M_N^2 M_{\ell_2}^2 \right] \\ &= \frac{1}{16\pi} G_F^2 f_{M'}^2 |V_{q_u q_d}|^2 M_M^2 M_N \, \lambda^{1/2} \left(1, \frac{y^{'}}{y_N}, \frac{y_{\ell_2}}{y_N} \right) \\ &\times \left[y_N - y' - 2y_{\ell_2} - \frac{y_{\ell_2}}{y_N} (y' - y_{\ell_2}) \right] , \end{aligned} \tag{5.10b}$$

where again the notations (5.6) were used. We notice that the algebraic factorization of the Q function, Eq. (E.10), reflects the factorization (5.8), as can be seen by inspection of the expressions (5.10a) and (5.10b).

It can be checked that the result for the LC processes $M^{\pm} \to \ell_1^{\pm} N \to \ell_1^{\pm} \ell_2^{\mp} M^{'\pm}$ is the same

as the result (5.8)-(5.9)

$$\Gamma(M^{\pm}\to \ell_1^{\pm}N\to \ell_1^{\pm}\ell_2^{\mp}M'^{\pm}) = \frac{1}{\Gamma_N}\Gamma(M^{\pm}\to \ell_1^{\pm}N)\Gamma(N\to \ell_2^{\mp}M'^{\pm}) \tag{5.11a}$$

$$= \frac{|B_{\ell_1 N}|^2|B_{\ell_2 N}|^2}{\Gamma_N}\overline{\Gamma}(M^{\pm}\to \ell_1^{\pm}N)\overline{\Gamma}(N\to \ell_2^{\pm}M'^{\mp}) \quad (\ell_1\neq\ell_2), \tag{5.11b}$$

where the canonical decay widths ($\overline{\Gamma}$'s) are again those of Eqs. (5.10). We recall that we consider the scenario with two on-shell neutrinos N_j ($j=1,2$) with almost degenerate masses: $\Delta M_N \ll M_{N_1}$, where $\Delta M_N \equiv M_{N_2}-M_{N_1}>0$. In this case, it turns out that the expression for the LV decay width becomes more complicated, see Eq. (4.5). With the notation (5.2) for the mixing coefficients, it can be written in the following form:

$$\begin{aligned}\Gamma(B^{\pm}\to \mu^{\pm}e^{\pm}\pi^{\mp}) &= \overline{\Gamma}\times\Big\{|B_{\mu N_1}|^2|B_{eN_1}|^2+\frac{\widetilde{\mathcal{K}}_1}{\widetilde{\mathcal{K}}_2}|B_{\mu N_2}|^2|B_{eN_2}|^2\\ &\quad+\frac{4\widetilde{\mathcal{K}}_1}{(\widetilde{\mathcal{K}}_1+\widetilde{\mathcal{K}}_2)}|B_{\mu N_1}||B_{eN_1}||B_{\mu N_2}||B_{eN_2}|\\ &\times\quad\left(\delta(y)\cos\theta_{21}^{(\mathrm{LV})}\mp\frac{\eta(y)}{y}\sin\theta_{21}^{(\mathrm{LV})}\right)\Big\},\end{aligned} \tag{5.12}$$

where $\overline{\Gamma}$ is given in Eq. (5.5), with $M_N\equiv M_{N_1}\approx M_{N_2}$, the angle $\theta_{21(\mathrm{LV})}$ is a combination of the phases of the heavy-light mixing coefficients

$$\theta_{21}^{(\mathrm{LV})}=\arg(B_{\mu N_2})+\arg(B_{eN_2})-\arg(B_{\mu N_1})-\arg(B_{eN_1}). \tag{5.13}$$

The functions $\delta(y)$ and $\eta(y)/y$ appearing in Eq. (5.12) are functions of the parameter $y\equiv\Delta M_N/\Gamma_N$ only, where Γ_N is the arithmetic average of the total decay widths of N_1 and N_2. The factors (functions) $\delta(y)$ and $\eta(y)/y$ represent the effects of the N_1-N_2 overlap in the decay width, in the real and imaginary parts of the N_1-N_2 interference terms, respectively. Therefore, $\delta(y)$ and $\eta(y)/y$ go to zero when $y\gg 1$, i.e., when no overlap.

Finally, the coefficients $\widetilde{\mathcal{K}}_j$ appearing in Eq. (5.12) are the combinations of the mixing coefficients appearing in the total decay widths presented in Equations (3.13) as $\widetilde{\mathcal{K}}_j^{Ma}$.

As mentioned earlier, in addition to the above LV decay width, there exist also the LC decay width $\Gamma(B^{\pm}\to\mu^{\pm}e^{\mp}\pi^{\pm})$, which in the case of scenario of one on-shell neutrino N coincides with the LV expression (5.5). In the scenario with two on-shell almost degenerate neutrinos N_j, the expression is slightly different from LV case Eq. (5.12), namely only the angle $\theta_{21}^{(\mathrm{LV})}$, Eq. (5.13), is now replaced by the following angle:

$$\theta_{21}^{(\mathrm{LC})}=\arg(B_{\mu N_2})-\arg(B_{eN_2})-\arg(B_{\mu N_1})+\arg(B_{eN_1}). \tag{5.14}$$

We shall consider, from now on, the case when there is an almost degeneracy of the two heavy neutrinos ($\Delta M_N\ll M_N\equiv M_{N_1}$) and at the same time the degeneracy ΔM_N is significantly larger than the (extremely small) decay width Γ_N:

$$\Delta M_N \ll M_N \text{ and } y\equiv\frac{\Delta M_N}{\Gamma_N}\gg 1. \tag{5.15}$$

In this case, we can see from Figs. 3.10 and 3.11 that the functions $\delta(y)$ and $\eta(y)/y$ become very small. Therefore, the N_1-N_2 overlap term in $\Gamma(B^\pm \to \mu^\pm e^\pm \pi^\mp)$ becomes negligible. As a result, Eq. (5.12) reduces to the following form, where we make use of the identities (5.8)-(5.10):

$$\begin{aligned}\Gamma(B^\pm \to \mu^\pm e^\pm \pi^\mp) &\approx \sum_{j=1}^{2} \Gamma(B^\pm \to \mu^\pm N_j \to \mu^\pm e^\pm \pi^\mp) && (5.16a)\\ &= \overline{\Gamma}(B^\pm \to \mu^\pm N)\overline{\Gamma}(N \to e^\pm \pi^\mp) \\ &\times \left\{ \frac{1}{\Gamma_{N_1}} |B_{\mu N_1}|^2 |B_{eN_1}|^2 + \frac{1}{\Gamma_{N_2}} |B_{\mu N_2}|^2 |B_{eN_2}|^2 \right\}. && (5.16b)\end{aligned}$$

The decay width presented hitherto does not contain an important suppression (acceptance) factor. Namely, the on-shell neutrino N_j travels before decaying. The decay will be detected if the on-shell neutrino decays during the passage of the neutrino through the detector. If the length of the detector is L, then the probability P_N of decay of N there is

$$\begin{aligned}P_N(L) = 1 - \exp\left(-\frac{t}{\tau_N \gamma_N}\right) &= 1 - \exp\left(-\frac{L}{\tau_N \gamma_N \beta_N}\right) && (5.17a)\\ \approx L/(\tau_N \gamma_N \beta_N) \quad &\text{if } P_N \ll 1. && (5.17b)\end{aligned}$$

In the second identity of Eq. (5.17a) we took into account that $L = \beta_N t$ where β_N ($\lesssim 1$) is the velocity of the N neutrino in the lab frame. Further, $\gamma_N = (1-\beta_N^2)^{-1/2}$ is the Lorentz lab time dilation factor, typically $\gamma_N > 2$. The N lifetime in the rest is $\tau_N = 1/\Gamma_N$. Therefore, $\gamma_N \tau_N$ is the N lifetime in the lab frame. The formula (5.17b) holds if $P_N \ll 1$, and we shall assume this to be the case in the considered cases.

This decay-within-the-detector probability P_N has been presented in details in Appendix C. It is convenient to define the corresponding canonical, independent of mixing, probability $\overline{A}$

$$\begin{aligned}\overline{A}(L) &= 1\text{m} \times \frac{\overline{\Gamma}(M_N)}{\gamma_N} && (5.18a)\\ \Rightarrow P_N(L) &\approx \left(\frac{L}{1\text{m}}\right) \times \overline{A}\, \widetilde{\mathcal{K}}. && (5.18b)\end{aligned}$$

The quantity $\overline{A}$ is presented, for $\gamma_N = 2$, in Fig. C.2 as a function of M_N.

The effective (true) decay widths and branching ratios are those multiplied by P_N. However, since we have two different (but almost mass degenerate) neutrinos N_j, we have for each of them a different decay probability

$$P_{N_j}(L) \approx \left(\frac{L}{1\text{m}}\right) \times \overline{A}\, \widetilde{\mathcal{K}}_j = \frac{L}{\gamma_N} \Gamma_{N_j}, \tag{5.19}$$

where $\widetilde{\mathcal{K}}_j$ is given in Eq. (3.15), and in the second equality we used the relations (5.18) and (3.13). The canonical probability $\overline{A}$, Eq. (5.18), is common to both neutrinos N_j because they have practically the same mass and thus the same kinematics (and hence the same Lorentz factor γ_N). The coefficients $\mathcal{N}_{\ell N}$($\sim 10^0$-10^1) in $\widetilde{\mathcal{K}}_j$ are common to both neutrinos N_j (because they have practically equal mass); but the mixings $B_{\ell N_j}$ can be, in principle, quite different for

the two neutrinos, and thus the two mixing factors $\widetilde{\mathcal{K}}_j$ $(j=1,2)$ may differ significantly from each other.

Combining the probabilities (5.19) with the decay width (5.16b) leads to the effective (true) decay width, where the dependence on the two decay widths Γ_{N_j} cancels out

$$\begin{aligned}\Gamma_{\rm eff}(B^\pm\to\mu^\pm e^\pm\pi^\mp;L) &\approx \sum_{j=1}^{2}\Gamma(B^\pm\to\mu^\pm N_j\to\mu^\pm e^\pm\pi^\mp)P_{N_j}(L) &(5.20a)\\ &\approx \frac{L}{\gamma_N\beta_N}\overline{\Gamma}(B^\pm\to\mu^\pm N)\overline{\Gamma}(N\to e^\pm\pi^\mp)\\ &\times \left[|B_{\mu N_1}|^2|B_{eN_1}|^2+|B_{\mu N_2}|^2|B_{eN_2}|^2\right]. &(5.20b)\end{aligned}$$

This implies that the effective differential decay, with respect to the distance L between the two vertices of the process, is

$$\begin{aligned}\frac{d}{dL}\Gamma_{\rm eff}(B^\pm\to\mu^\pm e^\pm\pi^\mp;L) &\approx \frac{1}{\gamma_N\beta_N}\overline{\Gamma}(B^\pm\to\mu^\pm N)\overline{\Gamma}(N\to e^\pm\pi^\mp)\\ &\times \left[|B_{\mu N_1}|^2|B_{eN_1}|^2+|B_{\mu N_2}|^2|B_{eN_2}|^2\right], &(5.21)\end{aligned}$$

which is independent of the distance L.

For the LC processes $B^\pm\to\mu^\pm e^\mp\pi^\pm$, the result is the same as in the above LV processes, due to the equality of the LC decay width (5.11) with the LV decay width (5.8)-(5.9) [cf. also Eqs. (5.10)]. Therefore, when $\delta(y),\eta(y)/y\ll 1$ (i.e., when the conditions (5.15) hold), we have

$$\begin{aligned}\frac{d}{dL}\Gamma_{\rm eff}(B^\pm\to\mu^\pm e^\mp\pi^\pm;L) &= \frac{d}{dL}\Gamma_{\rm eff}(B^\pm\to\mu^\pm e^\pm\pi^\mp;L), &(5.22a)\\ \Gamma_{\rm eff}(B^\pm\to\mu^\pm e^\mp\pi^\pm;L) &= \Gamma_{\rm eff}(B^\pm\to\mu^\pm e^\pm\pi^\mp;L). &(5.22b)\end{aligned}$$

The present upper bounds for the $|B_{\ell N_j}|^2$ mixing coefficients appearing in these expressions, in the considered mass range $M_N\approx$ 1-5 GeV, are $|B_{\ell N_j}|^2\sim 10^{-7}$-$10^{-4}$, cf. [45].[1]

5.2 The effects of neutrino oscillation

In the previous Section, important effects of neutrino oscillation of the propagating on-shell neutrino were not accounted for. As we shall see, these effects lead to a modulation, i.e., L-dependence of the effective decay widths obtained in the previous Section, where L is the distance traveled by the on-shell neutrino between it production and detection point ($L=\beta_N t$).

We shall follow the lines of the approach of Ref. [67] to neutrino oscillations. For the LV decays $B^+\to\mu^+N_j\to\mu^+e^+\pi^-$ of Fig. 5.1, the relevant interactions at the first (production) vertex are $-B^*_{\mu N_j}\overline{\mu}^c\gamma^\eta(1+\gamma_5)N_jW^{(+)}_\eta$, and the neutrino state produced at this vertex is

$$|\psi\rangle_{(B^+)}\sim B^*_{\mu N_1}|N_1(p_{N_1})\rangle+B^*_{\mu N_2}|N_2(p_{N_2})\rangle, \tag{5.23}$$

[1] The present upper bounds for $|B_{\tau N}|^2$ are higher than that, but are expected to become significantly lower in the future.

where the momenta of the two physical on-shell neutrinos are slightly different from each other, because $\Delta M_N \neq 0$ (we recall: $\Delta M_N \ll M_N$). We have

$$p_{N_j} = (E_{N_j}, 0, 0, p^3_{N_j}), \qquad E_{N_j} = \sqrt{M^2_{N_j} + (p^3_{N_j})^2}, \tag{5.24}$$

where the restriction to one spatial dimension ($\hat{z}$) was made, because the processes with oscillation require the neutrino to propagate far from the production vertex. At the second vertex of the LV process Fig. 5.1, the relevant coupling is $B^*_{eN_j}\overline{N_j}\gamma^\delta(1-\gamma_5)eW^{(+)}_\delta$. The detection of the neutrino there can be described by an operator at the detector space-time location $z = (t, 0, 0, L)$ where $L = \beta_N t$. This operator is the annihilation operator $B^*_{eN_j}\hat{b}_{(N_j)}(p_{N_j}; z) = B^*_{eN_j}\hat{b}_{(N_j)}(p_{N_j})\exp(-ip_{N_j}\cdot z)$ acting at the aforementioned component $|N_j(p_{N_j})\rangle \sim \hat{b}_{(N_j)}(p_{N_j})^\dagger|0\rangle$ ($j = 1, 2$). Since $\hat{b}_{(N)}(p_N)\hat{b}_{(N)}(p_N)^\dagger|0\rangle = \text{const}|0\rangle$, this implies the following detection amplitude:[2]

$$\mathcal{A}(B^+ \to \mu^+e^+\pi^-; L) \sim B^*_{\mu N_1}B^*_{eN_1}\exp(-ip_{N_1}\cdot z) + B^*_{\mu N_2}B^*_{eN_2}\exp(-ip_{N_2}\cdot z). \tag{5.25}$$

The L dependence of the effective (true) decay width of the considered process is proportional to the absolute square of the above amplitude

$$\frac{d}{dL}\Gamma^{(\text{osc})}_{\text{eff}}(B^+ \to \mu^+e^+\pi^-; L) \equiv \frac{1}{dL}\Gamma^{(\text{osc})}_{\text{eff}}(BB^+ \to \mu^+e^+\pi^-; L < L' < L + dL)$$
$$\sim |\mathcal{A}(B^+ \to \mu^+e^+\pi^-)|^2 \tag{5.26a}$$
$$\sim \left\{\sum_{j=1}^{2}|B_{\mu N_j}|^2|B_{eN_j}|^2 + 2\text{Re}\left[B^*_{\mu N_1}B^*_{eN_1}B_{\mu N_2}B_{eN_2}\exp\left[i(p_{N_2} - p_{N_1})\cdot z\right]\right]\right\}. \tag{5.26b}$$

The superscript "(osc)" indicates that this is the (differential) effective decay width with oscillation effects included. The oscillation term, in comparison with the expression (5.21), is new and introduces L-dependence in the otherwise L-independent differential decay width $d\Gamma_{\text{eff}}/dL$ of Eq. (5.21). This oscillation term comes from the interference term in the square of the amplitude (5.25). Therefore, by comparing the obtained expression (5.26) with (5.21), we can obtain the complete expression for the effective differential decay width with oscillation effects included

$$\frac{d}{dL}\Gamma^{(\text{osc})}_{\text{eff}}(B^+ \to \mu^+e^+\pi^-; L) \approx \frac{1}{\gamma_N\beta_N}\overline{\Gamma}(B^\pm \to \mu^\pm N)\overline{\Gamma}(N \to e^\pm\pi^\mp)$$
$$\times\left\{\sum_{j=1}^{2}|B_{\mu N_j}|^2|B_{eN_j}|^2 + 2\text{Re}\left[B^*_{\mu N_1}B^*_{eN_1}B_{\mu N_2}B_{eN_2}\exp\left[i(p_{N_2} - p_{N_1})\cdot z\right]\right]\right\}. \tag{5.27}$$

The oscillation term here contains two on-shell 4-momenta $p_{N_j} = (E_{N_j}, 0, 0, p^3_{N_j})$ ($j = 1, 2$) which are related by the on-shellness conditions $p_{N_j}\cdot p_{N_j} = M^2_{N_j}$ and by the condition

$$\beta_{N_2} - \beta_{N_1} \equiv \frac{p^3_{N_2}}{E_{N_2}} - \frac{p^3_{N_1}}{E_{N_1}} \approx 0. \tag{5.28}$$

[2] We use the metric $(1, -1, -1, -1)$ for the scalar products. It is our understanding that the authors of Ref. [67] use the metric $(-1, 1, 1, 1)$.

This condition comes from the following interpretation. The N_1 and N_2 amplitudes interfere at L if both of them are there appreciable. The neutrinos N_1 and N_2 in general separate as they travel from their production to their detection vertex. Interference is then possible there only if this separation $|\Delta L_{12}| \equiv |(\beta_{N_2} - \beta_{N_1})|t$ (with: $t = L/\beta_N$) is smaller than the spread of the wavepacket $\Delta L_{\rm wp} \equiv \beta_N \Delta T$, cf. Ref. [67]

$$\frac{|\beta_{N_2} - \beta_{N_1}|}{|\beta_{N_2} + \beta_{N_1}|} \ll \frac{\Delta T}{t} \ (\ll 1). \tag{5.29}$$

Stated otherwise, the following hierarchy is assumed:

Figure 5.3: *Graphical representation of the hierarchy Eq. (5.30) of the lengths ΔL_{12}, $\Delta L_{\rm wp}$ and the detector length L. The two interaction vertices (the production and the decay vertex of the neutrino N) are denoted as v_1 and v_2, respectively. Note that at the production vertex (v_1) the wavepackets of N_1 and N_2 are not mutually displaced, unlike in the decay vertex (v_2).*

$$|\Delta L_{12}| \left(\equiv \frac{|\beta_{N_2} - \beta_{N_1}|L}{\beta_N} \right) \ \ll \ \Delta L_{\rm wp} \, (\equiv \beta_N \Delta T) \ \ll \ L, \tag{5.30}$$

cf. also Fig. 5.3.

In order to express the oscillation phase $\phi(L) \equiv (p_{N_2} - p_{N_1}) \cdot z$ in Eq. (5.27) [$\Leftrightarrow$ (5.29)] in a convenient form, the condition (5.28) can be used. Since $\beta_{N_2} \equiv p_{N_2}^3/E_{N_2}$ and $\beta_{N_1} \equiv p_{N_1}^3/E_{N_1}$ are close in value, hence they are close to the value of $\beta_N \equiv (p_{N_2}^3 + p_{N_1}^3)/(E_{N_2} + E_{N_1})$. It can be checked that the latter velocity is practically equal to the arithemtic average $(1/2)(\beta_{N_2} + \beta_{N_1})$. Therefore,

$$z = (t, 0, 0, L) \approx t(1, 0, 0, \beta_N) = \frac{t}{(E_{N_2} + E_{N_1})}(p_{N_2} + p_{N_1}) \tag{5.31}$$

Therefore, the oscillation phase is [67]

$$\begin{aligned} \phi(L) \equiv (p_{N_2} - p_{N_1}) \cdot z \ &= \ t \frac{(M_{N_2}^2 - M_{N_1}^2)}{(E_{N_1} + E_{N_2})} \approx t M_N \frac{\Delta M_N}{E_N} \\ &\approx \ \frac{L}{\beta_N} M_N \frac{\Delta M_N}{E_N} = L \frac{\Delta M_N}{\beta_N \gamma_N}, \end{aligned} \tag{5.32}$$

where it was taken into account that $p_{N_j}^2 = M_{N_j}^2$, and $M_{N_1}^2 - M_{N_2}^2 = 2 M_N \Delta M_N$ (where: $0 < \Delta M_N \equiv M_{N_2} - M_{N_1} \ll M_{N_1} \equiv M_N$). As stressed in Ref. [67], this expression for the oscillation angle is valid always, not just for relativistic neutrinos N_j, whenever the relation (5.29) is fulfilled. For example, if the neutrinos are nonrelativistic, we have $\phi(L) \approx (L/\beta_N)\Delta M_N$. The obtained oscillation phase allows us to define the oscillation length $L_{\rm osc}$ as

$$\phi(L_{\rm osc}) \ = \ 2\pi \ \Rightarrow \ L_{\rm osc} = \frac{2\pi \beta_N \gamma_N}{\Delta M_N}. \tag{5.33}$$

Using the expression (5.32), the differential decay width (5.27) can now be written in a more explicit form

$$\frac{d}{dL}\Gamma_{\rm eff}^{(\rm osc)}(B^+\to\mu^+e^+\pi^-;L)\approx\frac{1}{\gamma_N\beta_N}\overline{\Gamma}(B^\pm\to\mu^\pm N)\overline{\Gamma}(N\to e^\pm\pi^\mp)$$
$$\times\left\{\sum_{j=1}^{2}|B_{\mu N_j}|^2|B_{eN_j}|^2+2|B_{\mu N_1}||B_{eN_1}||B_{\mu N_2}||B_{eN_2}|\cos\left(L\frac{\Delta M_N}{\beta_N\gamma_N}+\theta_{21}^{(\rm LV)}\right)\right\} \quad (5.34)$$

where the constant phase $\theta_{21}^{(\rm LV)}$ is defined in Eq. (5.13). We can integrate the differential decay width (5.34) over dL length to the full length L between the vertices. If $L\gg L_{\rm osc}$, this then gives then gives the full effective decay width of Eq. (5.20b), because the oscillation term $\sim\cos(\phi(L)+\theta_{12})$ gives a relatively negligible contribution when integrated over several "oscillation wavelengths" $L_{\rm osc}$. If, on the other hand, we do not assume $L\gg L_{\rm osc}$, the integration of the expression (5.34) gives

$$\Gamma_{\rm eff}^{(\rm osc)}(B^+\to\mu^+e^+\pi^-;L)\approx\frac{L}{\gamma_N\beta_N}\overline{\Gamma}(B^\pm\to\mu^\pm N)\overline{\Gamma}(N\to e^\pm\pi^\mp)\left\{\sum_{j=1}^{2}|B_{\mu N_j}|^2|B_{eN_j}^2|+\right.$$
$$\left.\frac{L_{\rm osc}}{\pi L}|B_{\mu N_1}||B_{eN_1}||B_{\mu N_2}||B_{eN_2}|\left[\sin\left(2\pi\frac{L}{L_{\rm osc}}+\theta_{21}^{(\rm LV)}\right)-\sin(\theta_{21}^{(\rm LV)})\right]\right\}. \quad (5.35)$$

Until now we considered the case of oscillation effects in LV decays $B^+\to\mu^+e^+\pi^-$. It can be checked that for the charge-conjugate LV decays $B^-\to\mu^-e^-\pi^+$ the previous derivation can be repeated, with the only replacements $B_{\ell N_j}^*\mapsto B_{\ell N_j}$ and $B_{\ell N_j}\mapsto B_{\ell N_j}^*$. Instead of Eq. (5.25) we now have

$$\mathcal{A}(B^-\to\mu^-e^-\pi^+;L)\sim B_{\mu N_1}B_{eN_1}\exp(-ip_{N_1}\cdot z)+B_{\mu N_2}B_{eN_2}\exp(-ip_{N_2}\cdot z). \quad (5.36)$$

This implies that in the result (5.34) we now get $\theta_{21}\mapsto-\theta_{21}$, so that we can extend the results (5.34) and (5.35) to both LV cases ($B^\pm$)

$$\frac{d}{dL}\Gamma_{\rm eff}^{(\rm osc)}(B^\pm\to\mu^\pm e^\pm\pi^\mp;L)\approx\frac{1}{\gamma_N\beta_N}\overline{\Gamma}(B^\pm\to\mu^\pm N)\overline{\Gamma}(N\to e^\pm\pi^\mp)$$
$$\times\left\{\sum_{j=1}^{2}|B_{\mu N_j}|^2|B_{eN_j}^2|+2|B_{\mu N_1}||B_{eN_1}||B_{\mu N_2}||B_{eN_2}|\cos\left(2\pi\frac{L}{L_{\rm osc}}\pm\theta_{21}^{(\rm LV)}\right)\right\}, \quad (5.37)$$

$$\Gamma_{\rm eff}^{(\rm osc)}(B^\pm\to\mu^\pm e^\pm\pi^\mp;L)\approx\frac{L}{\gamma_N\beta_N}\overline{\Gamma}(B^\pm\to\mu^\pm N)\overline{\Gamma}(N\to e^\pm\pi^\mp)\left\{\sum_{j=1}^{2}|B_{\mu N_j}|^2|B_{eN_j}^2|+\right.$$
$$\left.\frac{L_{\rm osc}}{\pi L}|B_{\mu N_1}||B_{eN_1}||B_{\mu N_2}||B_{eN_2}|\left[\sin\left(2\pi\frac{L}{L_{\rm osc}}\pm\theta_{21}^{(\rm LV)}\right)\mp\sin(\theta_{21}^{(\rm LV)})\right]\right\}. \quad (5.38)$$

For the LC processes $B^\pm\to\mu^\pm e^\mp\pi^\pm$, cf. Fig. 5.2, in the case of no oscillation effects the results for the decay widths are the same as for the LV processes, cf. Eqs. (5.20)-(5.22). When oscillations are accounted for, the results are almost the same as in the just considered LV

processes, except that for the decay amplitudes [cf. Eqs. (5.25) and (5.36) for LV case] we have some of the heavy-light mixing elements $B_{\ell N_j}$ complex-conjugated and others not

$$\mathcal{A}(B^+ \to \mu^+ e^- \pi^+; L) \sim B^*_{\mu N_1} B_{eN_1} \exp(-ip_{N_1}\cdot z) + B^*_{\mu N_2} B_{eN_2} \exp(-ip_{N_2}\cdot z), \quad (5.39a)$$

$$\mathcal{A}(B^- \to \mu^- e^+ \pi^-; L) \sim B_{\mu N_1} B^*_{eN_1} \exp(-ip_{N_1}\cdot z) + B_{\mu N_2} B^*_{eN_2} \exp(-ip_{N_2}\cdot z). \quad (5.39b)$$

This then leads to the following results, in analogy with the LC results (5.37)-(5.38) where now only the phase angle $\theta_{21}^{(\mathrm{LV})}$ gets replaced by a different phase angle $\theta_{21}^{(\mathrm{LC})}$ given in Eq. (5.14):

$$\frac{d}{dL}\Gamma^{(\mathrm{osc})}_{\mathrm{eff}}(B^\pm \to \mu^\pm e^\mp \pi^\pm; L) \approx \frac{1}{\gamma_N \beta_N}\overline{\Gamma}(B^\pm \to \mu^\pm N)\overline{\Gamma}(N \to e^\pm \pi^\mp) \times \left\{ \sum_{j=1}^{2} |B_{\mu N_j}|^2 |B^2_{eN_j}| + 2|B_{\mu N_1}||B_{eN_1}||B_{\mu N_2}||B_{eN_2}| \cos\left(2\pi \frac{L}{L_{\mathrm{osc}}} \pm \theta_{21}^{(\mathrm{LC})}\right)\right\}, \quad (5.40)$$

$$\Gamma^{(\mathrm{osc})}_{\mathrm{eff}}(B^\pm \to \mu^\pm e^\pm \pi^\mp; L) \approx \frac{L}{\gamma_N \beta_N}\overline{\Gamma}(B^\pm \to \mu^\pm N)\overline{\Gamma}(N \to e^\pm \pi^\mp)\left\{ \sum_{j=1}^{2} |B_{\mu N_j}|^2 |B^2_{eN_j}| + \frac{L_{\mathrm{osc}}}{\pi L}|B_{\mu N_1}||B_{eN_1}||B_{\mu N_2}||B_{eN_2}| \left[\sin\left(2\pi \frac{L}{L_{\mathrm{osc}}} \pm \theta_{21}^{(\mathrm{LC})}\right) \mp \sin(\theta_{21}^{(\mathrm{LC})})\right]\right\}. \quad (5.41)$$

All the formulas with oscillation effects, derived in this Section, can be extended in a straightforward way to the oscillation effects in the semihadronic decays with two equal flavors of produced charged leptons, i.e., $M^\pm \to \ell^\pm \ell^\pm M'^\mp$ and $M^\pm \to \ell^\pm \ell^\mp M'^\pm$; and more specifically, $B^\pm \to \mu^\pm \mu^\pm \pi^\mp$ and $B^\pm \to \mu^\pm \mu^\mp \pi^\pm$.

In Appendix F we show that the wavefunction approach of Ref. [39] (cf. also [68]) to the considered LV and LC processes with on-shell neutrinos is consistent, within their approximations, with the amplitude approach presented here and based on the method of Ref. [67].

5.3 Oscillation length and measurement of the modulation

For the described oscillation modulation to be well defined and detectable, several conditions have to be fulfilled. Among them is the hierarchy (5.30) between the length L between the production and the decay vertex, the width L_{wp} of the wavepacket, and the separation ΔL_{12} between the two wavepackets at the second vertex (cf. Fig. 5.3 and Ref. [67]). Yet another necessary condition for the detection of the oscillation is that the maximal detected length L between the two vertices (we shall call it simply the total detector length, $L_{\mathrm{max}} \equiv L_{\mathrm{det}}$) is larger than or comparable with the oscillation length L_{osc} [Eq. (5.33)]. For the measurement of the oscillation modulation effects in practice, the more convenient case is $L_{\mathrm{osc}} \sim L_{\mathrm{det}}$ than $L_{\mathrm{osc}} < L_{\mathrm{det}}$, i.e.,

$$L_{\mathrm{osc}} \left(\equiv \frac{2\pi \beta_N \gamma_N}{\Delta M_N}\right) \sim L_{\mathrm{max}} \ (\equiv L_{\mathrm{det}}). \quad (5.42)$$

Further, if the decay probability $P_{N_j}(L_{\mathrm{det}})$ for the decay of N_j $(j = 1, 2)$ within the detector, Eqs. (C.2)-(5.19), is significant, i.e., if $P_{N_j}(L_{\mathrm{det}}) \sim 1$, then the oscillation is not well-defined because it disappears within one of less oscillation cycle due the the decay of N_j. Therefore,

for the oscillation to be well-defined, we have to require $P_{N_j}(L_{\rm det}) \ll 1$. This means, according to Eq. (5.17b) and using Eq. (5.42), the following:

$$(L_{\rm osc} \equiv) \frac{2\pi\beta_N\gamma_N}{\Delta M_N} \sim L_{\rm det} \ll \frac{\beta_N\gamma_N}{\Gamma_{N_j}}. \tag{5.43}$$

This implies that we have $1/\Delta M_N \ll 1/\Gamma_{N_j}$ $(j = 1, 2)$, meaning that the condition $y(\equiv \Delta M_N/\Gamma_N) \gg 1$ of Eq. (5.15) is fulfilled when we have well-defined and detectable oscillation.[3] We recall that this condition $(y \gg 1)$ was assumed throughout the derivation of the oscillation formulas of the previous Section so that the (otherwise problematic) overlap terms with $\delta(y)$ and $\eta(y)/y$ factors in the expression (5.12) could be neglected.

The oscillation length can be estimated in the following way. Let us assume that the near mass-degeneracy $(y \gg 1)$ is in the interval: $1 \ll y(\equiv \Delta M_N/\Gamma_N) \lesssim 10^2$, i.e.,

$$\Delta M_N \lesssim 10^2 \Gamma_N. \tag{5.44}$$

Further, let us take that in the total decay widths Γ_{N_j}, Eqs. (3.13)-(3.15), the dominating contribution in the mixing factors $\widetilde{\mathcal{K}}_j$ is from ℓ-component, i.e., $\widetilde{\mathcal{K}}_j \approx \mathcal{N}_{\ell N}|B_{\ell N_j}|^2$ $(j = 1, 2;$ $\ell = e$ or μ or $\tau)$. Stated otherwise, we assume that $|B_{\ell N_j}|^2$ is the largest among the mixings $|B_{eN_j}|^2$, $|B_{\mu N_j}|^2$ and $|B_{\tau N_j}|^2$. Then we have

$$\begin{aligned} \Gamma_{N_j} &= \left(\frac{\mathcal{N}_{\ell N}}{10}\right) \times \left(\frac{|B_{\ell N_j}|^2}{10^{-5}}\right) \times 4.57 \times 10^{-18}\ \text{GeV} \\ &= \left(\frac{\mathcal{N}_{\ell N}}{10}\right) \times \left(\frac{|B_{\ell N_j}|^2}{10^{-5}}\right) \times \frac{1}{43.5\ \text{m}}. \end{aligned} \tag{5.45}$$

For $M_N =$ 1-5 GeV, and taking N to be Majorana neutrino, we have $\mathcal{N}_{eN} \approx \mathcal{N}_{\mu N} \approx$ 6-10, and $\mathcal{N}_{\tau N} \approx$ 3-5, hence the factor $\mathcal{N}_{\ell N}/10$ in Eq. (5.45) is ~ 1. The factor $|B_{\ell N_j}|^2/10^{-5}$ in Eq. (5.45) can be ~ 1, or larger or smaller, cf. Table 5.1 for some present upper bounds.

Table 5.1: *Presently known upper bounds for the squares $|B_{\ell N}|^2$ of the heavy-light mixing matrix elements, for various specific values of M_N. We excluded the upper bounds for $|B_{eN}|^2$ from $0\nu\beta\beta$ decay, which are uncertain due to possible cancellation effects. See also Figs. 3-5 of Ref. [69]. For each upper bound value, the corresponding experiment (reference) is indicated.*

$M_N[GeV]$	$\lvert B_{eN}\rvert^2$	$\lvert B_{\mu N}\rvert^2$	$\lvert B_{\tau N}\rvert^2$
1.0	3×10^{-7} ([70])	1×10^{-7} ([55])	3×10^{-3} ([56])
2.1	4×10^{-5} ([56])	3×10^{-5} ([71])	2×10^{-4} ([56])
3.0	2×10^{-5}([56])	2×10^{-5}([56])	4×10^{-5}([56])
4.0-5.0	1×10^{-5} ([56])	1×10^{-5} ([56])	1×10^{-5} ([56]

The oscillation length (5.33) can then be estimated

$$L_{\rm osc} = \frac{2\pi|\vec{p}_N|}{M_N\Delta M_N} \gtrsim \frac{|\vec{p}_N|}{M_N}\frac{2\pi}{10^2\Gamma_N} \sim \frac{|\vec{p}_N|}{M_N}\frac{1}{10\Gamma_N} \tag{5.46a}$$

$$\sim \frac{|\vec{p}_N|}{M_N}\frac{1}{10} \times \left(\frac{10}{\mathcal{N}_{\ell N}}\right) \times \frac{2\times10^{-5}}{(|B_{\ell N_1}|^2 + |B_{\ell N_2}|^2)} \times 5\times10^1\ \text{m} \sim \frac{|\vec{p}_N|}{M_N}\frac{10^{-4}}{|B_{\ell N_j}|^2}\ \text{m} \sim \frac{10^{-4}}{|B_{\ell N_j}|^2}\ \text{m}. \tag{5.46b}$$

[3] $\Gamma_N \equiv (1/2)(\Gamma_{N_1} + \Gamma_{N_2})$ according to the definition (3.37).

In the estimate (5.46a) we assumed the inequality (5.44), and in the estimate (5.46b) we took into account the relation (5.45), as well as the identity (3.37) for Γ_N; and at the end we assumed that the produced on-shell neutrinos N_j are semirelativistic, i.e., $|\vec{p}_N| \sim M_N$ (~ 1 GeV). Using the estimate (5.46b), and recalling that $|B_{\ell N_j}|^2$ is the largest among the mixings $|B_{eN_j}|^2$, $|B_{\mu N_j}|^2$ and $|B_{\tau N_j}|^2$, we can see from Table 5.1 that for $M_N =$ 1-5 GeV we can take $|B_{\ell N_j}|^2 = |B_{\tau N_j}|^2$, whose upper bounds are given in the right column of Table 5.1. This implies that, at present, we can expect the values $L_{\rm osc} \sim$ 0.1-10 m for the oscillation length. Of course, implicitly we assumed that the energies of the (B or B_c) mesons, which decay, are not very high so that the assumption $|\vec{p}_N| \sim M_N$ would be justified. If $L_{\rm osc} > 10$ m, we would need quite a large detector, cf. Eqs. (5.42) and (5.43).

If we have $L_{\rm osc} \sim$ 0.1-1 m ($\sim L_{\rm det}$), our formulas (5.37)-(5.38) for LV decays and (5.40)-(5.41) for LC decays indicate that such oscillations can be detected and measured, once a sufficient number of such decays is detected, with the first (production) and the second (decay) vertices being within the detector. In this way, the oscillation length $L_{\rm osc} \propto 1/\Delta M_N$ could be determined, and thus the mass difference ΔM_N ($\ll M_N$).

It is also interesting that these formulas indicate that in such a case the phases $\theta_{21}^{\rm (LV)}$ and $\theta_{21}^{\rm (LC)}$ could be measured as well. These phases could be determined, for example, by comparing the modulation of the measured differential effective decay widths $d\Gamma_{\rm eff}^{\rm (osc)}(B^{\pm}; L)/dL$ for the B^+ and B^- decays into $\mu e\pi$, because the phase difference between the two oscillatory modulations is $2 \times \theta_{21}$, cf. Eq. (5.37) for LV and Eq. (5.40) for LC case. The factor $\sin\theta_{21}$ appears in the CP asymmetry factor $\mathcal{A}_{\rm CP} \propto \sin\theta_{21}$ for these processes. For example, this asymmetry for the LV case is

$$\mathcal{A}_{\rm CP}^{\rm (LV)}(B) \equiv \frac{\Gamma(B^- \to \mu^- e^- \pi^+) - \Gamma(B^+ \to \mu^+ e^+ \pi^-)}{\Gamma(B^- \to \mu^- e^- \pi^+) + \Gamma(B^+ \to \mu^+ e^+ \pi^-)} \tag{5.47a}$$

$$\propto P \sin\theta_{21}^{\rm (LV)} \frac{y}{y^2+1}, \tag{5.47b}$$

where $y \equiv \Delta M_N/\Gamma_N$ [cf. the notation (3.37)], and factor $P \sim 1$ depends principally on the ratios of mixings $|B_{\ell N_2}|/|B_{\ell N_1}|$ ($\ell = \mu, e$) and ratio $\widetilde{\mathcal{K}}_1/\widetilde{\mathcal{K}}_2$ [cf. the notation (3.15)]. This factor $\mathcal{A}_{\rm CP}$ can be substantial if $y \equiv \Delta M_N/\Gamma_N$ is not too small, e.g. if $y \sim 10$. We refer to Section 4 for more details on this. An interesting aspect here is that, by the described measurement of the angle θ_{21} we could conclude that the CP asymmetry $\mathcal{A}_{\rm CP}$ is nonzero even in the case when $y \gg 1$, i.e., when this asymmetry is practically unmeasurable.

The differential decay width $d\Gamma_{\rm eff}^{\rm (osc)}(B \to \mu e\pi; L)/dL$ of Eqs. (5.37) and (5.40) is presented schematically in Fig. 5.4, where L is the distance between the two vertices, and $L_{\rm max} = L_{\rm det}$. In order to interpret how to measure this differential decay width, we recall that this quantity is the limit $(1/\Delta L) \times \Gamma_{\rm eff}^{\rm (osc)}(B \to \mu e\pi; L < L' < L + \Delta L)$ when $\Delta L \to 0$ (i.e., $\Delta L \ll L_{\rm osc}$), and here L' is the distance between the production (μ-N_j) and the decay (N_j-e-π) vertex. To measure such a quantity, a sufficiently high number of events for each chosen bin $L < L' < L + \Delta L$ would have to be measured (with $\Delta L \ll L_{\rm osc}$ and $L \leq L_{\rm det}$).

There may exist another complication in such measurements. Namely the length $L_{\rm osc}$ can vary in the detected events of the considered decays because $L_{\rm osc} \propto \beta_N \gamma_N \propto |\vec{p}_N| \equiv |\vec{p}_e + \vec{p}_\pi|$. In principle, the 3-momentum $\vec{p}_N \equiv \vec{p}_e + \vec{p}_\pi$ can be measured in each such decay, i.e., $L_{\rm osc}$ can be determined in each such event. The graphical representation Fig. 5.4 refers to a class of events which, among themselves, have approximately equal value of $L_{\rm osc}$, i.e., approximately equal $|\vec{p}_N|$. If the decaying $B^{\pm}$ (or $B_c^{\pm}$) mesons were at rest in the lab frame, then the value of

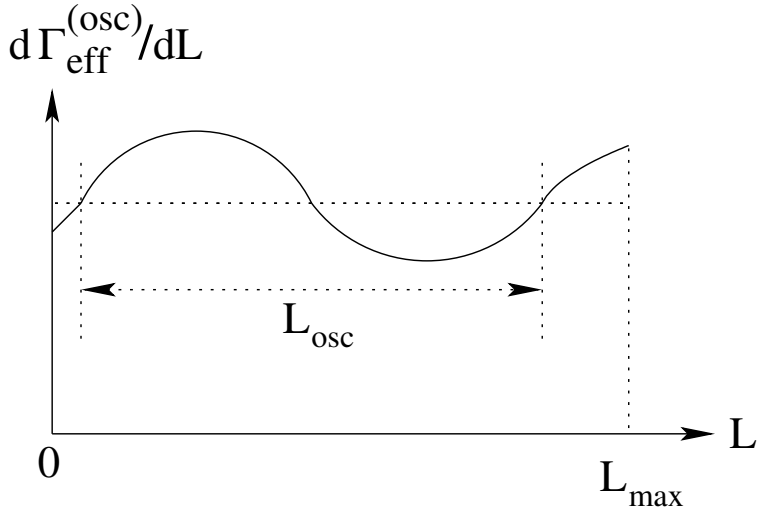

Figure 5.4: *Graphical schematical representation of the differential decay rate* $d\Gamma_{\rm eff}^{\rm (osc)}(B \to \mu e\pi; L)/dL$, *cf. Eqs. (5.37) and (5.40).*

$|\vec{p}_N|$ is such a frame would be fixed by kinematics, namely

$$|\vec{p}_N^{\,(0)}| = \frac{1}{2} M_B \, \lambda^{1/2} \left(1, \frac{M_N^2}{M_B^2}, \frac{M_\mu^2}{M_B^2}\right), \tag{5.48}$$

where the notation (5.6b) is used.

In reality the B mesons coming into the detector have energies $E_B > M_B$. Let us assume that the incoming B mesons in the lab frame have all approximately the same 3-momentum $\vec{p}_B = |\vec{p}_B|\hat{z}$ parallel to the direction $\hat{z}$ of the tube of the detector where both vertices are detected, and that the detector tube is relatively narrow. Then the vector $\vec{p}_N$ in the detected events is the 3-momentum which can be obtained from $\vec{p}_N^{\,(0)} = |\vec{p}_N^{\,(0)}|\hat{z}$ [cf. Eq. (5.48)] by a constant boost in the direction $-\hat{z}$, bringing us from the B rest frame into the lab frame where B's have the (approximately) constant 3-momentum $|\vec{p}_B|\hat{z}$. Thus the lab 3-momentum $\vec{p}_N = |\vec{p}_N|\hat{z}$ is approximately constant also in such a case. In such a case $L_{\rm osc}$ would be approximately the same for all the detected events $B \to \mu N \to \mu e\pi$ in the tube, and the oscillation modulation as indicated in Fig. 5.4 could be measured, including the phase θ_{21} relevant for CP violation.

Chapter 6

Conclusions

CP violation in the (sterile) neutrino sector may have important implications for the thermal generation of dark matter and baryon asymmetry of the universe [72]. We investigated the possibility of detection of CP violation in two different types of the decays, the leptonic ($\pi^{\pm} \to e^{\pm} N_j \to e^{\pm} e^{\pm} \mu^{\mp} \nu$) and the semihadronic decays ($M^{\pm} \to \ell_1^{\pm} N_j \to \ell_1^{\pm} \ell_2^{\pm} M^{'\mp}$), where M and $M^{'}$ are pseudoscalar mesons, $M = K, D, D_s, B, B_c$ and $M^{'} = \pi, K, D, D_s$, and the charged leptons are $\ell_1, \ell_2 = e, \mu$. We assumed that such decays occur by means of exchange of on-shell intermediate neutrinos at the tree level, but are suppressed by the heavy-light neutrino mixing elements of the PMNS matrix.

In the leptonic decay scenario ($\pi^{\pm} \to e^{\pm} e^{\pm} \mu^{\mp} \nu$), the decays can be lepton-number-conserving (LC), or lepton-number-violating (LV). If the N_j neutrinos are of Dirac nature, only LC decays take place; if they are of Majorana nature, both LC and LV decays take place. In Ref. [27] such decays were studied with a view to ascertain the nature of the intermediate neutrino N_j, and it was shown there that it may be possible to do this in the future pion factories where the number of produced charged pions will be exceedingly high. On the other hand, the semihadronic decays ($M^{\pm} \to \ell_1^{\pm} \ell_2^{\pm} M^{'\mp}$), are lepton-number-violation (LV) processes [25], and in such processes the neutrino must be Majorana type.

In this thesis, I investigated the possibility to establish the CP violation in both aforementioned types of decays. Such a CP violation originates from the interference between the N_1 and N_2 exchange processes and the existence of possible CP-violating phases in the PMNS mixing matrix. We showed that such signals of CP violation could be detected in the future pion factories (leptonic scenario) and in the future SHiP experiment (semihadronic scenario) if we have, at least, two sterile neutrinos in the mentioned mass intervals and such that their masses are almost degenerate. A similar phenomenon of (resonant) CP violation was investigated earlier [73], in neutrino decays and neutrino-mediated scattering, but with a more complicated formalism involving loops-effects. Our formalism is simpler, involving tree-level formulation and neutrino propagators with finite decay widths Γ_{Nj}.

In CP asymmetries detection, the crucial point is the expression for the imaginary part of the product of the propagators of two Majorana neutrinos Eqs. (3.35), when the difference of masses $\Delta M_N \equiv M_{N_2} - M_{N_1}$ (> 0) of the two sterile neutrinos becomes small enough, comparable to the total decay widths of these neutrinos, $0.33\ \Gamma_N \leq \Delta M_N \leq 5\ \Gamma_N$. In such a case, the mentioned imaginary part becomes large and leads to a large CP-violating decay width difference $S_-(M) \equiv S(M^-) - S(M^+)$. We show that in such a case, and provided that a specific CP-violating difference θ_{21} of the phases of heavy-light neutrino mixings is not very small ($|\theta_{21}| \ll 1$), the decay width difference $S_-(M)$ becomes comparable with the sum of the decay widths $S_+(M) \equiv S(M^-) + S(M^+)$ and the corresponding CP ratio $\mathcal{A}_{\rm CP}(M) \equiv S_-(M)/S_+(M)$ thus becomes $\mathcal{A}_{\rm CP}(M) \sim 1$. It is interesting that the requirement of the near degeneracy of the two sterile neutrinos (with $M_{N_j} \sim 1$ GeV), at which we arrive by requiring appreciable CP violation, fits well into the well-motivated νMSM model [29–34], where the near degeneracy

of the two sterile neutrinos with mass $M_{N_j} \sim 1$ GeV is obtained by requiring that the third (the lightest) sterile neutrino be the dark matter candidate. The results of our calculation can thus be interpreted in the framework of the νMSM model or more general low-scale seesaw models [74], namely that if the model is experimentally confirmed then it is possible that significant neutrino sector CP violation effects will be detected as well.

Moreover we considered the phenomenon of neutrino oscillations in semileptonic decays of B mesons via on-shell heavy nearly mass-degenerate Majorana neutrinos N_j ($j = 1, 2$): the lepton number violating (LV) decays $B^\pm \to \mu^\pm N_j \to \mu^\pm e^\pm \pi^\mp$, and the lepton number conserving (LC) decays $B^\pm \to \mu^\pm N_j \to \mu^\pm e^\mp \pi^\pm$. Since the neutrinos contributing to such decays have to be on-shell (the off-shell neutrinos give completely negligible contributions), the relevant flavor analogs are not ν_μ and ν_e Eqs. (5.1), but the truncated combinations $\mathcal{N}_1$ and $\mathcal{N}_2$ Eqs. (5.2)-(5.3), which are combinations of only the heavy mass neutrinos N_1 and N_2. The central results of the work are Eqs. (5.37) and (5.40) for the LV and LC differential effective decay rates $d\Gamma^{(\rm osc)}_{\rm eff}(L)/dL$. These quantities must be interpreted as $(1/\Delta L) \times \Gamma^{(\rm osc)}_{\rm eff}(L < L' < L + \Delta L)$, where L' is the measured distance between the production vertex (μ-N) and the decay vertex (N-e-π), and ΔL is considerably smaller than the oscillation length $L_{\rm osc} \equiv 2\pi|\vec{p}_N|/(M_N \Delta M_N)$. Here, $\vec{p}_N$ is the (approximately constant) 3-momentum of the intermediate N_j's, and mass quantities are $0 < \Delta M_N \equiv M_{N_2} - M_{N_1} \ll M_{N_1} \equiv M_N$. We argued that it is possible to have $L_{\rm osc} \sim$ 0.1-10 m if the 3-momenta $\vec{p}_B$ and thus $\vec{p}_N$ are not too large. If the detector length is comparable with $L_{\rm osc}$, and a sufficient number of mentioned decays is detected, we argued that it will be conceivable to measure the L-dependence of the differential decay width $d\Gamma^{(\rm osc)}_{\rm eff}(L)/dL$, i.e., the oscillation modulation effects. By measuring these effects, the value of $L_{\rm osc}$ could be discerned and thus the value of the mass difference ΔM_N ($\ll M_N$). Moreover, by measuring such effects it would be possible to discern the phase θ_{21}, cf. Eqs. (5.13) and (5.14), which plays an important role in the CP violation.

Appendix A

Explicit Formulas of $\pi^+ \to e^+e^+\mu^-\nu_e$

A.1 Square Matrix Elements

Here we write down the explicit formulas for the direct (DD^*), crossed (CC^*) and direct-crossed interference (DC^*, CD^*) elements [$T^{(X)}(DD^*)$, $T^{(X)}(CC^*)$, $T^{(X)}(DC^*)$, $T^{(X)}(CD^*)$] appearing in Eqs. (3.4). For the lepton number violating (LV) processes in Figs. 3.1 and 3.2, these are:

$$T^{(LV)}(DD^*) = 256(p_2\cdot p_\nu)\left[-M_\pi^2(p_1\cdot p_\mu)+2(p_1\cdot p_\pi)(p_\mu\cdot p_\pi)\right] , \tag{A.1a}$$

$$T^{(LV)}(CC^*) = 256(p_1\cdot p_\nu)\left[-M_\pi^2(p_2\cdot p_\mu)+2(p_2\cdot p_\pi)(p_\mu\cdot p_\pi)\right] , \tag{A.1b}$$

$$\begin{aligned} T_\pm^{(LV)}(DC^*) = 128\Big\{ & (p_1\cdot p_\nu)\left[M_\pi^2(p_2\cdot p_\mu)-2(p_2\cdot p_\pi)(p_\mu\cdot p_\pi)\right] \\ & +(p_2\cdot p_\nu)\left[M_\pi^2(p_1\cdot p_\mu)-2(p_1\cdot p_\pi)(p_\mu\cdot p_\pi)\right] \\ & -(p_1\cdot p_2)\left[M_\pi^2(p_\nu\cdot p_\mu)-2(p_\nu\cdot p_\pi)(p_\mu\cdot p_\pi)\right]\Big\} \\ & \mp i\Big\{ -(p_1\cdot p_\pi)\epsilon(p_2,p_\nu,p_\mu,p_\pi)+(p_2\cdot p_\pi)\epsilon(p_1,p_\nu,p_\mu,p_\pi) \\ & -(p_\nu\cdot p_\pi)\epsilon(p_1,p_2,p_\mu,p_\pi)+(p_\mu\cdot p_\pi)\epsilon(p_1,p_2,p_\nu,p_\pi)\Big\} , \end{aligned}$$

$$T_\pm^{(LV)}(CD^*) = \left(T_\pm^{(LV)}(DC^*)\right)^* , \tag{A.1c}$$

where we denoted

$$\epsilon(q_1,q_2,q_3,q_4) \equiv \epsilon^{\eta_1\eta_2\eta_3\eta_4}(q_1)_{\eta_1}(q_2)_{\eta_2}(q_3)_{\eta_3}(q_4)_{\eta_4} , \tag{A.2}$$

and $\epsilon^{\eta_1\eta_2\eta_3\eta_4}$ is the totally antisymmetric Levi-Civita tensor with the sign convention $\epsilon^{0123}=+1$.

For the lepton number conserving (LC) process in Figs. 3.3 and 3.4, the corresponding

expressions are:

$$\begin{aligned}
T^{(LC)}(DD^*) &= 256(p_\mu\cdot p_\nu)\Big[(p_1\cdot p_2)\left(M_\pi^4 - M_\pi^2M_e^2 - 4M_\pi^2(p_1\cdot p_\pi) + 4(p_1\cdot p_\pi)^2\right) \\
&\quad +2M_e^2(p_2\cdot p_\pi)(M_\pi^2 - p_1\cdot p_\pi)\Big]\,, \qquad \text{(A.3a)}\\
T^{(LC)}(CC^*) &= 256(p_\mu\cdot p_\nu)\Big[(p_1\cdot p_2)\left(M_\pi^4 - M_\pi^2M_e^2 - 4M_\pi^2(p_2\cdot p_\pi) + 4(p_2\cdot p_\pi)^2\right) \\
&\quad +2M_e^2(p_1\cdot p_\pi)(M_\pi^2 - p_2\cdot p_\pi)\Big]\,, \qquad \text{(A.3b)}\\
T^{(LC)}(DC^*) &= 256(p_\mu\cdot p_\nu)\Big[(p_1\cdot p_2)(M_\pi^2 - 2p_1\cdot p_\pi)(M_\pi^2 - 2p_2\cdot p_\pi) \\
&\quad +M_e^2\left(-2(p_2\cdot p_\pi)^2 + M_\pi^2(p_2\cdot p_\pi) + M_\pi^2M_e^2\right) \\
&\quad +M_e^2(p_1\cdot p_\pi)(M_\pi^2 - 2p_1\cdot p_\pi)\Big]\,, \\
T^{(LC)}(CD^*) &= \left(T^{(LC)}(DC^*)\right)^*\,. \qquad \text{(A.3c)}
\end{aligned}$$

A.2 Explicit formula for $\Gamma^{(X)}$ when $M_e \neq 0$

The formula (3.21) is obtained by performing the integration of the differential decay width $d\Gamma^{(LV)}/dE_\mu$ over the muon energy E_μ, in the rest frame of the N_j neutrino. The expression for $d\Gamma^{(LV)}/dE_\mu$ is written explicitly, e.g., in Appendix A of Ref. [27]. This gives

$$\begin{aligned}
\Gamma^{(LV)}(DD^*)_{jj} &= K_\pi^2\,\frac{1}{2!}\frac{1}{2M_\pi(2\pi)^8}\int d_4\,|P_j^{(LV)}(D)|^2\,T^{(LV)}(DD^*) \qquad \text{(A.4a)}\\
&= K_\pi^2\,\frac{1}{2!}\frac{1}{2M_\pi(2\pi)^8}\int d_4\,\frac{\pi}{M_{N_j}\Gamma_{N_j}}\delta\left((p_\pi - p_1)^2 - M_{N_j}^2\right)M_{N_j}^2\,T^{(LV)}(DD^*) = \cdots \qquad \text{(A.4b)}\\
&= K_\pi^2\,\frac{1}{(2\pi)^4}\frac{M_{N_j}}{\Gamma_{N_j}M_\pi^3}\lambda^{1/2}(M_\pi^2, M_{N_j}^2, M_e^2)\times\frac{1}{2M_{N_j}}\left[M_\pi^2(M_{N_j}^2 + M_e^2) - (M_{N_j}^2 - M_e^2)^2\right] \\
&\quad\times\int_{M_\mu}^{(M_{N_j}^2+M_\mu^2-M_e^2)/(2M_e)} dE_\mu E_\mu\sqrt{E_\mu^2 - M_\mu^2}\,\frac{(M_{N_j}^2 - 2M_{N_j}E_\mu + M_\mu^2 - M_e^2)^2}{(M_{N_j}^2 - 2M_{N_j}E_\mu + M_\mu^2)}\,. \qquad \text{(A.4c)}
\end{aligned}$$

The ellipses in Eq. (A.4b) indicate the analytic integrations over the four-particle final phase space of the process of Fig. 3.1 with the exception of E_μ (in the rest frame of N_j), performed in Ref. [27]. Eq. (A.4c) then uses the differential decay width $d\Gamma^{(LV)}(DD^*)/dE_\mu$ obtained in Ref. [27].[1] The integration in Eq. (A.4c) can be performed explicitly (in Ref. [27] it was performed only in the limit $M_e = 0$), and the result is Eq. (3.21) with notations (3.22) and the

[1] Eq. (A.7) of that reference, with the corresponding replacements: $m_M \mapsto M_\pi$, $m_N \mapsto M_{N_j}$, $m_\ell \mapsto M_\mu$, $m_1 = m_2 \mapsto M_e$.

function $\mathcal{F}(x_j, x_{ej})$ given explicitly here

$$\begin{aligned}\mathcal{F}(x_j,x_{ej}) = \Bigg\{ & \lambda^{1/2}(1,x_j,x_{ej})\big[(1+x_j)(1-8x_j+x_j^2) - x_{ej}(7-12x_j+7x_j^2) \\ & -7x_{ej}^2(1+x_j)+x_{ej}^3\big] - 24(1-x_{ej}^2)x_j^2\ln 2 \\ & +12\Bigg[-x_j^2(1-x_{ej}^2)\ln x_j + (2x_j^2 - x_{ej}^2(1+x_j^2))\ln(1+x_j+\lambda^{1/2}(1,x_j,x_{ej})-x_{ej}) \\ & +x_{ej}^2(1-x_j^2)\ln\left(\frac{(1-x_j)^2+(1-x_j)\lambda^{1/2}(1,x_j,x_{ej})-x_{ej}(1+x_j)}{x_{ej}}\right)\Bigg]\Bigg\}\,, \end{aligned} \tag{A.5}$$

It turns out that the integration over the differential decay width of the lepton number conserving case, $d\Gamma^{(LC)}/dE_\mu$,

$$\begin{aligned}\Gamma^{(LC)}(DD^*)_{jj} = {} & K_\pi^2\,\frac{1}{(2\pi)^4}\frac{M_{N_j}}{\Gamma_{N_j}M_\pi^3}\lambda^{1/2}(M_\pi^2,M_{N_j}^2,M_e^2)\times\frac{1}{96M_{N_j}^2} \\ & \times\int_{M_\mu}^{(M_{N_j}^2+M_\mu^2-M_e^2)/(2M_e)} dE_\mu \frac{1}{\left[M_\mu^2+M_{N_j}(-2E_\mu+M_{N_j})\right]^3} \\ & \times\Bigg\{8\sqrt{(E_\mu^2-M_\mu^2)}M_{N_j}\left[(2E_\mu-M_{N_j})M_{N_j}-M_\mu^2+M_e^2\right]^2 \\ & \times\Big[M_\pi^2M_{N_j}^2 - M_{N_j}^4 + M_e^2(M_\pi^2+2M_{N_j}^2) - M_e^4\Big] \\ & \times\Big[8E_\mu^3M_{N_j}^2 - 2M_\mu^2M_{N_j}(M_\mu^2+M_{N_j}^2+2M_e^2) - 2E_\mu^2M_{N_j}\left(5(M_\mu^2+M_{N_j}^2)+M_e^2\right) \\ & +E_\mu\left(3M_\mu^4+10M_\mu^2M_{N_j}^2+3M_{N_j}^4+3M_e^2(M_\mu^2+M_{N_j}^2)\right)\Big]\Bigg\} \end{aligned} \tag{A.6}$$

gives the same result as the $X = LV$ case, i.e., Eqs. (3.21) with (A.5). In Eq. (A.6) we inserted the differential decay width $d\Gamma^{(LC)}(DD^*)_{jj}/dE_\mu$ as obtained in Eq. (A.14) of Ref. [27].

Appendix B

Partial decay widths of heavy neutrino N

The formulas for the leptonic decay and semimesonic decay widths of a sterile neutrino N have been obtained in Ref. [45] (Appendix C there), for the masses $M_N \sim 1$ GeV. Nonetheless, for the higher values of the masses M_N, the calculation of the semihadronic decay widths becomes increasingly complicated because not all the resonances are known. Therefore, in Refs. [26, 75] an inclusive approach was proposed for the calculation of the total contribution to the semihadronic decay width of N, by replacing the various (pseudoscalar and vector) meson channels by quark-antiquark channels. This inclusive approach, based on duality, was applied for high masses $M_N \geq M_{\eta'} \approx 0.958$ GeV. Here we summarize the formulas given in Ref. [26] for the decay width channels (see also: [45]). The leptonic channels are:

$$2\Gamma(N \to \ell^- \ell'^+ \nu_{\ell'}) = |B_{\ell N}|^2 \frac{G_F^2}{96\pi^3} M_N^5 I_1(y_\ell, 0, y_{\ell'})(1 - \delta_{\ell\ell'}) \,, \tag{B.1a}$$

$$\begin{aligned}\Gamma(N \to \nu_\ell \ell'^- \ell'^+) = |B_{\ell N}|^2 \frac{G_F^2}{96\pi^3} M_N^5 \Big[& (g_L^{(\mathrm{lept})} g_R^{(\mathrm{lept})} + \delta_{\ell\ell'} g_R^{(\mathrm{lept})}) I_2(0, y_{\ell'}, y_{\ell'}) \\ & + \Big((g_L^{(\mathrm{lept})})^2 + (g_R^{(\mathrm{lept})})^2 + \delta_{\ell\ell'}(1 + 2 g_L^{(\mathrm{lept})}) \Big) I_1(0, y_{\ell'}, y_{\ell'}) \Big]\end{aligned} \tag{B.1b}$$

$$\sum_{\nu_\ell} \sum_{\nu'} \Gamma(N \to \nu_\ell \nu' \bar{\nu}') = \sum_{\ell} |B_{\ell N}|^2 \frac{G_F^2}{96\pi^3} M_N^5 \,. \tag{B.1c}$$

In Eq. (B.1a) factor 2 is to be included only in the Majorana case, because in such case both decays $N \to \ell^- \ell'^+ \nu_{\ell'}$ and $N \to \ell^+ \ell'^- \nu_{\ell'}$ contribute ($\ell \neq \ell'$). In the Dirac case, only one half of the expression (B.1a) contributes.

If $M_N < M_{\eta'} \approx 0.968$ GeV, the following semimesonic decays contribute, involving pseudoscalar (P) and vector (V) mesons:

$$2\Gamma(N \to \ell^- P^+) = |B_{\ell N}|^2 \frac{G_F^2}{8\pi} M_N^3 f_P^2 |V_P|^2 F_P(y_\ell, y_P) \ , \tag{B.2a}$$

$$\Gamma(N \to \nu_\ell P^0) = |B_{\ell N}|^2 \frac{G_F^2}{64\pi} M_N^3 f_P^2 (1 - y_P^2)^2 \ , \tag{B.2b}$$

$$2\Gamma(N \to \ell^- V^+) = |B_{\ell N}|^2 \frac{G_F^2}{8\pi} M_N^3 f_V^2 |V_V|^2 F_V(y_\ell, y_V) \ , \tag{B.2c}$$

$$\Gamma(N \to \nu_\ell V^0) = |B_{\ell N}|^2 \frac{G_F^2}{2\pi} M_N^3 f_V^2 \kappa_V^2 (1 - y_V^2)^2 (1 + 2y_V^2) \ , \tag{B.2d}$$

where factor 2 in the charged meson channels is again to be taken only in the Majorana case, because both decays $N \to \ell^- M^{'+}$ and $N \to \ell^+ M^{'-}$ contribute ($M^{'} = P, V$). The factors V_P and V_V are the corresponding CKM matrix elements involving the valence quarks of the mesons; and f_P and f_V are the corresponding decay constants. The pseudoscalar mesons which may contribute are: $P^\pm = \pi^\pm, K^\pm$; $P^0 = \pi^0, K^0, \bar{K}^0, \eta$. The vector mesons which may contribute are: $V^\pm = \rho^\pm, K^{*\pm}$; $V^0 = \rho^0, \omega, K^{*0}, \bar{K}^{*0}$.[1] When $M_N \geq M_{\eta'}$ (= 0.9578 GeV), the above semimesonic decay modes are replaced [26], in the spirit of duality, by the following quark-antiquark decay modes:

$$2\Gamma(N \to \ell^- U \bar{D}) = |B_{\ell N}|^2 \frac{G_F^2}{32\pi^3} M_N^5 |V_{UD}|^2 I_1(y_\ell, y_U, y_D) \ , \tag{B.3a}$$

$$\Gamma(N \to \nu_\ell q \bar{q}) = |B_{\ell N}|^2 \frac{G_F^2}{32\pi^3} M_N^5 \left[g_L^{(q)} g_R^{(q)} I_2(0, y_q, y_q) + \left((g_L^{(q)})^2 + (g_R^{(q)})^2 \right) I_1(0, y_q, y_q) \right] \ . \tag{B.3b}$$

In Eq. (B.3) we have to take the factor 2 only for the Majorana case. In the formulas (B.1)-(B.3) we denoted $y_x \equiv M_X/M_N$ ($X = \ell, \nu_\ell, P, V, q$), and in Eqs. (B.3) we denoted: $U = u, c$; $D = d, s, b$; $q = u, d, c, s, b$. The values of quark masses which we used were: $M_u = M_d = 3.5$ MeV; $M_s = 105$ MeV; $M_c = 1.27$ GeV; $M_b = 4.2$ GeV. The SM neutral current couplings in Eqs. (B.1b) and (B.3b) are

$$g_L^{(\mathrm{lept})} = -\frac{1}{2} + \sin^2\theta_W \ , \quad g_R^{(\mathrm{lept})} = \sin^2\theta_W \ , \tag{B.4a}$$

$$g_L^{(U)} = \frac{1}{2} - \frac{2}{3}\sin^2\theta_W \ , \quad g_R^{(U)} = -\frac{2}{3}\sin^2\theta_W \ , \tag{B.4b}$$

$$g_L^{(D)} = -\frac{1}{2} + \frac{1}{3}\sin^2\theta_W \ , \quad g_R^{(U)} = \frac{1}{3}\sin^2\theta_W \ . \tag{B.4c}$$

[1] For the values of the decay constants f_P and f_V, see, e.g., Table 1 in Ref. [26].

The neutral current couplings κ_V of the neutral vector mesons are:

$$\kappa_V = \frac{1}{3}\sin^2\theta_W \quad (V=\rho^0,\omega)\ , \tag{B.5a}$$

$$\kappa_V = -\frac{1}{4}+\frac{1}{3}\sin^2\theta_W \quad (V=K^{*0},\bar{K}^{*0})\ . \tag{B.5b}$$

The kinematical expressions I_1, I_2, F_P and F_V are:

$$I_1(x,y,z) = 12\int_{(x+y)^2}^{(1-z)^2}\frac{ds}{s}(s-x^2-y^2)(1+z^2-s)\lambda^{1/2}(s,x^2,y^2)\lambda^{1/2}(1,s,z^2)\ , \tag{B.6a}$$

$$I_2(x,y,z) = 24yz\int_{(y+z)^2}^{(1-x)^2}\frac{ds}{s}(1+x^2-s)\lambda^{1/2}(s,y^2,z^2)\lambda^{1/2}(1,s,x^2)\ , \tag{B.6b}$$

$$F_P(x,y) = \lambda^{1/2}(1,x^2,y^2)\left[(1+x^2)(1+x^2-y^2)-4x^2\right]\ , \tag{B.6c}$$

$$F_V(x,y) = \lambda^{1/2}(1,x^2,y^2)\left[(1-x^2)^2+(1+x^2)y^2-2y^4\right]\ , \tag{B.6d}$$

where λ function is written in Eq. (3.22a). Using these formulas, the total decay width $\Gamma(N_j\to$ all) can be calculated, and coefficients $\mathcal{N}_{\ell N_j}$ of Eq. (3.15) at the mixing terms $|B_{\ell N_j}|^2$ can be evaluated and are presented in Figs. B.1 and B.2. The small kink in the curves of Figs. B.1 and B.2 at $M_N = M_{\eta'}$ ($= 0.9578$ GeV) appears due to the replacement there (i.e., for $M_N \geq M_{\eta'}$) of the semihadronic decay channel contributions by the quark-antiquark channel contributions; we see that the duality works quite well there, with the exception of the case $\ell=\tau$ because of the large τ lepton mass.

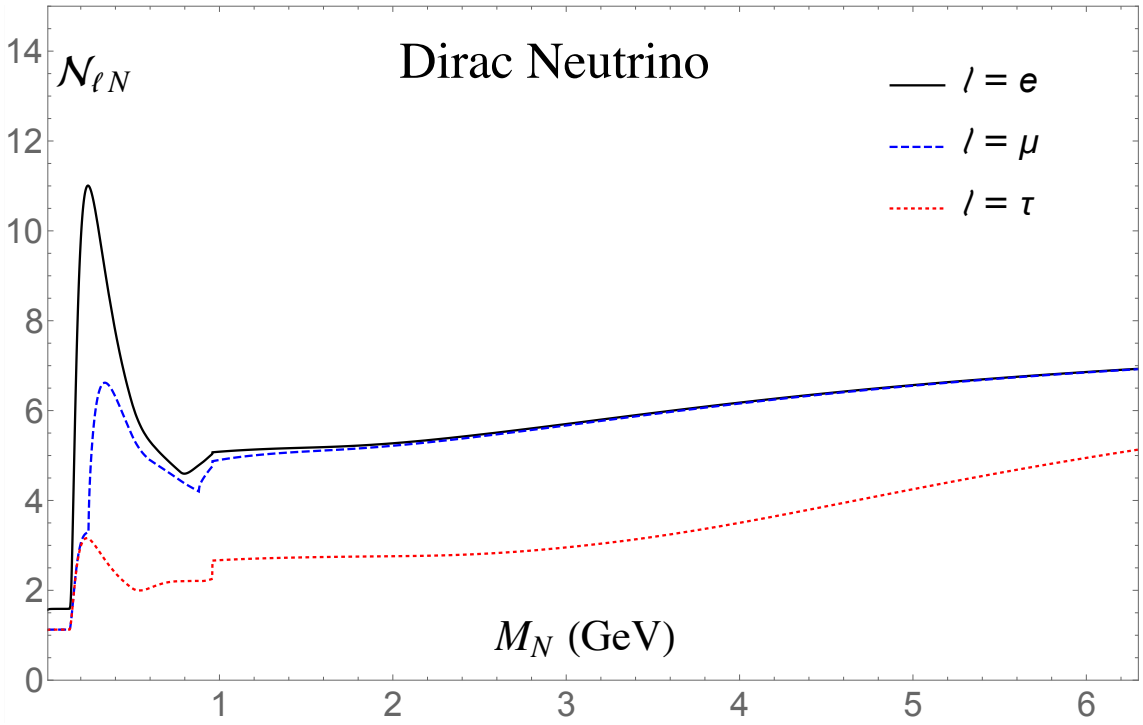

Figure B.1: *The effective mixing coefficients $\mathcal{N}_{\ell N}$ $(\ell = e, \mu, \tau)$ appearing in Eqs. (3.13)-(3.15), as a function of the mass M_N of the Dirac neutrino.*

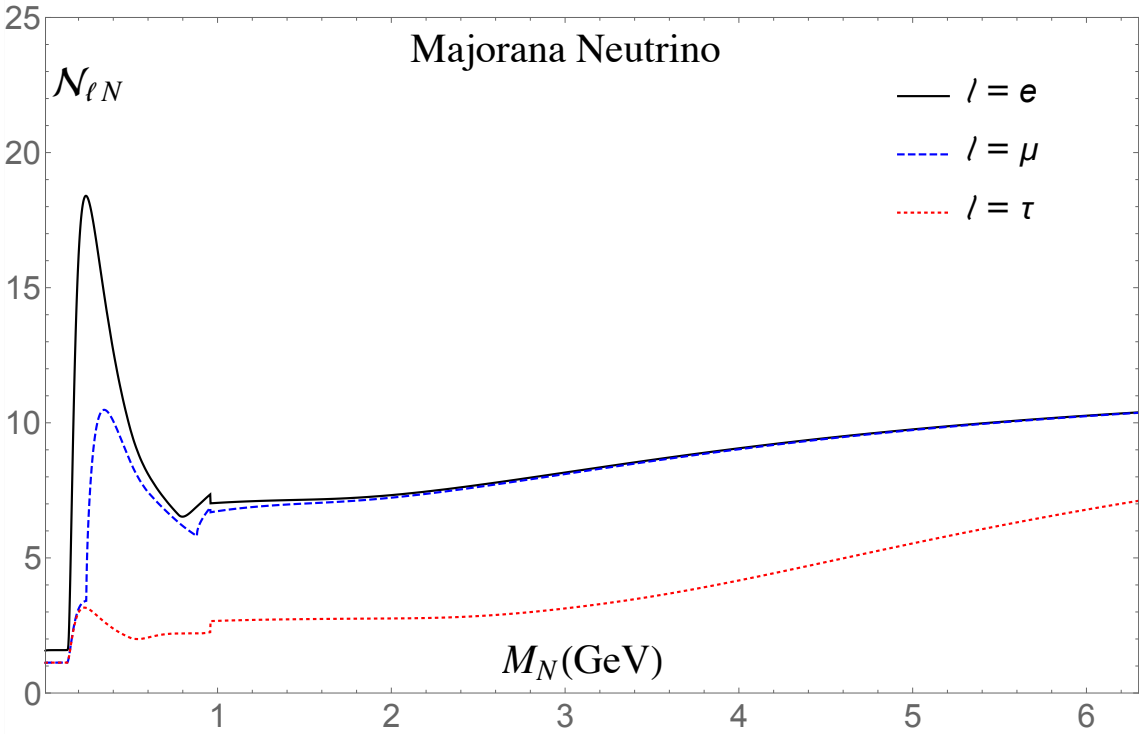

Figure B.2: *The effective mixing coefficients $\mathcal{N}_{\ell N}$ $(\ell = e, \mu, \tau)$ appearing in Eqs. (3.13)-(3.15), as a function of the mass M_N of the Majorana neutrino N.*

Appendix C

The acceptance factor

In experiments which try to detect and investigate the LV decay modes of the mesons $M^{\pm}$, the (expected) number $N_M \sim 10^N$ of produced mesons $M^{\pm}$ (per year, for example) is known. The value of the corresponding branching ratios of the LV decay modes: $\mathrm{Br}(M^{\pm} \to \ell_1^{\pm}\ell_2^{\pm}M'^{\mp}) \equiv \Gamma(M^{\pm} \to \ell_1^{\pm}\ell_2^{\pm}M'^{\mp})/\Gamma(M^{\pm} \to \text{all})$ or $\mathrm{Br}(\pi^{\pm} \to \ell_1^{\pm}\ell_1^{\pm}\ell_2^{\mp}\nu_{\ell_2}) \equiv \Gamma(\pi^{\pm} \to \ell_1^{\pm}\ell_1^{\pm}\ell_2^{\mp}\nu_{\ell_2})/\Gamma(\pi^{\pm} \to \text{all})$, then becomes important. In principle, if $\mathrm{Br}(M^{\pm} \to \ell_1^{\pm}\ell_2^{\pm}M'^{\mp})$ or $\mathrm{Br}(\pi^{\pm} \to \ell_1^{\pm}\ell_1^{\pm}\ell_2^{\mp}\nu_{\ell_2}) > 10^{-N}$, then such decay modes could be detected. Further, if an experiment produces approximately equal numbers of M^+ and M^- mesons, then the branching ratios of experimental significance for the decays $M^{\pm} \to \ell_1^{\pm}\ell_2^{\pm}M'^{\mp}$ and $\pi^{\pm} \to \ell_1^{\pm}\ell_1^{\pm}\ell_2^{\mp}\nu_{\ell_2}$ are:

$$\mathrm{Br}(M) \equiv \frac{S_+(M)}{[\Gamma(M^- \to \text{all}) + \Gamma(M^+ \to \text{all})]} \approx \frac{S_+(M)}{2\Gamma(M^- \to \text{all})} , \tag{C.1a}$$

$$\mathcal{A}_{\mathrm{CP}}(M)\mathrm{Br}(M) = \frac{S_-(M)}{[\Gamma(M^- \to \text{all}) + \Gamma(M^+ \to \text{all})]} \approx \frac{S_-(M)}{2\Gamma(M^- \to \text{all})} , \tag{C.1b}$$

where we use the notation of Eqs. (3.29a)-(5.47a) and (4.29a)-(4.29b) and $M = \pi, K, D, Ds, B, B_C$. Here we understand that $M = \pi$ means $\pi^{\pm} \to \ell_1^{\pm}\ell_1^{\pm}\ell_2^{\mp}\nu_{\ell_2}$ and $M = K, D, Ds, B, Bc$ means $M^{\pm} \to \ell_1^{\pm}\ell_2^{\pm}M'^{\mp}$. We also used the fact that in the considered cases of pseudoscalar mesons $M^{\pm}$ the total decay widths $\Gamma(M^- \to \text{all})$ and $\Gamma(M^+ \to \text{all})$ are practically equal. $\mathrm{Br}(M)$ represents the average of the branching ratios of M^+ and M^- for these decays, while $\mathcal{A}_{\mathrm{CP}}(M)\mathrm{Br}(M)$ is the corresponding branching ratio for the (CP-violating) difference.

Nonetheless, in experiments we must also take into account the acceptance (suppression) factor in the detection of these decays, which appears due to the small length of the detector in comparison to the relatively large lifetime of the (on-shell) sterile neutrinos N_j. Stated otherwise, most of the on-shell neutrinos, produced in the decay $M^{\pm} \to \ell_1^{\pm}N_j$, are expected to survive long enough time to travel through the detector and decay (into $\ell_2^{\pm}M'^{\mp}$) outside the detector.

Only when $M = B$ or B_c, a large part of the produced neutrinos N_j can decay within the 1 meter long detector (see the arguments later on).

This effect suppresses the number of detected decays and should be taken into account. The acceptance (suppression) factor is the probability of the on-shell neutrino N to decay inside the detector of length L

$$P_{N_j} \approx \frac{L}{\gamma_{N_j}\tau_{N_j}\beta_{N_j}} \sim \frac{L}{\gamma_{N_j}\tau_{N_j}} = \frac{L\Gamma_{N_j}}{\gamma_{N_j}} = \frac{L\overline{\Gamma}(M_{N_j})}{\gamma_{N_j}}\widetilde{\mathcal{K}}_j \equiv \overline{A}(M_{N_j})\widetilde{\mathcal{K}}_j , \tag{C.2}$$

where γ_{N_j} is the time dilation (Lorentz) factor $\gamma_{N_j} = (1-\beta_{N_j}^2)^{-1/2}$ ($\sim$ 1-10) in the lab system. We took into account that the speed of neutrino is $\beta_{N_j} \sim 1$. The quantity $\overline{\Gamma}(M_{N_j})$ ($\propto M_{N_j}^5$) and the factor $\widetilde{\mathcal{K}}_j$ ($\propto |B_{\ell N_j}|^2$) were defined in Eqs. (3.14) and (3.15), respectively. The quantity $\overline{A}(M_{N_j}) \equiv (L\overline{\Gamma}(M_{N_j})/\gamma_{N_j})$ can be called "canonical acceptance," and depends heavily on the neutrino mass: $\overline{A} \propto M_{N_j}^5$. In Figs. C.1 and C.2 we present the values of this canonical acceptance as a function of the neutrino mass M_N, for the choice $L = 1$ m ($= 5.064{\cdot}10^{15}$ GeV^{-1}) and $\gamma_N = 2$.

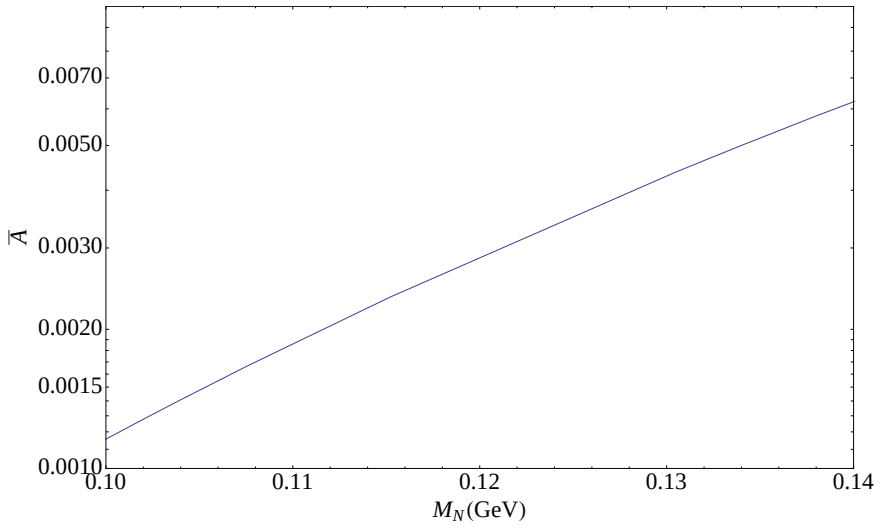

Figure C.1: *The canonical acceptance $\overline{A}(M_N) \equiv (L\overline{\Gamma}(M_N)/\gamma_N)$ as a function of the neutrino mass M_N in the relevant on-shell range for the pion decay. In the curve, we took for the length of the detector the value $L = 1$ m and for the time dilation factor the value $\gamma_N = 2$.*

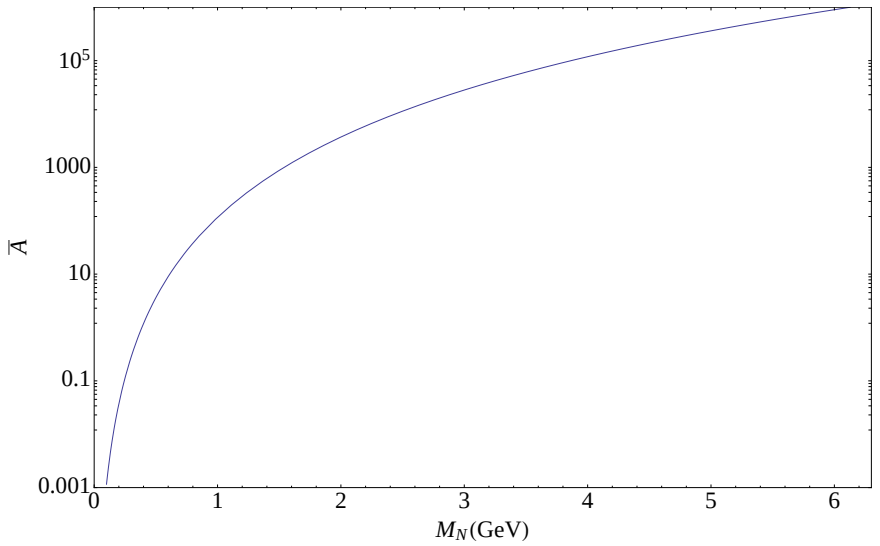

Figure C.2: *The canonical acceptance $\overline{A}(M_N) \equiv (L\overline{\Gamma}(M_N)/\gamma_N)$ as a function of the neutrino mass M_N. In the curve, we took for the length of the detector the value $L = 1$ m and for the time dilation factor the value $\gamma_N = 2$.*

The values of $\overline{A}$ for other cases of the values of L and γ_N are obtained directly from the presented curve by taking into account that $\overline{A} \propto L/\gamma_N$. The realistic acceptance factor is then obtained by Eq. (C.2), where $\widetilde{\mathcal{K}}_j \sim |B_{\ell N_j}|^2$ $(j = 1, 2)$ are the heavy-light mixing factors defined in Eq. (3.15) with coefficients $\mathcal{N}_{\ell N}$ there of ~ 10 according to Figs. B.1 and B.2. Combining the results of Figs. B.1 and B.2 with Eq. (3.15), we can write rough approximations for $\widetilde{\mathcal{K}}_j$

$$\widetilde{\mathcal{K}}_j^{Ma} \approx 1.6|B_{eN_j}|^2 + 1.1|B_{\mu N_j}|^2 + 1.1|B_{\tau N_j}|^2 \quad (\pi \text{ decays}) , \tag{C.3a}$$

$$\widetilde{\mathcal{K}}_j^{Di} \approx 1.6|B_{eN_j}|^2 + 1.1|B_{\mu N_j}|^2 + 1.1|B_{\tau N_j}|^2 \quad (\pi \text{ decays}) , \tag{C.3b}$$

$$\widetilde{\mathcal{K}}_j^{Ma} \approx 15|B_{eN_j}|^2 + 8|B_{\mu N_j}|^2 + 2|B_{\tau N_j}|^2 \quad (K \text{ decays}) , \tag{C.3c}$$

$$\widetilde{\mathcal{K}}_j^{Ma} \approx 7(|B_{eN_j}|^2 + |B_{\mu N_j}|^2) + 2|B_{\tau N_j}|^2 \quad (D, D_s \text{ decays}) , \tag{C.3d}$$

$$\widetilde{\mathcal{K}}_j^{Ma} \approx 8(|B_{eN_j}|^2 + |B_{\mu N_j}|^2) + 3|B_{\tau N_j}|^2 \quad (B, B_c \text{ decays}) . \tag{C.3e}$$

The rough upper bounds for $|B_{\ell N}|^2$, for $\ell = e, \mu, \tau$, are given in Table C.1 for the typical ranges of our interest: M_N around 0.13; 0.25; 1; 3 GeV – relevant for the decays of π; K; (D, D_s); (B, B_c), respectively (see also Table C.2 for several specific values of M_N).

TABLE C.1: *Present rough upper bounds for $|B_{\ell N}|^2$ $(\ell = e, \mu, \tau)$ for M_N in the ranges around the values* 0.13, 0.25, 1, 3 *GeV; and the canonical acceptance factor $\overline{A}(M_N)$ (for $L = 1$ m and $\gamma_N = 2$).*

M_N [GeV]	$\lvert B_{eN}\rvert^2$	$\lvert B_{\mu N}\rvert^2$	$\lvert B_{\tau N}\rvert^2$	$\overline{A}$
≈ 0.13	10^{-8}	10^{-6}	10^{-4}	$4 \cdot 10^{-3}$
≈ 0.25	10^{-8}	10^{-7}	10^{-4}	0.11
≈ 1.0	10^{-7}	10^{-7}	10^{-2}	115.
≈ 3.0	10^{-6}	10^{-4}	10^{-4}	$3 \cdot 10^4$

The present upper bounds for $|B_{eN}|^2$, in the mentioned range of M_N, are largely determined by the neutrinoless double beta decay experiments [49, 50, 76] $(0\nu\beta\beta)$. The upper bounds for $|B_{\mu N}|^2$ come from searches of peaks in the spectrum of μ in pion and kaon decays [51] and from decay searches [51–56, 77, 78]. The upper bounds for $|B_{\tau N}|^2$ come from CC interactions (if τ is produced) and from NC interactions [56–58]. In Table C.2 we present the upper bounds on $|B_{\ell N}|^2$ for specific chosen values of M_N in the mentioned interval.

Table C.2: *Present upper bounds for the squares $|B_{\ell N}|^2$ of the heavy-light mixing matrix elements, for various specific values of M_N.*

$M_N[GeV]$	$\lvert B_{eN}\rvert^2$	$\lvert B_{\mu N}\rvert^2$	$\lvert B_{\tau N}\rvert^2$
0.1	$(1.5 \pm 0.5) \times 10^{-8}$	$(6.0 \pm 0.5) \times 10^{-6}$	$(8.0 \pm 0.5) \times 10^{-4}$
0.3	$(2.5 \pm 0.5) \times 10^{-9}$	$(3.0 \pm 0.5) \times 10^{-9}$	$(1.5 \pm 0.5) \times 10^{-1}$
0.5	$(2.0 \pm 0.5) \times 10^{-8}$	$(6.5 \pm 0.5) \times 10^{-7}$	$(2.5 \pm 0.5) \times 10^{-2}$
0.7	$(3.5 \pm 0.5) \times 10^{-8}$	$(2.5 \pm 0.5) \times 10^{-7}$	$(9.0 \pm 0.5) \times 10^{-3}$
1.0	$(4.5 \pm 0.5) \times 10^{-8}$	$(1.5 \pm 0.5) \times 10^{-7}$	$(3.0 \pm 0.5) \times 10^{-3}$
2.0	$(1.0 \pm 0.5) \times 10^{-7}$	$(2.5 \pm 0.5) \times 10^{-5}$	$(3.0 \pm 0.5) \times 10^{-4}$
3.0	$(1.5 \pm 0.5) \times 10^{-7}$	$(2.5 \pm 0.5) \times 10^{-5}$	$(4.5 \pm 0.5) \times 10^{-5}$
4.0	$(2.5 \pm 0.5) \times 10^{-7}$	$(1.5 \pm 0.5) \times 10^{-5}$	$(1.5 \pm 0.5) \times 10^{-5}$
5.0	$(3.0 \pm 0.5) \times 10^{-7}$	$(1.5 \pm 0.5) \times 10^{-5}$	$(1.5 \pm 0.5) \times 10^{-5}$
6.0	$(3.5 \pm 0.5) \times 10^{-7}$	$(1.5 \pm 0.5) \times 10^{-5}$	$(1.5 \pm 0.5) \times 10^{-5}$

The upper bounds have in some cases strong dependence on the precise values of M_N, and for further details we refer to the corresponding figures in Ref. [45].

The corresponding values of the canonical acceptance factor $\overline{A}(M_N)$ are also included in Table C.1.

Combining Eqs. (C.2) with (C.3) and Table C.1, we obtain for the acceptance factor P_{N_j} the following estimates and upper bounds relevant for the π decays ($M_N \approx 0.13$ GeV), K decays ($M_N \approx 0.25$ GeV), D and D_s decays ($M_N \approx 1$ GeV), and B and B_c decays ($M_N \approx 3$ GeV):

$$\begin{aligned} P_{N_j}(M_N \approx 0.13\text{GeV}) &\approx (6.4|B_{eN_j}|^2 + 4.4|B_{\mu N_j}|^2)10^{-3} \quad (+4.4|B_{\tau N_j}|^2)10^{-3} \\ &\lesssim 10^{-11} + 10^{-9} \quad (+10^{-7}) \,, \end{aligned} \tag{C.4a}$$

$$\begin{aligned} P_{N_j}(M_N \approx 0.25\text{GeV}) &\approx 1.7|B_{eN_j}|^2 + 0.9|B_{\mu N_j}|^2 \quad (+0.2|B_{\tau N_j}|^2) \\ &\lesssim 10^{-8} + 10^{-7} \quad (+10^{-5}) \,, \end{aligned} \tag{C.4b}$$

$$\begin{aligned} P_{N_j}(M_N \approx 1\text{GeV}) &\approx 0.8 \cdot 10^3|B_{eN_j}|^2 + 0.8 \cdot 10^3|B_{\mu N_j}|^2 \quad (+2 \cdot 10^2|B_{\tau N_j}|^2) \\ &\lesssim 10^{-4} + 10^{-4} \quad (+10^{0}) \,, \end{aligned} \tag{C.4c}$$

$$\begin{aligned} P_{N_j}(M_N \approx 3\text{GeV}) &\approx 3 \cdot 10^5|B_{eN_j}|^2 + 3 \cdot 10^5|B_{\mu N_j}|^2 \quad (+1 \cdot 10^5|B_{\tau N_j}|^2) \\ &\lesssim 10^{0} + 10^{0} \quad (+10^{0}) \,, \end{aligned} \tag{C.4d}$$

The upper bounds for P_{N_j} in Eqs. (C.4) are written as a sum of the contributions of upper bounds from $|B_{eN_j}|^2$, $|B_{\mu N_j}|^2$ and $|B_{\tau N_j}|^2$ separately. Further, the contributions of $|B_{\tau N_j}|^2$ are included in Eqs. (C.4) optionally, in the parentheses, because the upper bounds of the mixings $|B_{\tau N_j}|^2$ are still very high and are expected to be reduced significantly in the foreseeable future. The upper bounds which give results higher than one are replaced by one (10^0), because the acceptance (decay probability) P_{N_j} can never be higher than one by definition.

Appendix D

Delta function approximation for the imaginary part of the propagator product

In this Appendix we investigate the expression for the imaginary part of the propagator product, $\mathrm{Im}(P_1(D)P_2(D)^*)$, Eq. (3.35). For convenience we introduce in this Appendix the following simplified notations x, M^2, Δ and ξ:

$$x \equiv p_N^2, \quad M^2 \equiv M_{N_1}^2, \tag{D.1a}$$

$$\Delta \equiv \Delta M_N^2 \equiv M_{N_2}^2 - M_{N_1}^2, \tag{D.1b}$$

$$\Gamma_{N_1} = \xi\Gamma_N, \quad \Gamma_{N_2} = (2-\xi)\Gamma_N. \tag{D.1c}$$

We note that $\Delta > 0$ by convention; and $0 < \xi < 2$. Further, $\Gamma_{N_1} + \Gamma_{N_2} = 2\Gamma_N$, in accordance with the definition of Γ_N Eq. (3.13). Since we always have $\Gamma_{N_j} \ll M_{N_j}$ (the neutrinos N_j are sterile), the relation (3.34) holds, i.e.,

$$\frac{\Gamma_{N_j} M_{N_j}}{(x - M_{N_j}^2)^2 + \Gamma_{N_j}^2 M_{N_j}^2} = \pi\delta(x - M_{N_j}^2). \tag{D.2}$$

We can write the right-hand side of Eq. (3.35a) for $\mathrm{Im}(P_1(D)P_2(D)^*)$ as

$$\mathrm{Im}\,(P_1(D)P_2(D)^*) = \mathcal{R}_1 + \mathcal{R}_2 \tag{D.3}$$

where $\mathcal{R}_1$ and $\mathcal{R}_2$ can be written, in our notation, as

$$\mathcal{R}_1 = \frac{(x - M^2)(2-\xi)\Gamma_N\sqrt{M^2+\Delta}}{[(x-M^2)^2 + \xi^2\Gamma_N^2 M^2]\,[(x - M^2 - \Delta)^2 + (2-\xi)^2\Gamma_N^2(M^2+\Delta)]} \tag{D.4a}$$

$$= \eta_1 \times \frac{\pi}{\Delta}\delta(x - M^2 - \Delta), \tag{D.4b}$$

$$\mathcal{R}_2 = -\frac{\xi\Gamma_N M(x - M^2 - \Delta)}{[(x-M^2)^2 + \xi^2\Gamma_N^2 M^2]\,[(x - M^2 - \Delta)^2 + (2-\xi)^2\Gamma_N^2(M^2+\Delta)]} \tag{D.4c}$$

$$= \eta_2 \times \frac{\pi}{\Delta}\delta(x - M^2), \tag{D.4d}$$

In Eqs. (D.4b) and (D.4d), the identity (D.2) was used, and we introduced two (dimensionless) parameters η_j $(j = 1, 2)$. We want to obtain these two parameters η_j. They can be obtained by integrating analytically the explicit expressions (D.4a) and (D.4c) for $\mathcal{R}_j(x)$ over x. For

example, integration of $\mathcal{R}_1(x)$ gives

$$\int_{-\infty}^{+\infty} dx \frac{(x-M^2)(2-\xi)\Gamma_N\sqrt{M^2+\Delta}}{[(x-M^2)^2+\xi^2\Gamma_N^2M^2]\,[(x-M^2-\Delta)^2+(2-\xi)^2\Gamma_N^2(M^2+\Delta)]} = \frac{\pi\Delta}{(\Delta^2+4\Gamma_N^2M_*^2)}, \tag{D.5}$$

where

$$M_*^2 = \frac{1}{2}M^2\left[(2-\xi(2-\xi))+\xi(2-\xi)\sqrt{1+\Delta/M^2}\right]+\frac{1}{4}(2-\xi)^2\Delta \tag{D.6a}$$

$$= M^2\left[1+(1-\xi/2)\frac{\Delta}{M^2}+\mathcal{O}\left(\frac{\Delta^2}{M^4}\right)\right]. \tag{D.6b}$$

The integration in Eq. (D.5) can be evaluated in the range $]-\infty,\infty[$, due to *Dirac delta* structure in the integrand (Dirac delta functions have narrows peaks for possitive $x \approx M_{Nj}$).

Therefore, in the case of near degeneracy ($\Delta \ll M^2$) we have $M_*^2 = M^2$. If we now use in the integration over dx the expression (D.4b) instead, take into account $M_*^2 = M^2$ in the case of near degeneracy, and compare with (D.5), we obtain the following expression for the parameter η_1 by comparison with (D.5):

$$\eta_1\frac{1}{\Delta} = \frac{\Delta}{(\Delta^2+4\Gamma_N^2M^2)} \quad (\Delta \ll M^2), \tag{D.7a}$$

$$\eta_1 = \frac{y^2}{y^2+1} \quad \left(y \equiv \frac{\Delta}{(2M\Gamma_N)},\ \Delta \ll M^2\right), \tag{D.7b}$$

where in Eq. (D.7b) we use the usual notation in this paper $y \equiv (M_{N_2}-M_{N_1})/\Gamma_N = \Delta/(2M\Gamma_N)$. Here we note that $\Delta \equiv (M_{N_2}^2-M_{N_1}^2) = (M_{N_2}-M_{N_1})2M_{N_1}$ in the case of near degeneracy $\Delta \ll M^2 \equiv M_{N_1}^2$.

Doing the same procedure with the quantity $\mathcal{R}_2$, we obtain for η_2 the very same result as for η_1

$$\eta_1 = \eta_2 = \frac{y^2}{y^2+1} \quad (\Delta \ll M^2). \tag{D.8}$$

Appendix E

Explicit formulas of $M^{\pm} \to \ell_1^{\pm}\ell_2^{\pm}M^{'\mp}$

E.1 The matrix element $\mathcal{T}(M^{\pm})$ for the decay of Fig. 4.1 can be written in the form.

$$\mathcal{T}(M^{\pm}) = K_{M\pm}\sum_{j=1}^{2} k_j^{(\pm)} M_{N_j}\left[P_j(D)T_{M\pm}(D) + P_j(C)T_{M\pm}(C)\right] \ , \tag{E.1}$$

where $j = 1, 2$ refer to the contributions of the exchanges of the two intermediate neutrinos N_j, and $X = D, C$ refer to the contribution of the direct and crossed channels, respectively, cf. Fig. 4.1. In Eq. (E.1), $k_j^{(\pm)}$ are the heavy-light mixing factors defined in Eq. (3.7); $P_j(X)$ $(j = 1, 2; X = D, C)$ are the propagator functions of N_j neutrino for the D and C channel, Eqs. (3.6), and $K_{\pm}$ are the constants coming from the vertices

$$K_{M-} = -G_F^2 V_{Q_u Q_d} V_{q_u q_d} f_M f_{M'} \ , \qquad K_{M+} = (K_{M-})^* \ , \tag{E.2}$$

where f_M and $f_{M'}$ are the decay constants of $M^{\pm}$ and $M^{'\mp}$, and $V_{Q_u Q_d}$ and $V_{q_u q_d}$ are the CKM elements for $M^{\pm}$ and $M^{'\mp}$: M^+ has the valence quark content $Q_u\bar{Q}_d$; $M^{'+}$ has $q_u\bar{q}_d$. The functions $T_{M\pm}(D)$ and $T_{M\pm}(C)$ appearing in the amplitude (E.1) can be written as

$$T_{M\pm}(D) = \overline{u}_{\ell_2}(p_2)\not{p}_{M'}\not{p}_{M}(1 \mp \gamma_5)v_{\ell_1}(p_1) \ , \tag{E.3a}$$
$$T_{M\pm}(C) = \overline{u}_{\ell_2}(p_2)\not{p}_{M}\not{p}_{M'}(1 \mp \gamma_5)v_{\ell_1}(p_1) \ , \tag{E.3b}$$

where the spinors are written in the helicity basis. Squaring and summing over the final helicities leads to the square $|\mathcal{T}(M^{\pm})|^2$ of the total decay amplitude (E.1) as given in Eq. (4.5) in conjuntion with Eqs. (3.7)-(3.5), where the quadratic expressions $T_{M\pm}(X)T_{M\pm}(Y)^*$ $(X, Y = D, C)$ appearing in the normalized decay widths $\widetilde{\Gamma}_{\pm}(XY^*)_{ij}$ in Eq. (4.7) are

$$\begin{aligned} T_{M\pm}(D)T_{M\pm}(D)^* &= 8\big[M_M^2 M_{M'}^2(p_1\cdot p_2) - 2M_M^2(p_1\cdot p_{M'})(p_2\cdot p_{M'}) - 2M_{M'}^2(p_1\cdot p_M)(p_2\cdot p_M) \\ &\quad +4(p_1\cdot p_M)(p_2\cdot p_{M'})(p_M\cdot p_{M'})\big] \equiv T_M(D)T_M(D)^* \ , \end{aligned} \tag{E.4a}$$
$$\begin{aligned} T_{M\pm}(C)T_{M\pm}(C)^* &= 8\big[M_M^2 M_{M'}^2(p_1\cdot p_2) - 2M_M^2(p_1\cdot p_{M'})(p_2\cdot p_{M'}) - 2M_{M'}^2(p_1\cdot p_M)(p_2\cdot p_M) \\ &\quad +4(p_2\cdot p_M)(p_1\cdot p_{M'})(p_M\cdot p_{M'})\big] \equiv T_M(C)T_M(C)^* \ , \end{aligned} \tag{E.4b}$$
$$\begin{aligned} T_{M\pm}(D)T_{M\pm}(C)^* &= 16\Big\{M_M^2(p_1\cdot p_{M'})(p_2\cdot p_{M'}) + M_{M'}^2(p_1\cdot p_M)(p_2\cdot p_M) - \frac{1}{2}M_M^2 M_{M'}^2(p_1\cdot p_2) \\ &\quad +(p_M\cdot p_{M'})\left[-(p_1\cdot p_M)(p_2\cdot p_{M'}) - (p_2\cdot p_M)(p_1\cdot p_{M'}) + (p_M\cdot p_{M'})(p_1\cdot p_2)\right] \\ &\quad \mp i(p_M\cdot p_{M'})\epsilon(p_M, p_1, p_2, p_{M'})\Big\} \end{aligned} \tag{E.4c}$$
$$T_{M\pm}(C)T_{M\pm}(D)^* = (T_{M\pm}(D)T_{M\pm}(C)^*)^* = T_{M\mp}(D)T_{M\mp}(C)^* = (T_{M\mp}(C)T_{M\mp}(D)^*)^* \ , \tag{E.4d}$$

where in these expressions the summation over the (final) helicities of the leptons ℓ_1 and ℓ_2 is implied, and we denoted

$$\epsilon(q_1,q_2,q_3,q_4) \equiv \epsilon^{\eta_1\eta_2\eta_3\eta_4}(q_1)_{\eta_1}(q_2)_{\eta_2}(q_3)_{\eta_3}(q_4)_{\eta_4} \ , \tag{E.5}$$

and $\epsilon^{\eta_1\eta_2\eta_3\eta_4}$ is the totally antisymmetric Levi-Civita tensor with the sign convention $\epsilon^{0123} = +1$.

The expressions (E.4), in conjunction with the definitions (4.7), imply for the canonical decay widths $\widetilde{\Gamma}_{M\pm}(XY^*)_{ij}$ of Eq. (4.7) various symmetry relations, among them that $\widetilde{\Gamma}_{M\pm}(DD^*)$ and $\widetilde{\Gamma}_{M\pm}(CC^*)$ are both self-adjoint (2×2) matrices and that elements of the D-C interference matrices $\widetilde{\Gamma}_{M\pm}(CD^*)$ and $\widetilde{\Gamma}_{M\pm}(DC^*)$ are related

$$\widetilde{\Gamma}_M(DD^*)_{ij} = \left(\widetilde{\Gamma}_M(DD^*)_{ji}\right)^* , \qquad \widetilde{\Gamma}_M(CC^*)_{ij} = \left(\widetilde{\Gamma}_M(CC^*)_{ji}\right)^* , \tag{E.6a}$$

$$\widetilde{\Gamma}_{M\pm}(CD^*)_{ij} = \left(\widetilde{\Gamma}_{M\pm}(DC^*)_{ji}\right)^* . \tag{E.6b}$$

When the two final leptons are the same ($\ell_1 = \ell_2$), we can use the fact that the integration d_3 over the final particles is symmetric under $(p_1 \leftrightarrow p_2)$ (because $M_{\ell_1} = M_{\ell_2}$), and we have additional symmetry relations

$$\widetilde{\Gamma}_M(DD^*)_{ij} = \widetilde{\Gamma}_M(CC^*)_{ij} \ , \tag{E.7a}$$

$$\widetilde{\Gamma}_{M\pm}(CD^*)_{ij} = \widetilde{\Gamma}_{M\pm}(DC^*)_{ij} \ , \tag{E.7b}$$

and the (2×2) D-C interference matrices $\widetilde{\Gamma}_{M\pm}(CD^*)$ become self-adjoint, too.

E.2 Explicit expression for the function Q.

The expression (4.17) can be obtained by using in the integration over the phase space of three final particles [Eqs. (4.3)-(4.4)], for the contribution of the N_j neutrino, the identity

$$d_3\left(M(p_M) \to \ell_1(p_1)\ell_2(p_2)M'(p_{M'})\right) =$$

$$d_2\left(M(p_M) \to \ell_1(p_1)N_j(p_N)\right) dp_N^2 d_2\left(N_j(p_N) \to \ell_2(p_2)M'(p_{M'})\right) \tag{E.8a}$$

$$d_2\left(M(p_M) \to \ell_2(p_2)N_j(p_N)\right) dp_N^2 d_2\left(N_j(p_N) \to \ell_1(p_1)M'(p_{M'})\right) \ , \tag{E.8b}$$

where the first identity can be used for the DD^* contribution (where $p_N = p_M - p_1$) and the second for the CC^* contribution (where $p_N = p_M - p_2$). Using the identity (3.34) in the DD^* contribution, and the analogous identity for the CC^* contribution, the integration over dp_N^2 becomes trivial, and the d_2-type of integrations are straightforward.[1] The resulting expression for $\overline{\Gamma}(DD^*)_{jj}$ is then the expression Eq. (4.17) with the notations (4.19) and (4.23), where the

[1] This is equivalent to the factorization approach $\Gamma(M \to \ell_1 N_j)\mathrm{Br}(N_j \to \ell_2 M')$ valid when N_j is on-shell.

function Q has the form

$$\begin{aligned} Q(x; x_{\ell_1}, x_{\ell_2}, x') &= \left\{ \frac{1}{2}(x - x_{\ell_1})(x - x_{\ell_2})(1 - x - x_{\ell_1}) \left(1 - \frac{x'}{x} + \frac{x_{\ell_2}}{x}\right) \right. \\ &\quad + \big[- x_{\ell_1} x_{\ell_2}(1 + x' + 2x - x_{\ell_1} - x_{\ell_2}) - x_{\ell_1}^2(x - x') + x_{\ell_2}^2(1 - x) \\ &\quad \left. + x_{\ell_1}(1 + x)(x - x') - x_{\ell_2}(1 - x)(x + x') \big] \right\} . \qquad \text{(E.9)} \\ &= \frac{1}{2}\left[(1 - x)x + x_{\ell_1}(1 + 2x - x_{\ell_1})\right] \left[x - x' - 2x_{\ell_2} - \frac{x_{\ell_2}}{x}(x' - x_{\ell_2}) \right] \qquad \text{(E.10)} \end{aligned}$$

Appendix F

The quantum mechanics approach to oscillation.

In this Appendix, we show that the amplitude approach to on-shell oscillations in the considered processes, as presented in the main text of this work and following mainly the amplitude approach of Ref. [67], is consistent with the usual (quantum mechanics) approach to neutrino oscillation [39] (cf. also [68]) applied to these processes (within the approximations used in such approaches).

We recall that the relevant e- and μ-flavor analogs in the considered processes are the combinations (5.3a) of only the two almost mass-degenerate heavy neutrino eigenfields N_j ($j = 1, 2$), because the other components (including the light neutrino mass eigenfields ν_1, ν_2, ν_3) are off-shell or are assumed off-shell in the considered processes. Following the usual (quantum mechanics) approaches to neutrino oscillation, cf. [39] (cf. also [68]), the e and μ "heavy" flavor analogs $\mathcal{N}_\alpha$ ($\alpha = 1, 2$) of the heavy neutrino mass eigenstates N_j ($j = 1, 2$), cf. Eqs. (5.2), are represented as quantum mechanical states [cf. Eq. (5.3a) for the corresponding fields]

$$|\mathcal{N}_\alpha\rangle = \mathcal{B}^*_{\alpha 1}|N_1\rangle + \mathcal{B}^*_{\alpha 2}|N_2\rangle, \tag{F.1a}$$

$$|\overline{\mathcal{N}}_\alpha\rangle = \mathcal{B}_{\alpha 1}|N_1\rangle + \mathcal{B}_{\alpha 2}|N_2\rangle \quad (\alpha = 1, 2), \tag{F.1b}$$

where in Eq. (F.1b) we assumed that the physical neutrinos N_j are Majorana. Here we used the notation (5.3b) for the 2×2 matrix $\mathcal{B}$ with normalized lines. In the wavefunction approach [39], these wavefunctions are in the Schrödinger representation, and consequently have the following evolution in time t:

$$|\mathcal{N}_\alpha(t)\rangle = \sum_{j=1}^{2} \mathcal{B}^*_{\alpha j} \exp(-iE_j t)|N_j\rangle = \sum_{\beta=1}^{2}\sum_{j=1}^{2} \mathcal{B}^*_{\alpha j} \exp(-iE_j t) \left(\mathcal{B}^{*-1}\right)_{j\beta} |\mathcal{N}_\beta\rangle, \tag{F.2a}$$

$$|\overline{\mathcal{N}}_\alpha(t)\rangle = \sum_{j=1}^{2} \mathcal{B}_{\alpha j} \exp(-iE_j t)|N_j\rangle = \sum_{\beta=1}^{2}\sum_{j=1}^{2} \mathcal{B}_{\alpha j} \exp(-iE_j t) \left(\mathcal{B}^{-1}\right)_{j\beta} |\overline{\mathcal{N}}_\beta\rangle, \tag{F.2b}$$

where we recall the notation (5.3b) used for the 2×2 matrix $\mathcal{B}$, and the inverse matrix is consequently

$$\mathcal{B}^{-1} = \frac{1}{\mathrm{Det}\mathcal{B}} \begin{bmatrix} \mathcal{B}_{22} & -\mathcal{B}_{12} \\ -\mathcal{B}_{21} & \mathcal{B}_{11} \end{bmatrix}, \tag{F.3}$$

and $\mathcal{B}^{*-1}$ is the complex conjugate of this. In Eqs. (F.2) the notation $E_j \equiv E_{N_j}$ is used for the energy of the neutrino mass eigenstate $|N_j\rangle$, where E_{N_j} is given in Eq. (5.24). The states $|N_j\rangle$ ($j = 1, 2$) are orthogonal to each other

$$\langle N_j|N_k\rangle = \delta_{jk}. \tag{F.4}$$

We note that the 2×2 matrix $\mathcal{B}$ matrix, Eq. (5.3b), although having its two lines normalized, is in general not unitary, and therefore

$$\langle \mathcal{N}_1 | \mathcal{N}_2 \rangle = \sum \mathcal{B}_{1j} \mathcal{B}^*_{2j} \neq 0, \quad \langle \mathcal{N}_1 | \overline{\mathcal{N}}_2 \rangle = \sum \mathcal{B}_{1j} \mathcal{B}_{2j} \neq 0, \tag{F.5}$$

i.e., the states of the "heavy" flavor analogs, $|\mathcal{N}_\alpha\rangle$ and/or $|\overline{\mathcal{N}}_\beta\rangle$, are in general not mutually orthogonal. As a consequence of Eqs. (F.4) and (5.3), these flavor analogs are normalized states

$$\langle \mathcal{N}_1 | \mathcal{N}_1 \rangle = \langle \mathcal{N}_2 | \mathcal{N}_2 \rangle = 1 = \langle \overline{\mathcal{N}}_1 | \overline{\mathcal{N}}_1 \rangle = \langle \overline{\mathcal{N}}_2 | \overline{\mathcal{N}}_2 \rangle. \tag{F.6}$$

In the LC decay $B^+ \to \mu^+ e^- \pi^+$, Fig. 5.2, the neutrino flavor state produced in the first (production) vertex is $|\mathcal{N}_2\rangle$, and the state disappearing at the second (decay) vertex is $|\mathcal{N}_1\rangle$, cf. Fig. F.1. Therefore, the relevant oscillation amplitude in this decay is $\langle \mathcal{N}_1 | \mathcal{N}_2(t) \rangle$.

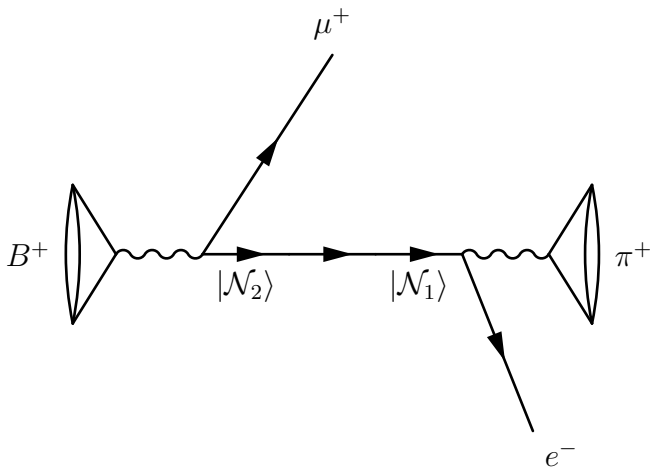

Figure F.1: *The LC decay $B^+ \to \mu^+ e^- \pi^+$: at the production vertex, $|\mathcal{N}_1\rangle$ state is produced; at the decay vertex, $|\mathcal{N}_2\rangle$ state is absorbed.*

Using the relations (F.2a) and (F.5)-(F.6), we obtain[1] the following expression for the relevant oscillation amplitude $\langle \mathcal{N}_1 | \mathcal{N}_2(t) \rangle$:

$$\begin{aligned} \langle \mathcal{N}_1 | \mathcal{N}_2(t) \rangle &= \left\{ \exp(-iE_{N_1} t) \mathcal{B}^*_{21} \left[\left(\mathcal{B}^{*-1}\right)_{11} + \left(\mathcal{B}^{*-1}\right)_{12} (\mathcal{B}_{11}\mathcal{B}^*_{21} + \mathcal{B}_{12}\mathcal{B}^*_{22}) \right] \right. \\ &\quad \left. + \exp(-iE_{N_2} t) \mathcal{B}^*_{22} \left[\left(\mathcal{B}^{*-1}\right)_{21} + \left(\mathcal{B}^{*-1}\right)_{22} (\mathcal{B}_{11}\mathcal{B}^*_{21} + \mathcal{B}_{12}\mathcal{B}^*_{22}) \right] \right\} \qquad \text{(F.7a)} \\ &= \frac{1}{\mathrm{Det}\mathcal{B}^*} \times \left\{ \exp(-iE_{N_1} t) \mathcal{B}^*_{21} \left[\mathcal{B}^*_{22} - \mathcal{B}^*_{12} (\mathcal{B}_{11}\mathcal{B}^*_{21} + \mathcal{B}_{12}\mathcal{B}^*_{22}) \right] \right. \\ &\quad \left. + \exp(-iE_{N_2} t) \mathcal{B}^*_{22} \left[-\mathcal{B}^*_{21} + \mathcal{B}^*_{11} (\mathcal{B}_{11}\mathcal{B}^*_{21} + \mathcal{B}_{12}\mathcal{B}^*_{22}) \right] \right\} \qquad \text{(F.7b)} \end{aligned}$$

Transforming Eq. (F.7a) to Eq. (F.7b), we used for $\mathcal{B}^{*-1}$ the complex conjugate of the identity (F.3). In this quantum mechanics approach, the terms in Eq. (F.7) with $\exp(-iE_{N_j} t)$ correspond to the terms $\exp(-ip_{N_j} \cdot z)$ of the corresponding amplitude $\mathcal{A}(B^+ \to \mu^+ e^- \pi^+)$ in Eq. (5.39a). If the two approaches are to be consistent with each other, then the ratio of the

[1] The algebra is performed in analogy with the usual quantum mechanics approach to light neutrino oscillations [39], except that now we have in general the nonorthogonality of the two flavor states Eq. (F.5).

coefficients at $\exp(-iE_{N_1}t)$ and $\exp(-iE_{N_2}t)$ in Eq. (F.7b) is equal to the ratio of the coefficients at $\exp(-ip_{N_1}\cdot z)$ and $\exp(-ip_{N_2}\cdot z)$ in Eq. (5.39a). This means that for the consistency we need to have[2]

$$\frac{\mathcal{B}^*_{22}-\mathcal{B}^*_{12}\left(\mathcal{B}_{11}\mathcal{B}^*_{21}+\mathcal{B}_{12}\mathcal{B}^*_{22}\right)}{-\mathcal{B}^*_{21}+\mathcal{B}^*_{11}\left(\mathcal{B}_{11}\mathcal{B}^*_{21}+\mathcal{B}_{12}\mathcal{B}^*_{22}\right)} \;=\; \frac{\mathcal{B}_{11}}{\mathcal{B}_{12}}. \tag{F.8}$$

By direct cross-multipliocation, it is straightforward to check that this identity really holds. In checking this identity, it is enough to use only the normalization of the lines of the $\mathcal{B}$ matrix, Eq. (5.3b): $|\mathcal{B}_{11}|^2+|\mathcal{B}_{12}|^2=1$.

In an analogous way, we can check that this quantum mechanics approach is consistent with the amplitude approach of the main text:

- also in the LC case $B^-\to\mu^-e^+\pi^-$: in the explanation above (Fig. F.1), the states $|\mathcal{N}_2\rangle$ and $|\mathcal{N}_1\rangle$ get replaced by $|\overline{\mathcal{N}}_2\rangle$ and $|\overline{\mathcal{N}}_1\rangle$, cf. Eqs. (F.1).
- also in the LV case $B^+\to\mu^+e^+\pi^-$: in the explanation above (Fig. F.1), the state $|\mathcal{N}_1\rangle$ gets replaced by $|\overline{\mathcal{N}}_1\rangle$, cf. Eqs. (F.1).
- also in the LV case $B^-\to\mu^-e^-\pi^+$: in the explanation above (Fig. F.1), the state $|\mathcal{N}_2\rangle$ gets replaced by $|\overline{\mathcal{N}}_2\rangle$, cf. Eqs. (F.1).

[2]Keeping in mind that, according to Eqs. (5.3), we have $B_{eN_j}=K_1\mathcal{B}_{1j}\propto\mathcal{B}_{1j}$ and $B_{\mu N_j}=K_2\mathcal{B}_{2j}\propto B_{2j}$.

Bibliography

[1] W. Pauli, "Dear radioactive ladies and gentlemen," *Phys.Today* **31N9** (1978) 27.

[2] C. Cowan, F. Reines, F. Harrison, H. Kruse, and A. McGuire, "Detection of the free neutrino: A Confirmation," *Science* **124** (1956) 103–104.

[3] G. Danby, J. Gaillard, K. A. Goulianos, L. Lederman, N. B. Mistry, *et al.*, "Observation of High-Energy Neutrino Reactions and the Existence of Two Kinds of Neutrinos," *Phys.Rev.Lett.* **9** (1962) 36–44.

[4] B. Pontecorvo, "Inverse beta processes and nonconservation of lepton charge," *Sov.Phys.JETP* **7** (1958) 172–173.

[5] **Super-Kamiokande** Collaboration, Y. Fukuda *et al.*, "Evidence for oscillation of atmospheric neutrinos," *Phys.Rev.Lett.* **81** (1998) 1562–1567, arXiv:hep-ex/9807003 [hep-ex].

[6] **SNO** Collaboration, Q. Ahmad *et al.*, "Direct evidence for neutrino flavor transformation from neutral current interactions in the Sudbury Neutrino Observatory," *Phys.Rev.Lett.* **89** (2002) 011301, arXiv:nucl-ex/0204008 [nucl-ex].

[7] **KamLAND** Collaboration, K. Eguchi *et al.*, "First results from KamLAND: Evidence for reactor anti-neutrino disappearance," *Phys.Rev.Lett.* **90** (2003) 021802, arXiv:hep-ex/0212021 [hep-ex].

[8] P. Minkowski, "$\mu \to e\gamma$ at a Rate of One Out of 10^9 Muon Decays?," *Phys.Lett.* **B67** (1977) 421–428.

[9] P. Ramond, "The Family Group in Grand Unified Theories," arXiv:hep-ph/9809459 [hep-ph].

[10] T. Yanagida, "HORIZONTAL SYMMETRY AND MASSES OF NEUTRINOS," *Conf.Proc.* **C7902131** (1979) 95–99.

[11] R. N. Mohapatra and G. Senjanovic, "Neutrino Mass and Spontaneous Parity Violation," *Phys.Rev.Lett.* **44** (1980) 912.

[12] G. Racah, "On the symmetry of particle and antiparticle," *Nuovo Cim.* **14** (1937) 322–328.

[13] W. Furry, "On transition probabilities in double beta-disintegration," *Phys.Rev.* **56** (1939) 1184–1193.

[14] H. Primakoff and S. P. Rosen, "Nuclear double-beta decay and a new limit on lepton nonconservation," *Phys.Rev.* **184** (1969) 1925–1933.

[15] H. Primakoff and P. S. Rosen, "BARYON NUMBER AND LEPTON NUMBER CONSERVATION LAWS," *Ann.Rev.Nucl.Part.Sci.* **31** (1981) 145–192.

[16] J. Schechter and J. Valle, "Neutrinoless Double beta Decay in SU(2) x U(1) Theories," *Phys.Rev.* **D25** (1982) 2951.

[17] M. Doi, T. Kotani, and E. Takasugi, "Double beta Decay and Majorana Neutrino," *Prog.Theor.Phys.Suppl.* **83** (1985) 1.

[18] S. R. Elliott and J. Engel, "Double beta decay," *J.Phys.* **G30** (2004) R183–R215, arXiv:hep-ph/0405078 [hep-ph].

[19] V. Rodin, A. Faessler, F. Simkovic, and P. Vogel, "Assessment of uncertainties in QRPA 0nu beta beta-decay nuclear matrix elements," *Nucl.Phys.* **A766** (2006) 107–131, arXiv:0706.4304 [nucl-th].

[20] L. S. Littenberg and R. E. Shrock, "Upper bounds on lepton number violating meson decays," *Phys.Rev.Lett.* **68** (1992) 443–446.

[21] L. S. Littenberg and R. Shrock, "Implications of improved upper bounds on —Delta L— = 2 processes," *Phys.Lett.* **B491** (2000) 285–290, arXiv:hep-ph/0005285 [hep-ph].

[22] C. Dib, V. Gribanov, S. Kovalenko, and I. Schmidt, "K meson neutrinoless double muon decay as a probe of neutrino masses and mixings," *Phys.Lett.* **B493** (2000) 82–87, arXiv:hep-ph/0006277 [hep-ph].

[23] A. Ali, A. Borisov, and N. Zamorin, "Majorana neutrinos and same sign dilepton production at LHC and in rare meson decays," *Eur.Phys.J.* **C21** (2001) 123–132, arXiv:hep-ph/0104123 [hep-ph].

[24] A. de Gouvea and J. Jenkins, "A Survey of Lepton Number Violation Via Effective Operators," *Phys.Rev.* **D77** (2008) 013008, arXiv:0708.1344 [hep-ph].

[25] G. Cvetic, C. Dib, S. K. Kang, and C. Kim *Phys.Rev.* **D82** (2010) 053010, arXiv:1005.4282 [hep-ph].

[26] J. C. Helo, S. Kovalenko, and I. Schmidt, "Sterile neutrinos in lepton number and lepton flavor violating decays," *Nucl.Phys.* **B853** (2011) 80–104, arXiv:1005.1607 [hep-ph].

[27] G. Cvetic, C. Dib, and C. Kim, "Probing Majorana neutrinos in rare $\pi^+ \to e^+e^+\mu^-\nu$ decays," *JHEP* **1206** (2012) 149, arXiv:1203.0573 [hep-ph].

[28] N. Cabibbo, "Time Reversal Violation in Neutrino Oscillation," *Phys.Lett.* **B72** (1978) 333–335.

[29] T. Asaka, S. Blanchet, and M. Shaposhnikov, "The nuMSM, dark matter and neutrino masses," *Phys.Lett.* **B631** (2005) 151–156, arXiv:hep-ph/0503065 [hep-ph].

[30] T. Asaka and M. Shaposhnikov, "The nuMSM, dark matter and baryon asymmetry of the universe," *Phys.Lett.* **B620** (2005) 17–26, arXiv:hep-ph/0505013 [hep-ph].

[31] D. Gorbunov and M. Shaposhnikov, "How to find neutral leptons of the νMSM?," *JHEP* **0710** (2007) 015, arXiv:0705.1729 [hep-ph].

[32] A. Boyarsky, O. Ruchayskiy, and M. Shaposhnikov, "The Role of sterile neutrinos in cosmology and astrophysics," *Ann.Rev.Nucl.Part.Sci.* **59** (2009) 191–214, arXiv:0901.0011 [hep-ph].

[33] M. Shaposhnikov, "Is there a new physics between electroweak and Planck scales?," arXiv:0708.3550 [hep-th].

[34] M. Shaposhnikov, "Neutrino physics within and beyond the three flavour oscillation," *J.Phys.Conf.Ser.* **408** (2013) 012015.

[35] W. Bonivento, A. Boyarsky, H. Dijkstra, U. Egede, M. Ferro-Luzzi, *et al.*, "Proposal to Search for Heavy Neutral Leptons at the SPS," arXiv:1310.1762 [hep-ex].

[36] S. Alekhin, W. Altmannshofer, T. Asaka, B. Batell, F. Bezrukov, *et al.*, "A facility to Search for Hidden Particles at the CERN SPS: the SHiP physics case," arXiv:1504.04855 [hep-ph].

[37] C. Itzykson and J. Zuber, "QUANTUM FIELD THEORY,".

[38] B. Kayser, F. Gibrat-Debu, and F. Perrier, "The Physics of massive neutrinos," *World Sci.Lect.Notes Phys.* **25** (1989) 1–117.

[39] S. Bilenky, "Introduction to the physics of massive and mixed neutrinos," *Lect.Notes Phys.* **817** (2010) 1–255.

[40] Z. Maki, M. Nakagawa, and S. Sakata, "Remarks on the unified model of elementary particles," *Prog.Theor.Phys.* **28** (1962) 870–880.

[41] J. Abad, J. Esteve, and A. Pacheco, "Neutrinoless Double Beta Decay of the Kaon in a Relativistic Quark Model," *Phys.Rev.* **D30** (1984) 1488.

[42] G. Cveti, C. Kim, and J. Zamora-Sa, "CP violations in $\pi^{\pm}$ Meson Decay," *J.Phys.* **G41** (2014) 075004, arXiv:1311.7554 [hep-ph].

[43] G. Cvetic, C. Dib, C. Kim, and J. Zamora-Saa, "Probing the Majorana neutrinos and their CP violation in decays of charged scalar mesons π, K, D, D_s, B, B_c," *Symmetry* **7** (2015) 726–773, arXiv:1503.01358 [hep-ph].

[44] "Project X and the Science of the Intensity Frontier." http://projectx.fnal.gov/pdfs/ProjectXwhitepaperJan.v2.pdf.

[45] A. Atre, T. Han, S. Pascoli, and B. Zhang, "The Search for Heavy Majorana Neutrinos," *JHEP* **0905** (2009) 030, arXiv:0901.3589 [hep-ph].

[46] G. Cveti, C. Kim, and J. Zamora-Sa, "CP violation in lepton number violating semihadronic decays of K, D, D_s, B, B_c," *Phys.Rev.* **D89** no. 9, (2014) 093012, arXiv:1403.2555 [hep-ph].

[47] C. O. Dib, M. Campos, and C. Kim, "CP Violation with Majorana neutrinos in K Meson Decays," *JHEP* **1502** (2015) 108, arXiv:1403.8009 [hep-ph].

[48] M. A. Ivanov and S. G. Kovalenko *Phys.Rev.* **D71** (2005) 053004, arXiv:hep-ph/0412198 [hep-ph].

[49] P. Benes, A. Faessler, F. Simkovic, and S. Kovalenko, "Sterile neutrinos in neutrinoless double beta decay," *Phys.Rev.* **D71** (2005) 077901, arXiv:hep-ph/0501295 [hep-ph].

[50] G. Belanger, F. Boudjema, D. London, and H. Nadeau, "Inverse neutrinoless double beta decay revisited," *Phys.Rev.* **D53** (1996) 6292–6301, arXiv:hep-ph/9508317 [hep-ph].

[51] A. Kusenko, S. Pascoli, and D. Semikoz, "New bounds on MeV sterile neutrinos based on the accelerator and Super-Kamiokande results," *JHEP* **0511** (2005) 028, arXiv:hep-ph/0405198 [hep-ph].

[52] **WA66** Collaboration, A. M. Cooper-Sarkar *et al.*, "Search for Heavy Neutrino Decays in the BEBC Beam Dump Experiment," *Phys.Lett.* **B160** (1985) 207.

[53] G. Bernardi, G. Carugno, J. Chauveau, F. Dicarlo, M. Dris, *et al.*, "FURTHER LIMITS ON HEAVY NEUTRINO COUPLINGS," *Phys.Lett.* **B203** (1988) 332.

[54] **FMMF** Collaboration, E. Gallas *et al.*, "Search for neutral weakly interacting massive particles in the Fermilab Tevatron wide band neutrino beam," *Phys.Rev.* **D52** (1995) 6–14.

[55] **NuTeV, E815** Collaboration, A. Vaitaitis *et al.*, "Search for neutral heavy leptons in a high-energy neutrino beam," *Phys.Rev.Lett.* **83** (1999) 4943–4946, arXiv:hep-ex/9908011 [hep-ex].

[56] **DELPHI** Collaboration, P. Abreu *et al.*, "Search for neutral heavy leptons produced in Z decays," *Z.Phys.* **C74** (1997) 57–71.

[57] **NOMAD** Collaboration, P. Astier *et al.*, "Search for heavy neutrinos mixing with tau neutrinos," *Phys.Lett.* **B506** (2001) 27–38, arXiv:hep-ex/0101041 [hep-ex].

[58] J. Orloff, A. N. Rozanov, and C. Santoni, "Limits on the mixing of tau neutrino to heavy neutrinos," *Phys.Lett.* **B550** (2002) 8–15, arXiv:hep-ph/0208075 [hep-ph].

[59] **Particle Data Group** Collaboration, J. Beringer *et al.*, "Review of Particle Physics (RPP)," *Phys.Rev.* **D86** (2012) 010001.

[60] G. Cvetic, C. Kim, G.-L. Wang, and W. Namgung, "Decay constants of heavy meson of 0- state in relativistic Salpeter method," *Phys.Lett.* **B596** (2004) 84–89, arXiv:hep-ph/0405112 [hep-ph].

[61] M. Drewes, "Private Communication,".

[62] D. Boyanovsky, "Nearly degenerate heavy sterile neutrinos in cascade decay: mixing and oscillations," *Phys.Rev.* **D90** no. 10, (2014) 105024, arXiv:1409.4265 [hep-ph].

[63] D. Boyanovsky and L. Lello, "Time evolution of cascade decay," *New J.Phys.* **16** (2014) 063050, arXiv:1403.6366 [hep-ph].

[64] D. Boyanovsky, "Spacetime evolution of heavy sterile neutrinos in cascade decays," *Nucl.Phys.* **B888** (2014) 248–270, arXiv:1406.5739 [hep-ph].

[65] L. Canetti, M. Drewes, T. Frossard, and M. Shaposhnikov, "Dark Matter, Baryogenesis and Neutrino Oscillations from Right Handed Neutrinos," *Phys.Rev.* **D87** no. 9, (2013) 093006, arXiv:1208.4607 [hep-ph].

[66] G. Cvetic, C. Kim, R. Kogerler, and J. Zamora-Saa, "Oscillation of heavy sterile neutrino in decay of $B \to \mu e \pi$," arXiv:1505.04749 [hep-ph].

[67] A. G. Cohen, S. L. Glashow, and Z. Ligeti, "Disentangling Neutrino Oscillations," *Phys.Lett.* **B678** (2009) 191–196, arXiv:0810.4602 [hep-ph].

[68] C. Giunti and C. W. Kim, "Quantum mechanics of neutrino oscillations," *Found.Phys.Lett.* **14** (2001) 213–229, arXiv:hep-ph/0011074 [hep-ph].

[69] F. F. Deppisch, P. S. B. Dev, and A. Pilaftsis, "Neutrinos and Collider Physics," arXiv:1502.06541 [hep-ph].

[70] **CHARM** Collaboration, F. Bergsma *et al.*, "A Search for Decays of Heavy Neutrinos in the Mass Range 0.5-GeV to 2.8-GeV," *Phys.Lett.* **B166** (1986) 473.

[71] **Belle** Collaboration, D. Liventsev *et al.*, "Search for heavy neutrinos at Belle," *Phys.Rev.* **D87** no. 7, (2013) 071102, arXiv:1301.1105 [hep-ex].

[72] L. Canetti, M. Drewes, and M. Shaposhnikov, "Sterile Neutrinos as the Origin of Dark and Baryonic Matter," *Phys.Rev.Lett.* **110** no. 6, (2013) 061801, arXiv:1204.3902 [hep-ph].

[73] S. Bray, J. S. Lee, and A. Pilaftsis, "Resonant CP violation due to heavy neutrinos at the LHC," *Nucl.Phys.* **B786** (2007) 95–118, arXiv:hep-ph/0702294 [HEP-PH].

[74] M. Drewes and B. Garbrecht, "Experimental and cosmological constraints on heavy neutrinos," arXiv:1502.00477 [hep-ph].

[75] V. Gribanov, S. Kovalenko, and I. Schmidt, "Sterile neutrinos in tau lepton decays," *Nucl.Phys.* **B607** (2001) 355–368, arXiv:hep-ph/0102155 [hep-ph].

[76] D. London, "Inverse neutrinoless double beta decay (and other Delta L = 2 processes)," arXiv:hep-ph/9907419 [hep-ph].

[77] **L3** Collaboration, O. Adriani *et al.*, "Search for isosinglet neutral heavy leptons in Z0 decays," *Phys.Lett.* **B295** (1992) 371–382.

[78] **CHARM II** Collaboration, P. Vilain *et al.*, "Search for heavy isosinglet neutrinos," *Phys.Lett.* **B343** (1995) 453–458.